Spring 6-5-2018

Maternal Angiotensinogen Genotype and Fetal Sex Impact Uteroplacental Function and the Developmental Origins of Stress-Induced Hypertension

Jessica Faith Hebert
Portland State University

Maternal Angiotensinogen Genotype and Fetal Sex Impact Uteroplacental Function and the Developmental Origins of Stress-Induced Hypertension

by

Jessica Faith Hebert

A dissertation submitted in partial fulfillment of the
requirements for the degree of

Doctor of Philosophy
in
Biology

Dissertation Committee:
Michael Bartlett, Chair
Terry Morgan
Justin Courcelle
Jason Podrabsky
Gwen Shusterman

Portland State University
2018

Abstract

Fetal growth restriction (FGR) is a common and potentially life-threatening complication that affects 5-10% of human pregnancies. Maternal genetic predisposition and fetal male sex are known risk factors, but the underlying mechanisms are unknown. To study a known maternal genetic risk factor and the impact of fetal sex, we employed a published transgenic (TG) mouse model, which was designed to mimic a common human angiotensinogen (AGT) promoter variant associated with a 20% increase in circulating AGT levels. We hypothesized that TG dams would deliver growth restricted pups and that the underlying mechanism would be related to differences in maternal uterine pregnancy-induced vascular remodeling, abnormal blood flow to the placenta, and placental damage. In addition, since growth restricted human males are at an increased risk of developing adult onset hypertension, which has been associated with reduced nephron development, we tested for developmental programming in our mouse model and the impact of fetal sex. Our results show that TG dams have reduced uterine and placental angiogenesis when their pups were males, but relatively normal angiogenesis in the female siblings compared with wild-type controls. The uterine placental bed in TG dams had abnormal pro-angiogenic/anti-angiogenic expression ratios that were related to differences in uterine natural killer cell activation and fetal sex. The abnormal phenotype could be rescued by delivering vascular endothelial growth factor (VEGF) to uterine endothelial cells. Male progeny from TG dams had abnormal kidney epigenetic changes, fewer nephrons as adults, and they developed stress-induced hypertension. We conclude that the combination of maternal genetic risk and fetal male sex affect uteroplacental angiogenesis leading to FGR and the programming of stress-induced hypertension.

Dedication

For Nancy Eris Hebert and Bobbi Kirk,
who I think would have enjoyed this story.
Thanks for raising great men,
even if they were probably tough on their placentas.

Acknowledgements

I am sincerely grateful for the mentorship of my advisor, Dr. Terry Morgan, without whom I would not have begun and completed this work. Thanks to my dissertation committee, Dr. Justin Courcelle, Dr. Jason Podrabsky, Dr. Gwen Shusterman, and Dr. Michael Bartlett, and to my other mentors and collaborators Dr. Elizabeth DuPriest and Dr. Helen Jones, for their generous advice and guidance. I am indebted to my peers for the commiseration and coffee, especially Dr. Catherine Dayger, Jess Millar, and Mayu Morita.

I am so thankful for the support and patience of my family and friends during these long years of study. None of this would have been possible without my parents, Rick and Joann Johnson. Thanks, Mom and Dad, for being supportive of my love for science, and thank you to my sister Erica Tuff for her humor and razor-sharp insight.

To my husband Royal: my gratitude exceeds the length of this dissertation. I love you and I could not have done this without you or our Lucymuppet.

To the therapists at Lewis & Clark Community Counseling Center, thank you for the tools I needed to survive, and then to thrive.

Finally, my deepest appreciation to the Holy Trinity of Scicomm: Bill Nye, Carl Sagan, and Stephen Hawking for inspiring me to share the science I love with the world.

Table of Contents

List of Tables

Chapter 2 Table

Chapter 3 Tables

List of Figures

Chapter 1

Chapter 2

Chapter 3

Chapter 4

Chapter 5

Preface

Chapter 2 has been resubmitted to the *Journal of Clinical Investigation*

Morgan TK, Hebert J, Roberts V, et al. "Vascular endothelial growth factor gene delivery to uterine spiral arteries rescues pregnancy-induced angiogenesis and prevents fetal growth restriction in transgenic mouse model of placental insufficiency"

Chapter 3 is in preparation for submission to *Biology of Reproduction*

Jessica F. Hebert, Jess A. Millar, et al. "Male fetal sex inhibits uteroplacental vascular growth in a mouse model of fetal growth restriction"

Chapter 4 has been submitted to the journal *Reproductive Sciences*

Elizabeth DuPriest, Jessica F. Hebert, Mayu Morita, et al. "Renal DNA methylation and the developmental programming of stress-induced hypertension in male mice"

Chapter 1

Dissertation Introduction: New Insights into the Roles of Maternal Genotype and Fetal Sex in the Pathophysiology of Placental Insufficiency

Fetal growth restriction (FGR) is a common and potentially life-threatening complication of pregnancy (1). It is defined as birthweight below the 10th percentile for gestational age (2). Not only does FGR increase perinatal morbidity and mortality, but accumulating evidence suggests the relative lack of appropriate nutrition in utero leads to profound epigenetic affects and abnormal fetal organ development culminating in a significantly increased risk of adult onset diseases like hypertension, diabetes, and cardiovascular disease (3, 4). FGR is a multifactorial disease, but the most common association is relative "placental insufficiency," which may be defined as reduced maternal nutrient supply (e.g. low protein diet, relative hypoxia [altitude]), or increased fetoplacental demand (exceptionally large placenta and/or baby, which is observed in maternal obesity and gestational diabetes; or multiple gestations [twins; triplets]) (1).

The underlying cause of placental insufficiency is not well understood, but the clinical syndrome includes more than just FGR: gestational hypertension (preeclampsia), preterm labor not caused by intra-amniotic infection, and developmental programming of many adult onset diseases are often comorbid (5–10). Abnormal blood flow to the placenta is thought to be the most common cause of placental insufficiency in these multifactorial syndromes (6), but the mechanisms affecting blood flow to the placenta are not well understood. The overarching hypothesis tested in this dissertation is that

differences in uteroplacental arterial growth and architecture may explain differences in uteroplacental blood flow and pregnancy outcomes, including developmental programming of adult onset disease.

Developmental Origins of Health and Disease (DOHAD)

Developmental Origins of Health and Disease (DOHAD) explores how early life events, from effects on the oocyte to gestational conditions to childhood illness, have impact on later adult onset disease (11). These events are often referred to as the "Barker Hypothesis" for David Barker, who described "programming" events, where early changes in structure or function resulted in increased risk of adult disease (12, 13). Some of the first DOHAD studies concerned the relationship between birthweight and adult disease, where young men whose mothers were starving in their first trimester during the Dutch famine of 1944-5 had significantly higher rates of obesity than men from mothers who did not suffer from the famine or experienced the famine during late pregnancy; it has been the prevailing thought that it is advantageous to the fetus to conserve resources that would be used for organ development as fat to help ensure survival after birth (14). Other early DOHAD experiments found links between low birthweight and a number of adult onset diseases, most notably cardiovascular and renal disease (15–18).

Fetal Growth and Uteroplacental Vascular Remodeling

Normal fetal growth requires proper uteroplacental vascular angiogenesis and pregnancy-induced uterine spiral artery vascular remodeling (19). Several factors are involved in blood vessel formation, which are comprised of a consecutive process known as vasculogenesis and angiogenesis. Both processes are required for proper growth and pruning of vascular beds in the maternal uterus and fetal placenta during pregnancy.

Known growth factors that encourage blood vessel formation and remodeling (angiogenic) and the regulators of those factors (antiangiogenic) significantly affect uteroplacental vascular development (20).

Vasculogenesis and angiogenesis are both critical processes in developing blood vessels, but they are distinctly different: vasculogenesis creates the original blood vessels, while angiogenesis acts upon existing blood vessels to make more vascular structures in response to conditions (21). Both are necessary in the developing placenta to meet the increased local demand for effective transport of oxygen, nutrients, and wastes via blood vessels. The placenta grows rapidly but also must be able to adjust to growing and changing demands over the course of gestation. Without sufficient development of uteroplacental arteries and fetoplacental capillaries, fetal growth is restricted (22, 23).

Vasculogenesis is defined as the differentiation of precursor cells into endothelial cells to form a de novo primitive vascular network. Vasculogenesis occurs early in gestation in human placental villi with angiogenesis following later (24). Vasculogenesis occurs at the fetomaternal interface, but also causes vascular changes in the uterine basal arteries in the first month of pregnancy (21). Vasculogenesis has three principle steps: the recruitment and development of hemangioblasts, the formation of hemangioblastic cords, and the formation of lumens to create endothelial tubes (25). Recruitment and development of progenitor cells occurs primarily through vascular endothelial growth factor (VEGF) signaling to the VEGFR-2 receptor. Fibroblastic growth factor 2 (FGF2) interacting with its receptor FGFR causes vasculogenesis to form cords of hemangioblastic progenitor cells. In addition to the VEGFR-2 receptor, VEGF also

begins to interact with VEGFR-1 (also known as Flt1) in order to form endothelial tube structures, the first blood vessels (22).

Angiogenesis, the growth and regulation of new capillaries from pre-existing blood vessels, follows vasculogenesis. Angiogenesis can be classified as non-branching or branching angiogenesis, where either blood vessels elongate or divide into highly branched capillary networks. In non-branching angiogenesis, existing endothelial tubes created by vasculogenesis can be lengthened either at the ends of the vessels, by proliferation, or by incorporation. Branching angiogenesis can occur by partitioning an existing tube longitudinally or by sprouting new side branches from an existing tube (26). VEGF binds to both VEGFR-1 and VEGFR-2 in angiogenesis; following branching or extension, vascular growth factor angiopoeitin-1 (Ang-1) recruits pericytes for the establishment and maintenance of the vessel walls (27). Increasing VEGF and placental growth factor (PLGF) increases both vessel number through branching angiogenesis and vascular permeability (28, 29). A balance of branching and non-branching angiogenesis is required for normal uteroplacental vascular growth: too little or too much branching may result in aberrant uteroplacental blood flow leading to placental damage and FGR.

Pregnancy-Induced Uterine Angiogenesis

Uterine spiral arteries are the most angiogenic vessels in the human body. During human female reproductive years these vessels are grown and shed each menstrual cycle. In pregnancy these vessels are stimulated to dilate dramatically creating funnel-like structures lined by invasive placental cells, which fix into widely open lumens that are not responsive to vasoconstrictors, essentially taking control of blood flow to the placenta (19). However, new data suggest the upstream radial arteries in the muscular wall of the

uterus may actually regulate the volume of blood flow to the placenta, while the dilated spiral arteries control the rate of flow (30, 31) The importance of uterine vascular angiogenesis is highlighted in mice (30, 32, 33). Mice do not have spiral arteries before they are pregnant. Unlike human females who grow spiral arteries each month of their menstrual cycle, female mice only grow them during pregnancy. A mouse gestation is approximately 19 days long. They grow spiral arteries off of the radial arteries from days 6-12 (33, 34). This angiogenic process followed by appropriate pruning creates 3-5 spiral artery branches from each radial artery in mice. It only occurs in the placental bed, which supports the idea that placental paracrine signaling, or an implantation wound healing process, is required for proper uterine angiogenesis. Notably, unlike humans, mouse placentas are not particularly invasive into the uterus and placental invasion does not appear to play a role in murine spiral artery remodeling; growth and remodeling is complete before the mouse placenta begins invading the uterine metrial triangle (35). A comparison of human and murine vascular structures is presented in Figure 1.1.

The mechanisms regulating murine spiral artery angiogenesis are beginning to be understood. It is currently thought that this process is largely dependent on the presence of placental implantation and activation of the maternal immune system in the metrial triangle (36). Specifically, maternal uterine natural killer (uNK) cell activation seems to play an essential role in proper spiral artery angiogenesis and uteroplacental blood flow.

uNK cells are abundant in the human placental bed (decidua basalis) (37). They are also abundant in the mouse metrial triangle (38). These specialized maternal immune cells in the uterus are unlike NK cells elsewhere in the body and do not attack and kill their targets (e.g. tumors, infections, fetal placenta). Instead, uNK cells are responsible

for producing vascular endothelial growth factor (VEGF), which is a key regulator of spiral artery angiogenesis (39, 40).

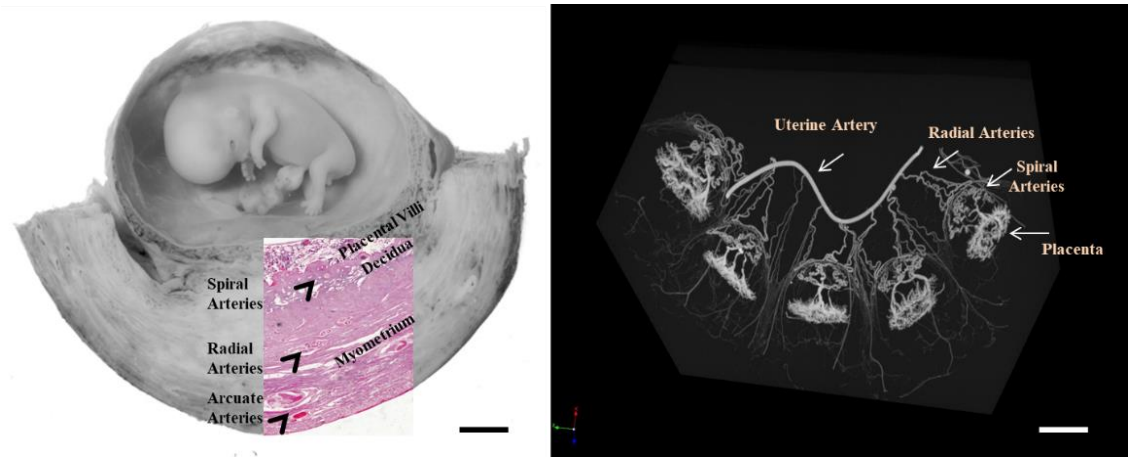

Figure 1.1. Uteroplacental arteries in human and mouse undergo angiogenesis and remodeling during pregnancy. In humans (seen at 10 weeks on the left), the decidual spiral arteries are already in place before implantation, but they grow by dilating in the first trimester. The upstream radial and arcuate arteries also grow longer and dilate during pregnancy. Mice (multiple uteroplacental units in a single gestation at d16.5, near term, on the right) grow their spiral arteries *de novo* during pregnancy from the radial arteries and comprise most of the angiogenic response to placentation. Scale bar is 1.0 cm. Human image courtesy of the *Centre for Trophoblast Research*; microCT scan courtesy of Dr. Monique Rennie.

Angiogenic/Anti-Angiogenic Factors: VEGF, PLGF, and sFlt1

A major critical molecular player in angiogenesis, vascular endothelial growth factor (VEGF) binds its receptor, cell-surface tyrosine kinase VEGFRs, to induce highly effective proliferation of endothelial cells, stimulate new blood vessel formation, and increase cellular permeability (41). The most abundant VEGF form, VEGF-A, is secreted by decidual cells containing high amounts of the progesterone receptor (PR). Ovarian steroid secretion activates PR and plays an important part in decidua formation early in pregnancy. In turn, VEGF-A binds VEGFR2 to signal a number or blood vessel proliferative and permeability signals; this binding scenario is particularly crucial in uterine angiogenesis and successful implantation (42). VEGFR2 shares many of the same signaling pathways as Ang II type I receptors, using phospholipase C production of

inositol triphosphate to stimulate protein kinase C activity and increase calcium levels (43). PLGF, structurally similar to VEGF, also binds VEGF receptor 1 (VEGFR-1, also known as Flt1). Like VEGF and Ang II, PLGF stimulates migratory and growth pathways via MAPK, but does not use PLC in order to activate those functions (44).

Soluble fms-like tyrosine kinase-1 (sFlt1), a splice variant of VEGFR-1/Flt1, is an antiangiogenic factor. sFlt1 has been observed at high levels in women with preeclampsia, even very early in pregnancy (45). Similar to Flt1, but without the cytoplasmic and transmembrane domains, sFlt1 binds free VEGF and PLGF, decreasing their efficacy on endothelial vascular formation and remodeling (10, 46). sFlt1 is suspected to be sensitive to eNOS activity: the absence of eNOS may prevent sFlt1 from forming entirely (47). This sensitivity to oxygen species may also support the claim that sFlt1 is released from the placenta in response to hypoxic conditions (48). By sequestering angiogenic factors VEGF and PLGF, sFlt1 inhibits proper uteroplacental vascular development.

Immune Responses and uNKs

Another piece of the FGR pathology puzzle surrounding vascular growth involves the multitude of immune and antibody responses which have a significant effect on growth and proliferation pathway signaling. Produced by CD4+ T cells, CD8+ T cells, and other immune and allergy response cells, cytokines can largely be divided into two families: type 1 (Th1-like), which favor immune response, and type 2 (Th2-like), which exhibit an antibody response. Type 1 cytokines include IFN-γ, TFNα, and interleukin(IL)-2 and 12, while the Type 2 family includes IL-4, IL-10, and TGF-β (49–51). Historically, type 1 cytokines have been regarded as detrimental to gestation and that

Th1 immunity to trophoblast cells results in loss of pregnancy, where a higher ratio of type 2 cytokines and Th2 trophoblastic immunity is associated with successful pregnancy (52–54). Cytokines help maintain a valuable balance in inflammatory reactions and cell survival, remodeling spiral arteries through both cell survival and apoptotic signals (55).

Some recent research argues that the Th1/Th2 ratio is limiting in terms of pregnancy prognosis, because it does not take into account the action of uNK cells (56). uNKs play a number of roles in the vascular growth of the early placenta, from producing growth factors to disrupting vascular smooth muscle cells, both actions critical to spiral artery remodeling (57). uNKs produce VEGF and Ang-1 early in pregnancy. The levels of these growth factors taper off by the end of the first trimester in humans (39). This agrees with an early activation of uNKs seen in mice, with a switching from an inactive-to-active state happening between GD6.5 and 8.5 in normal murine pregnancy, and uNKs predominantly conjugating with Th2-type CD8+ immune cells, indicating early gestation as a critical time for leukocyte interactions and immune regulation (58). uNK cells are extremely prevalent in early gestation, with 65-70% of the total lymphoid cell population represented by uNKs; this number decreases by mid-gestation and by term, they are completely absent (37, 59).

Although our knowledge of the pathogenesis of fetal growth restriction is incomplete, the growing evidence indicates that a delicate balance between angiogenic and antiangiogenic factors must be maintained to provide both ample and correctly remodeled uteroplacental blood vessels that meet fetal demands yet do not exceed mother’s ability to supply. Understanding these molecular influences on placental

structural development will allow us to develop better preventative and treatment measures to protect mother's health and the fetus' development to birth and beyond.

Fetal Sex Effects

A lingering question in uteroplacental biology is whether fetal sex may play a role in this process. Again, the mouse serves as an excellent model because each gestation produces multiple pups (usually 8-12/litter) and a mixture of fetal sexes that may be correlated with their corresponding uteroplacental vascular architecture. Fetal sex is thought to be an important covariate because outcomes for males in cases of placental insufficiency are much worse than their female siblings—in animal models and in humans (60–63). Males are more likely to be negatively impacted in utero by detrimental effects like maternal smoking and malnutrition (64, 65). They are more likely to suffer from developmental programming of adult onset diseases like cardiovascular disease and they have a shortened lifespan compared to FGR females (15, 16, 66–69).

Male offspring have a higher birthweight relative to placental weight (reduced fetal:placental ratio) than matched female controls, which suggests males may sacrifice placental development in favor of fetal development (63). Since the placenta is the bridge between maternal supply and fetal demand, sacrificing infrastructure in favor of short-term weight gains turns out to be a "dangerous" approach. The molecular mechanisms behind these observed effects and the degree to which male fetal sex affects uteroplacental vasculature have not been studied.

Angiotensinogen and Placental Insufficiency

Angiotensinogen (AGT), a member of the serpin (serine protease inhibitor) protein family, is the precursor and rate limiting substrate. Unlike many members of this

family, angiotensinogen does not inhibit serine proteolytic activity (70). AGT is primarily produced and released into plasma circulation by hepatocytes and is principally cleaved by enzymes in the kidney or lung to achieve a functional form (71). Angiotensinogen is comprised of a 453-amino acid chain, which is first cleaved by renin in response to decreased sodium concentration or blood pressure. This produces a 10-amino acid chain, angiotensin I (Ang I). Two terminal residues are cleaved from Ang I by angiotensin-converting enzyme (ACE) to create the 8-amino acid long functional form of angiotensinogen, angiotensin II (Ang II) (72). Ang I may be additionally cleaved by chymase, a serine protease produced by placental villous syncytiotrophoblasts, and thereby may also contribute to increased Ang II levels (73). Ang II affects both renal

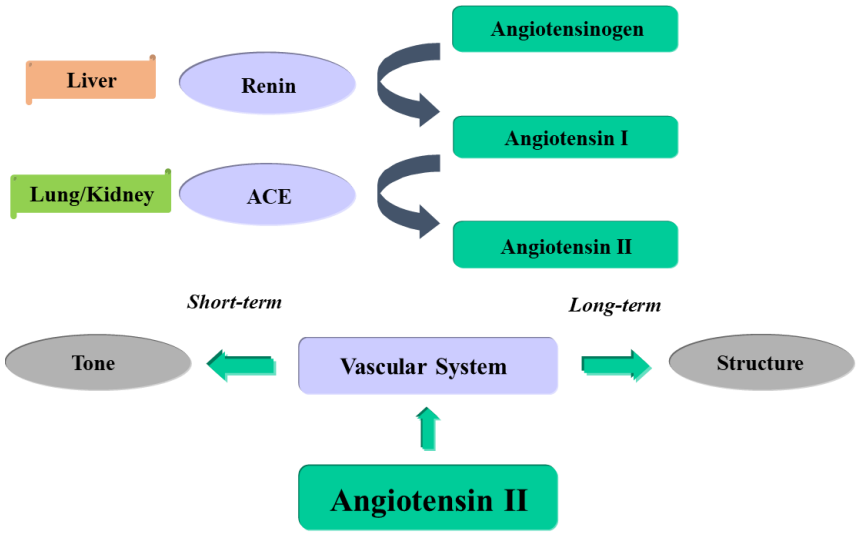

Figure 1.2. Systemic and tissue-specific renin-angiotensin systems.

function and blood pressure by stimulating both short and long-term vascular responses (74, 75). A summary of this process is illustrated in Figure 1.2.

Ang II type-I (AT1) receptors are G-protein coupled receptors that control blood pressure and volume by producing more vascular smooth muscle cells, inducing their

contraction, and decreasing renal blood flow (76). AT1 achieves this effect by stimulating phospholipase C (PLC), sodium-hydrogen antiporters, and water reabsorption. The primary role of PLC is hydrolyzing phosphatidylinositol 4,5-bisphosphate (IP2) to form inositol trisphosphate (IP3), which increases cellular concentrations of calcium. Calcium is crucial to vascular smooth muscle cell proliferation and contraction, the latter of which causes vasoconstriction by causing smooth muscle cells to contract around blood vessels (77). Via the formation of IP3, PLC also participates in the activation of protein kinase C (PKC), a phosphorylation cascade member responsible for activating transcription, permeability, and further cellular proliferation vital to vascular development (78). Other downstream effects of AT1 signaling include formation of reactive oxygen species (ROS) that can activate the mitogen-activated protein kinases (MAPK) to uncouple endothelial nitric oxide synthase (eNOS), a protein that participates in vasodilation as well as cell permeability (47, 79). Notably, angiotensin receptor 2 (AT2) is not highly expressed in the placenta, but is increased in the fetal kidney (73). It is possible that the observed increase of Ang II in growth-restricted pregnancies could therefore be linked to later onset adult renal dysfunction in FGR offspring.

Although Ang II is required for blood vessel growth and remodeling, excessive Ang II levels have a negative effect on placental development. A mutation in the human angiotensinogen promoter A(-6) is known to cause a 20% increase in circulating AGT levels. An elevation in AGT levels would cause similarly increased Ang II, and therefore, abnormal remodeling effects (80, 81). High calcium levels produced by Ang II stimulation of IP3 activity can also cause extreme smooth muscle cell contraction around blood vessels, leading to detrimental vasoconstriction (77). High Ang II concentrations

may negatively affect blood vessel growth by competitively inhibiting the angiopoietin receptor TIE-2, which acts as a critical receptor tyrosine kinase in blood vessel proliferation signaling pathways for vascular maturation in the endometrium (82).

Ang II can stimulate vascular remodeling through additional angiogenic growth-related receptors, primarily by transactivation through AT1. One of these, epithelial growth factor receptor (EGFR), regulates migration and hypertrophy of vascular smooth muscle cells when AT1 is bound to Ang II. EGFR has been reported to require AT1 receptor phosphorylation for activation for some functions (83). Ang II also stimulates the platelet-derived growth factor receptor (PDGFR) and insulin-like growth factor-1 receptor (IGF-1R) through transactivation by the AT1 receptor (84). PDGFR and IGF-1R both stimulate downstream ERK (a member of the MAPK cascade family) to induce fibrosis and hypertrophy, though the exact mechanism by which Ang II induces this action is unknown (85). Fibroblastic growth factor also regulates angiogenic changes, but it functions through a distinct MAPK pathway (85).

Maternal Risk Factors for Placental Insufficiency and Variant AGT Expression

Several influences have been previously identified as maternal risk factors for placental insufficiency: diet and BMI (86–88), altitude and environmental quality (89, 90), sick maternal vessels and failed maternal response (91–93), but we have focused on a genetic cause: an increase in maternal angiotensinogen. Placental insufficiency has been associated with a common variant of angiotensinogen, a substitution at angiotensinogen residue 235 methionine (M235) to threonine (T235); this mutation, which is tightly linked to a substitution of an adenine for a guanine in the angiotensinogen promoter region (G(-6)A), causes a 20% elevation in expression of angiotensinogen and, in turn,

angiotensin II (94, 95). M235 is considered a “protective” state. About 70% of the Caucasian population carries the protective M235 allele, while only about 2% of Central Africans and 15% of Asians do (96). T235 has specifically been cited as a genetic cause of placental insufficiency due to its reducing effect on the efficacy and number of uterine spiral arteries and increase in maternal hypertension (97, 98).

Working Hypothesis

We hypothesize that placental insufficiency leading to fetal growth restriction is a multifactorial disease process involving both maternal and fetal risk factors in mice. A summary of these known and hypothesized influences is shown in Figure 1.3.

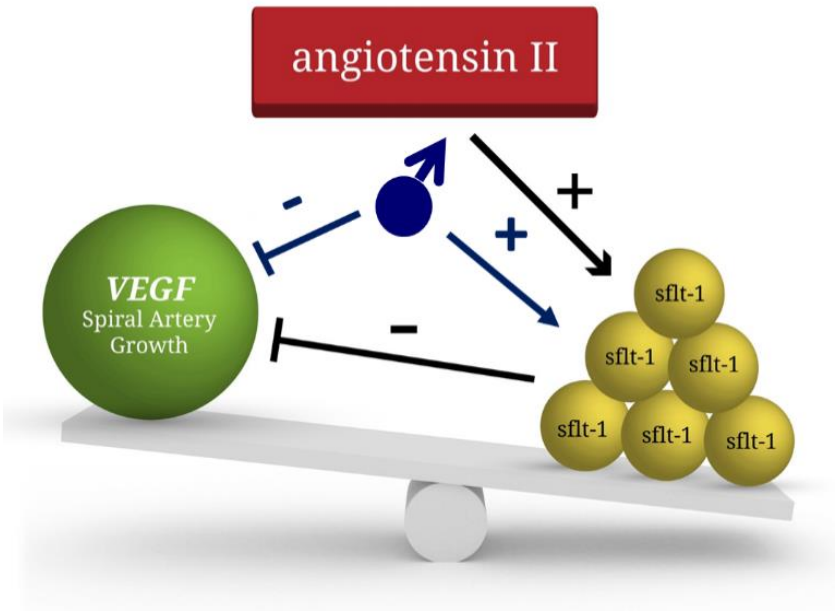

Figure 1.3. Maternal AGT genotype and fetal sex effects on angiogenic levels.

Mouse Model of Elevated Maternal Angiotensinogen Expression

To study the effects of elevated maternal AGT expression on uterine spiral artery angiogenesis and fetoplacental outcomes, we have studied a commercially available gene titration transgenic (TG) mouse model that has three copies of the mouse angiotensinogen

(AGT) gene in a C57BL/6J background (99, 100). The extra copy of the murine AGT gene leads to a 1.2-fold increase in circulating AGT compared with C57BL/6J wild-type (WT) two copy controls. This variant was made to mimic the common human AGT promoter variant (A-6G) associated with preeclampsia, FGR, and abnormal uterine spiral artery remodeling (80, 99, 101). This "physiologic" 20% increase in circulating AGT is associated with increased levels of sFlt1, which is a decoy receptor for VEGF and acts as an antiangiogenic sequestration mechanism effectively decreasing available VEGF and blocking angiogenesis (42).

A relatively early observation by our group leading to our working hypothesis was that pups from TG dams were growth restricted at both mouse GD16 (near-term; mouse gestation is 19 days) and at birth (Figure 1.4).

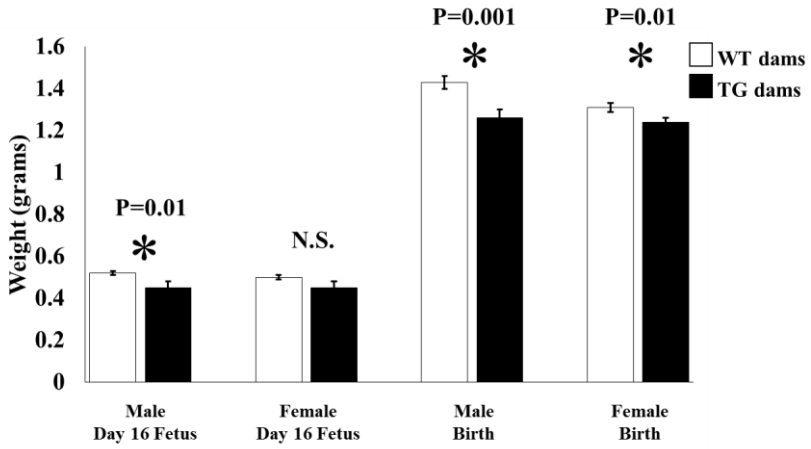

Figure 1.4. Relative fetal and birthweights of WT and TG dams. Males from TG dams are smaller than WT controls at day 16 gestation and birth, females only smaller at birth.

Because this mouse model had FGR, like human pregnancies with this AGT genotype, we decided to address three questions for this doctoral thesis. First, what is the impact of the maternal AGT genotype on pregnancy, including the effects on maternal

blood pressure, kidney function, uterine spiral artery growth, uteroplacental blood flow, placental damage, and fetal growth? Second, are there relationships between fetal sex and uteroplacental vascular growth mediators such as uNK activity, maternal spiral artery growth, placental vascular growth, placental transcriptomics, and placental nutrient delivery? Finally, do FGR progeny from TG dams show signs of developmental programming of adult onset disease, specifically cardiovascular disease (as seen in other models (102-105)), and what is the mechanism?

NOTE: All references for each chapter are provided at the end of this dissertation.

Chapter 2

Vascular Endothelial Growth Factor Gene Delivery to Uterine Spiral Arteries Rescues Pregnancy-induced Angiogenesis and Prevents Fetal Growth Restriction in Transgenic Mouse Model of Placental Insufficiency

Abstract

Pregnancy complications like gestational hypertension and fetal growth restriction are common and associated with increased maternal and neonatal morbidity and mortality. The causes are multifactorial, but abnormal uterine spiral artery remodeling and aberrant blood flow to the placenta are thought to be significant contributors. Spiral arteries undergo a monthly angiogenic process in menstruating women, but they are grown *de novo* in mice for the purpose of mediating blood flow to the fetal-placental unit. The molecular mechanisms regulating this process are not well understood, but mediators like vascular endothelial growth factor (VEGF), soluble fms-like tyrosine kinase-1 (sflt-1), and angiotensin II may play important roles. To better understand the relationship between VEGF, sflt-1, angiotensin II, and pregnancy outcomes, we used ultrasound-mediated microbubble conjugated VEGF gene delivery to target uterine endothelial cells in a previously characterized transgenic (TG) mouse model expressing 1.2-fold more angiotensinogen (AGT) than wild-type female controls. Luciferase gene transfer served as a "sham" negative control. We observed: 1) An isolated 20% increase in maternal AGT expression in TG dams is sufficient to cause increased angiotensin II production, maternal gestational hypertension, and fetal growth restriction; 2) TG dams have a reduced VEGF/sflt-1 ratio; 3) uterine spiral artery angiogenesis is reduced and blood flow

to the placenta is abnormal with signs of placental damage; 4) VEGF gene delivery to uterine blood vessels before mating leads to increased VEGF endothelial expression during early gestation (days 3-7.5), which rescues spiral artery angiogenesis and prevents fetal growth restriction. We conclude the AGT/VEGF axis plays a key role in regulating uterine angiogenesis and blood flow.

Introduction

Investigators use the term "placental insufficiency" to describe abnormal uteroplacental nutrient transport, placental damage, and associated pregnancy complications like gestational hypertension (preeclampsia), fetal growth restriction (FGR), and developmental programming effects (1-4). Although the underlying causes of placental insufficiency remain poorly understood, abnormal pregnancy-induced uterine spiral artery remodeling is one well-accepted mechanism (5-11).

Pregnancy-induced changes in uterine spiral artery remodeling may be recognized as early as the first trimester of pregnancy (7) with significant variation among women reported at term (6). The cause of this variation is uncertain, but it may begin with an imbalance in maternal angiogenic factors (1, 2, 12-15), shallow placental invasion (9), or both (16). Multiple studies support the hypothesis that angiogenic factors like vascular endothelial growth factor (VEGF) are essential for normal spiral artery growth and dilation during pregnancy (14, 15). Moreover, women with placental insufficiency are more likely to show abnormally increased placental production of the soluble VEGF receptor (sflt-1), which may inhibit VEGF activity (1, 2). The reason that human

placentas release more sflt-1 in pregnancies complicated by preeclampsia is not entirely clear, but the placenta is thought to be the primary source (2).

We hypothesize that elevated maternal angiotensin II activity may play a role in stimulating sflt-1 production during pregnancy and inhibiting normal spiral artery remodeling. Molecular variants of the maternal angiotensinogen (AGT) gene that cause increased angiotensin II availability are associated with preeclampsia and FGR (17-22). Similarly, maternal auto-antibodies that activate the angiotensin II type 1 (AT1) receptor are also at increased risk for preeclampsia and fundamental alterations in human uteroplacental vasculature (23). We suspect this may be because angiotensin II directly affects spiral artery remodeling (7, 24), or indirectly inhibits pregnancy-induced spiral artery growth by stimulating placental sflt-1 production (25).

To isolate the effects of elevated maternal angiotensin II production on sflt-1 production, spiral artery remodeling, and uteroplacental blood flow, we studied a gene-titration transgenic (TG) mouse model (26). This TG model has three copies of the murine AGT gene, which simulate the 20% increase in maternal AGT expression observed in women homozygous for the AGT A(-6)G promoter variant associated with preeclampsia and FGR (17, 22). In TG males, this construct leads to hypertension (26). In TG females, we have shown that they do not expand their blood volume during pregnancy (27), similar to women with preeclampsia (28). Unlike other TG models of placental insufficiency, which use genetic knockouts (29), or use over-expressed human genes (30), this 3-copy gene-titration model employs mouse AGT expressed at physiologic levels, which may more accurately reflect the underlying pathophysiology of placental insufficiency in women.

To better understand the relationship between VEGF, sflt-1, angiotensin II, and pregnancy outcomes, we used ultrasound-mediated microbubble conjugated VEGF or firefly *Luciferase* gene delivery to target uterine endothelial cells as previously described by our group to delivery VEGF to ischemic limbs in mice (31).

Methods

Murine Angiotensinogen Gene Titration Transgenic Model: Commercially available 3-copy transgenic (TG) mice (B6.129P2-Tg (AGTdup) 1Unc/J; The Jackson Laboratory, Bar Harbor, Maine) were backcrossed into C57BL/6J wild-type (WT controls) for at least ten generations using an IACUC approved protocol (eIACUC IS080). To control for potential "generational effects," all TG females in this study were "*de novo*" from WT dams mated with TG males. Mice were genotyped using a published PCR-based protocol (32) targeting the mouse AGT allele D8MIT56 (rs264414580). Systemic AGT expression was approximated by quantitative real-time RT-PCR using cDNA from fresh livers as described (26) and all experiments were performed in triplicate normalized to β-actin. Timed matings were performed and checked for vaginal plugs, which we designated as embryonic day 0.5 (33), with delivery confirmed at e19.5.

Maternal Tissue-Specific Angiotensin II Measurements: Ang II peptide with and without C-terminal [$^{13}C^{15}N$] stable isotope-labeling was synthesized (Thermo Fisher Scientific, Waltham, MA) as a control for LC-SRM analysis by the *Pacific Northwest National Laboratory*. Virgin and maternal kidney and uterine metrial triangle (e10.5) angiotensin II levels from TG and WT mice were measured using extracts that were spiked with 100 fmol heavy-isotope labeled Ang II, then loaded onto a reverse-phase C18 column on a

Agilent 1200 HPLC system (Agilent Technologies, Santa Clara, CA) for Ang II peptide enrichment. All sample fractions were analyzed using a nanoACQUITY UPLC system coupled online to a TSQ Vantage triple quadrupole mass spectrometer. The light-to-heavy peak area ratio (L/H) of the most abundant transition (349.52/371.20 and 352.86/371.20) was used for quantification of endogenous Ang II in each sample.

Maternal Serum sflt-1 Measurements: Maternal serum sflt-1 levels were measured using published protocols (29) and a commercially available ELISA (R&D Systems, Minneapolis, MN). Measurements were performed in triplicate from four-six animals from separate litters per group. Data were reported in pg /ml within the dynamic range of the assay compared with kit controls.

Mean Arterial Blood Pressure by Radio-Telemetry: Adult (11-13 weeks) virgin female mice were subcutaneously implanted with TA11PA-C10 radio transmitters (Data Sciences International, St. Paul, MN) catheterized into the common carotid artery. Following one week of recovery, virgin baseline mean arterial pressure (MAP) was reported as the continuous average over three days. Six WT and six TG dams were then mated with WT males and MAP was recorded from day 2.5 to delivery (day 19.5).

Renal Function and Glomerular Electron Microscopy: Virgin mice were trained in metabolic cages for ten days. Virgin blood samples (50ul) and 24 hour urine collections were then obtained for three days before timed mating. These pregnant mice were then housed in separate metabolic cages from day 5.5 to delivery. Blood samples (50 ul) and 24 hour urine collections were taken at day 10.5 and day 18.5 for analysis. All e18.5 pregnant females were euthanized and a portion of their kidneys were fixed in 2.5% glutaraldehyde for electron microscopy and examined for glomerular endotheliosis (34).

Urinary albumin was measured using a mouse specific ELISA kit (EXOCELL, Inc). Urinary and serum creatinine levels were measured by HPLC (35). 24 hour urinary albumin secretion was reported relative to urinary creatinine (ug/mg/day). Creatinine clearance was calculated as the concentration of urinary creatinine (mg/dl) x urine flow (ml/min) /plasma creatinine (mg/dl) to yield CrCl in mls/minute with an expected range of 0.125-0.250 for virgin and pregnant mice, respectively. Data were reported from virgin and day 18.5 WT and TG mice (n=6 animals per group.

Contrast-Enhanced Three-Dimensional MicroCT Imaging of Spiral Arteries: Four WT and four TG litters at day 16.5 were tested using published methods (38). In brief, pregnant mice were anesthetized with isoflurane and heparinized (0.05 ml at 100 IU/ml). The abdomen was opened and a catheter was introduced into the descending aorta. An infusion pump was used to slowly perfuse the lower body vasculature with heparinized xylocaine (0.05 ml heparin at 100IU/ml in 2% xylocaine) to clear the vasculature of blood; then yellow contrast agent (Microfil HV-122, Flow Tech Inc., Carver, MA) was infused until it filled the exposed uteroplacental arterial circulations (38). After infusion, the system was tied off; the uterus was removed, fixed in formalin, and mounted in agarose for micro-CT scanning. 3-dimensional datasets were acquired using a Quantum FX micro-CT scanner (Caliper Life Sciences). Vascular surface renderings were generated using the *Amira* software package (Visage Imaging, San Diego, California) and three representative uteroplacental units from each litter were used to measure the number, length, and coiling of the spiral arteries and central canals. Data were reported as the average per litter to generate a mean +/- SEM for each group.

Modeling Uteroplacental Blood Flow with Spiral Artery Architecture: Quantitative structural data was used to parameterize two computational models of uterine hemodynamics at d16.5. The first model represented the uterine vasculature from the uterine artery to the level of the labyrinth, as resistance vessels acting in series and parallel. The model incorporated spiral artery number, length, lumen diameters, and dimensions of the uterine artery, radial arteries and canals as described (38). The resistance of each individual vessel was defined using Poiseuille's Law ($R=8\mu L/\pi r^4$, where $\mu=3.36x10^{-3}$ Pa.s is the viscosity of blood, L is vessel length and r is vessel radius). The conductivity of blood into the labyrinth was defined as a function of capillary density from stereology and blood flow in the labyrinth was modelled as a porous medium. The second model used 3D segmentations of the vascular tree in individual WT and TG dams to define a vascular geometry for from the uterine artery to the labyrinth, with the vasculature truncated at the first branch of the labyrinth capillaries with diameter < 300 μm as labyrinth capillaries become indistinguishable from one another in imaging beyond this level. Blood flow in the 3D model was simulated using incompressible Navier-Stokes equations using ANSYS-CFX (Ansys Inc., Version 17.2) at the walls of the arteries no-slip boundary conditions were applied. Blood pressure at the uterine artery was predicted and compared with collected telemetry data described above. Distribution of blood flow across models was also compared to mean empirically collected microbubble ultrasound measurements of uteroplacental blood flow.

Uteroplacental Blood Flow by Microbubble-Enhanced Ultrasound: Uteroplacental blood flow was measured at day 16.5 in ten WT and six TG virgin females after timed mating using published methods by our group (36, 37). Briefly, sterile lipid microbubbles (5%

Definity [Lantheus Medical Imaging, Billerica, MA] dissolved in 0.9% saline) were continuously infused into the jugular vein. Data for each placenta were acquired using a Sequoia 512 ultrasound device (Siemens Medical Systems, Mountain View, CA) equipped with a linear-array (15L8) transducer. Flow rates and volumes were determined by microbubble destruction followed by replenishment kinetics. The acoustic beam was centered over the pelvis and the microbubbles within the beam path were destroyed by a brief (2 second) acoustic burst (1.9 mechanical index). Vascular perfusion was then estimated for the region of interest (ROI: i.e. uterine wall or placenta) by fitting replenishment data to $Intensity = A(1\text{-}e^{\beta\tau})$ where the re-entry rate constant (β) reflects the flux rate and is proportional to vascular conductance; and, the video intensity plateau (*A*) represents microvascular blood volume. Total microvascular blood flow was calculated as the product of *A* and β. Spiral artery transit times were calculated from the time they reappeared in the placenta relative to the uterine wall.

Umbilical Cord Artery Doppler: Timed gestations were used to measure fetal umbilical artery peak velocity at e16.5 by Doppler ultrasound using a *Vevo 660* (Visualsonics [SonoSite, Inc.], Toronto, Canada) in anesthetized pregnant mice (n=4 WT and n=4 TG dams; testing three pups per litter). Absent end-diastolic flow may be normally observed in WT pregnancies before day 15.5 (33), therefore all gestational day 16.5 results were restricted to the eight deliveries confirmed at e19.5. Waveforms were analyzed while blinded to maternal genotype and reported as +/- absent end-diastolic flow for each fetus (39).

Placental sflt-1, Heat Shock Protein 70 Expression, and Ultrastructure: Whole placentas dissected from the uterine wall were trimmed from four WT and four TG dams at day

18.5. Three placentas per litter were selected from both uterine horns for total protein extraction and two placentas from distal horns per litter were fixed in 2.5% glutaraldehyde for electron microscopy to evaluate for ultrastructural features of placental damage (40). Total placental protein was quantitated by routine BCA. Sflt-1 as measured as described above and reported as ng/mg total protein; heat shock protein 70 (HSP70) expression was assayed by Western blot (41) and measured by densitometry. Results were reported as the average per litter +/- SEM per group.

Microbubble VEGF and Luciferase Conjugated Gene Delivery to Uterine Vasculature: VEGF/luciferase plasmid cDNA charge-coupled to microbubbles were injected into the maternal circulation and targeted to regional endothelial cells as previously described by our group (31). Briefly, 1 $x10^9$ microbubbles coupled to 500 ug of cDNA were infused into the jugular vein. The uterus was visualized by ultrasound and pulsed at 0.6 MPa (Sonos 5500, Philips, MA) specifically in the uterine plane, which was highlighted by also injecting non-conjugated bubbles via catheter into the uterus. Transfected nulligravida TG and WT mice (six per group) were then mated with WT males and dated from the time of vaginal plug noting the number of days post-transfection. Mice were reliably plugged within 48 hours of transfection and similar to prior studies in male mice (31), pilot studies showed that luciferase/VEGF expression peaked at 3 days post transfection and persisted for 7-10 days in virgin uteri used to establish time course.

Statistical Analysis: Continuous data were analyzed using RS/1 software (Domain Manufacturing Corp). Groups were compared using the Kruskal-Wallis one-way ANOVA, or Mann-Whitney U test with post-hoc corrections. End-diastolic arterial blood flow waveforms (yes or no) in WT and TG litters were compared by Fisher's exact test.

Results

Elevated Maternal AGT Expression Leads to Hypertension and Fetal Growth Restriction

The genetic difference between TG and WT dams was the presence of the AGTdup construct in an otherwise shared black 6 background (3-copies versus 2-copies of the murine AGT gene, respectively). Breeding females were all 11-13 weeks old, nulligravida, and they were all bred with WT males. TG females expressed approximately 20% more AGT than WT controls (Figure 2.1A), similar to prior reports (26). Tissue-specific angiotensin II levels in the maternal kidneys and maternal metrial triangles were also increased in TG dams with 5-fold differences in the maternal kidneys and 2-fold differences in the uterine metrial triangles (Figure 2.1B-D).

TG dams had significantly elevated serum sflt-1 levels (Figure 2.1E), but this increase (30 ng/ml) was insufficient to cause glomerular endotheliosis or proteinuria (data not shown). WT controls increased their creatinine clearance by 20% by term (0.25 ml/min versus 0.20 ml/min in virgin females) while TG dams did not (0.15 mls/min) similar to women with preeclampsia (42). Total placental sflt-1 protein levels were 10% greater in TG dams compared with controls (62 +/- 13 ng/mg versus 56 +/- 4 ng/mg, respectively, although this difference did not achieve statistical significance).

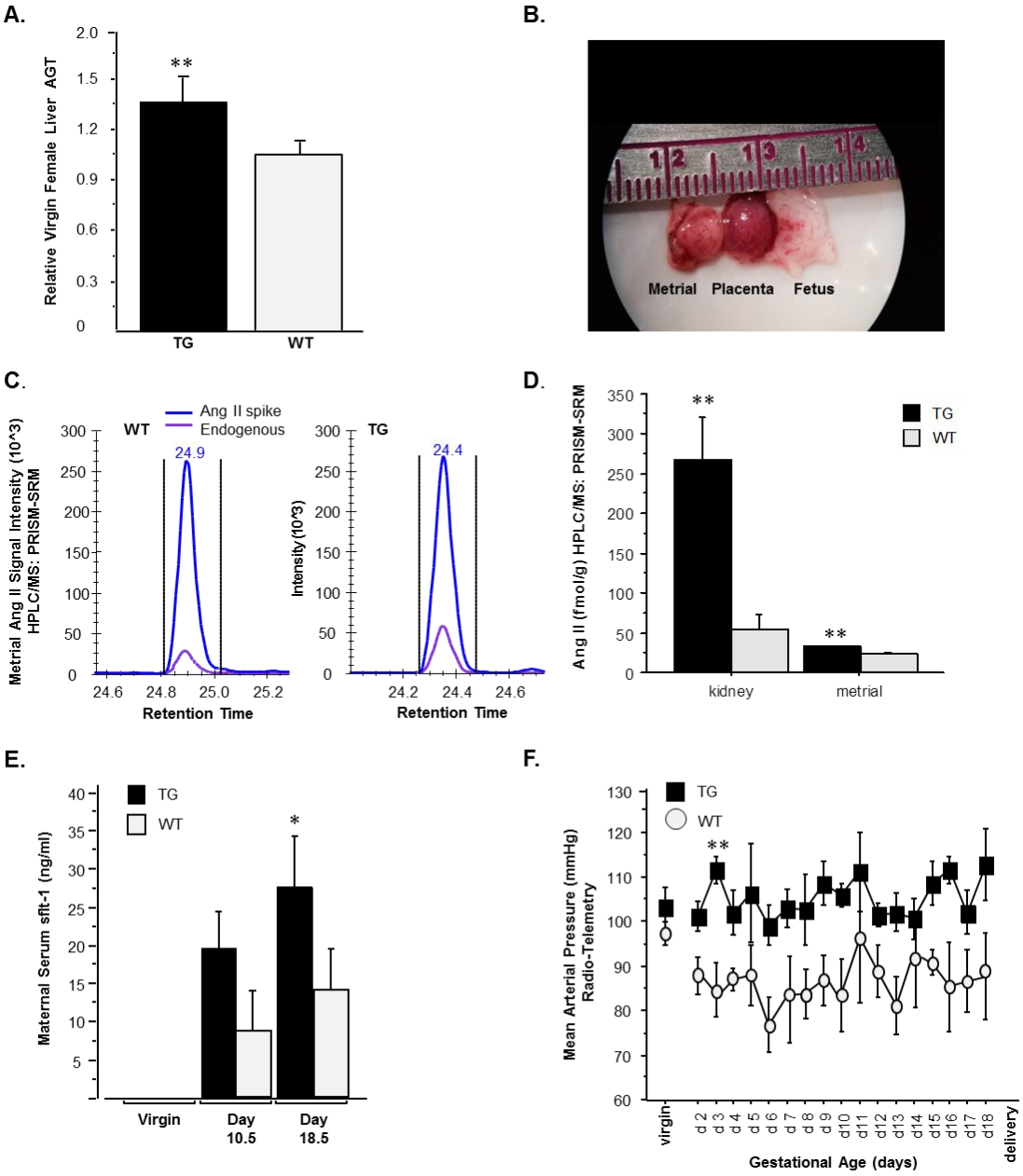

Figure 2.1. Elevated systemic maternal AGT expression leads to increased angiotensin II, elevated sflt-1, and maternal hypertension. A) AGTdup 3-copy transgenic (TG) mice backcrossed into C57BL/6J wild-type (WT) for more than ten generations show slightly increased liver AGT expression compared with controls (~20% increase). B) Microdissection of maternal uterine placental bed tissue (metrial triangle) away from placenta and fetus at mid-gestation for angiotensin II measurements by HPLC/MS (C) shows increased angiotensin II in metrial tissue and maternal kidneys of TG dams compared with WT controls (D). Maternal sflt-1 levels are elevated (E) and maternal blood pressure is elevated in TG dams. *P<0.05; **P<0.01.

Radio-telemetry revealed no difference in mean arterial pressure (MAP) between virgin TG and WT females, but during pregnancy TG dams failed to undergo normal drops in blood pressure, unlike WT controls (Figure 2.1F). Relatively elevated MAP could be reliably detected as early as e3.5 and persisted through gestation.

Fetal Growth Restriction

Fetal weights at day 16 were lower in TG dams compared with age-matched WT controls (Table 2.1). Placental weight was not decreased in TG dams (Table 2.1); therefore, the overall placental efficiency (fetal weight/placental weight) was reduced in their progeny. Newborn pups from TG dams were 7-10% smaller than WT controls.

Table 2.1. Fetal Growth Restriction in Maternal Angiotensinogen Overexpression Model

	Wild-Type (WT) (n=17)	Transgenic (TG) (n=15)	P-value
Litter size	8.1 +/- 0.16 (range 7-9)	6.5 +/- 0.75 (range 3-10)	P=0.29
Day 16.5 Progeny Fetal Weight	0.51 grams +/- 0.01	0.45 grams +/- 0.02	P=0.01
Placental Weight	0.088 grams +/- 0.002	0.095 grams +/- 0.002	P=0.03
Fwt/PLwt	5.8 +/- 0.16	4.8 +/- 0.28	P=0.01
Birthweight*	1.43 +/- 0.03	1.26 +/- 0.04	P=0.01

Preterm data are based on weights at day 16.5 after vaginal plug for n=7 WT and n=9 TG litters.
* Birthweight data are based on post-delivery day 1 for n=10 WT and n=6 TG litters.
Placental efficiency was defined as fetal weight (Fwt) divided by placental weight (PLwt).
Data are means +/- standard error (SEM). P-values based on nonparametric Mann-Whitney U-test.

Reduced Spiral Artery Angiogenesis in Transgenic Dams

WT and TG dams near term (day 16.5) were infused with contrast agent as described (38) to visualize and measure the maternal uteroplacental vascular anatomy. Three-dimensional surface renderings revealed a complex network of coiled spiral arteries in WT dams (4-6 per placental unit) that merged into larger central canals feeding

the placental labyrinth (Figure 2.2A). In contrast, the number of spiral arteries in TG dams was reduced by approximately 30% (Figure 2.2B, C); and, the length and number of spiral artery coils/mm were also reduced (Figure 2.2D). However, the diameter of central canals downstream to the spiral arteries were not significantly different between WT and TG dams (0.36+/-0.2 mm, 0.41+/-0.3 mm, p=0.23, respectively).

Hemodynamic Modeling using Blood Pressure and Uterine Vascular Architecture

We employed the mean maternal blood pressure at day 16.5 from each group and the mean uteroplacental arterial architecture derived from 3DmicroCT data from the uterine artery to the level of the placental labyrinth as resistance vessels acting in series and parallel. The resistance of each vessel type (uterine, radials, spiral arteries, labyrinth) was calculated using Poiseuille's Law and vessel length, radius, and numbers expected for WT mice were additionally compared with published values by Rennie et al. (38) for comparison. Modeling studies suggested that the structure of the spiral arteries should be the major driver of differences between WT and TG hemodynamics. Spiral artery structure played a dominant role in TG hemodynamics, but a more minor role in the WT group. In the WT group, the greater number of spiral arteries feeding each placenta effectively decreased flow resistance by 4.6 times compared with the TG group. Because resistance to flow was low in the WT group, structural variability in other levels of the uteroplacental vascular tree exerted greater effects, which should translate into greater variability in blood flow transit times in WT mice compared with TG dams. Overall, including differences in blood pressure at day 16.5 (WT ~85mmHg; TG ~112 mmHg) the predicted transit times of a volume bolus through the WT uteroplacental arterial network

would be expected to be 5-8 seconds; whereas TG dams are expected to have faster and narrower transit times in the range of 1-2 seconds (Figure 2.2F).

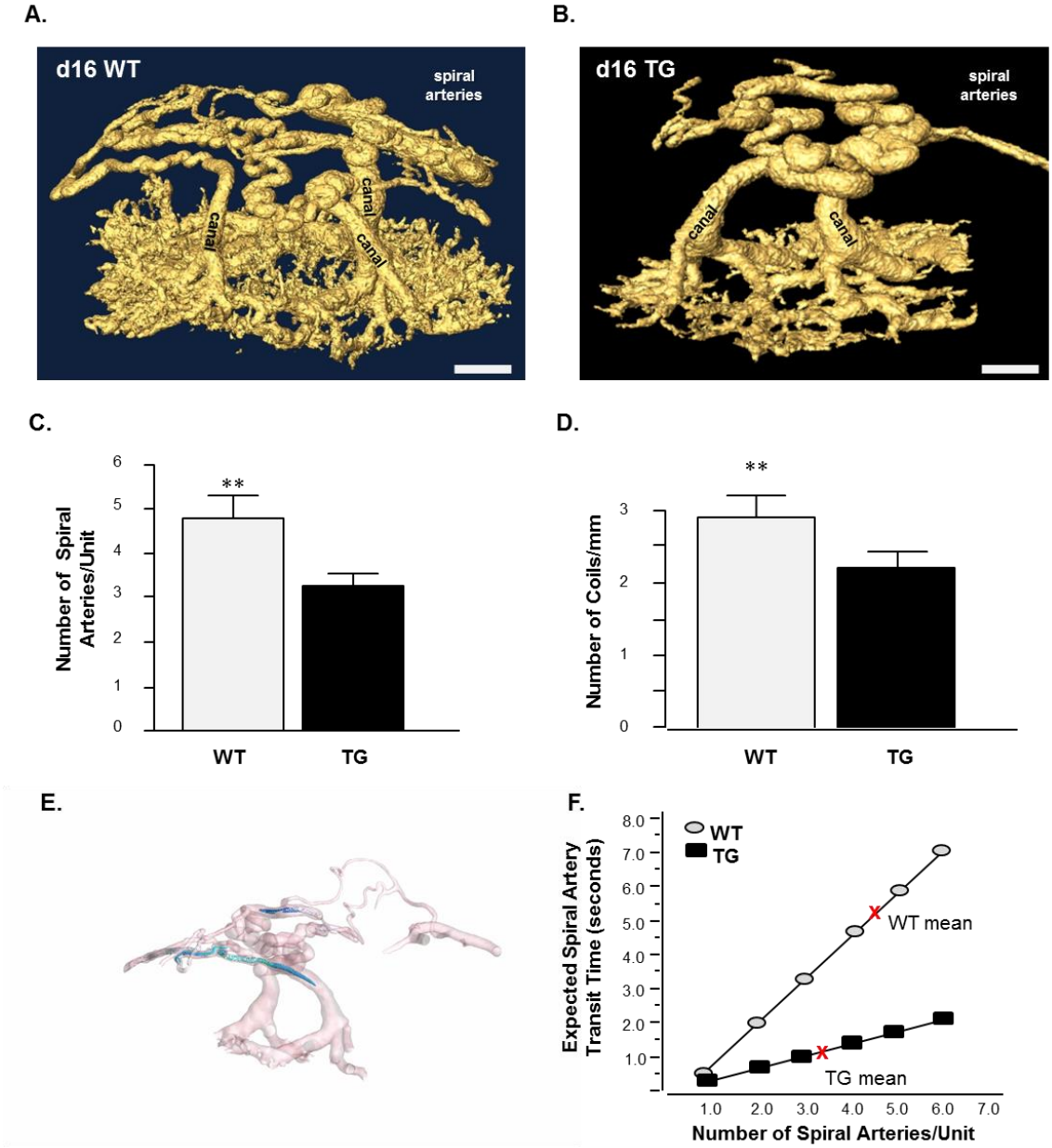

Figure 2.2. Abnormal spiral artery growth visualized by 3D microCT imaging and uteroplacental blood flow modeling estimates. Representative examples of iso-intensity surface renderings obtained from three-dimensional micro-CT imaging data collected at day 16.5 from wild-type (WT) controls (A) and transgenic (TG) dams (B). (C-D) Quantitative analysis of four litters per group imaging three implantation units/litter showed significantly more spiral arteries with more coils/mm in WT mice compared with TG dams. E) Average blood pressure and spiral artery architecture (diameter, length, branching, coiling) at day 16.5 for each maternal genotype was used to model the resistance and expected flow through these vessels, which suggested a slower flow rate through WT units (F) related to more spiral artery branching and lower mean blood pressure compared with TG dams. Scale bars are 1.0 mm.
** P<0.01.

Abnormal Uteroplacental Blood Flow in TG Mice

We used contrast-enhanced ultrasound to *quantify* blood flow velocities and volumes in TG dams and WT controls. We have previously used this microbubble enhanced imaging method to measure uteroplacental blood flow in non-human primates (36) and in women during the first trimester of pregnancy (37). Others have used it to measure uteroplacental blood flow in rats (43). Measurements are based on regional reappearance kinetics of microbubbles after targeted elimination by an ultrasound induced cavitation. In WT dams, the microbubbles reappeared rapidly in the uterine wall; transit time slowed down as they coiled through the spiral arteries and then they slowly filled the placental labyrinth (Figure 2.3A). In contrast, placentas from TG dams filled rapidly with similar reappearance kinetics to filling of the uterine wall (Figures 2.3B, C). Placental filling transit times in TG dams was within 2 seconds of cavitation, indicative of faster arterial conductance; whereas WT mice required 4-8 seconds (Figure 2.3D). These measurements were surprisingly similar to those predicted by our hemodynamic modeling based solely on blood pressure and uteroplacental architecture (Figure 2.2F). Quantitative analysis of total placental microvascular blood flow was not statistically significantly different between WT and TG dams at day 16.5 (Figure 2.3E). Since transit times through the TG circuit are 2-4 times faster than WT dams, this implies that smaller bolus volumes are transiting faster in TG dams. That is to say, TG dams had faster flow velocities of smaller flow volumes feeding their smaller placentas.

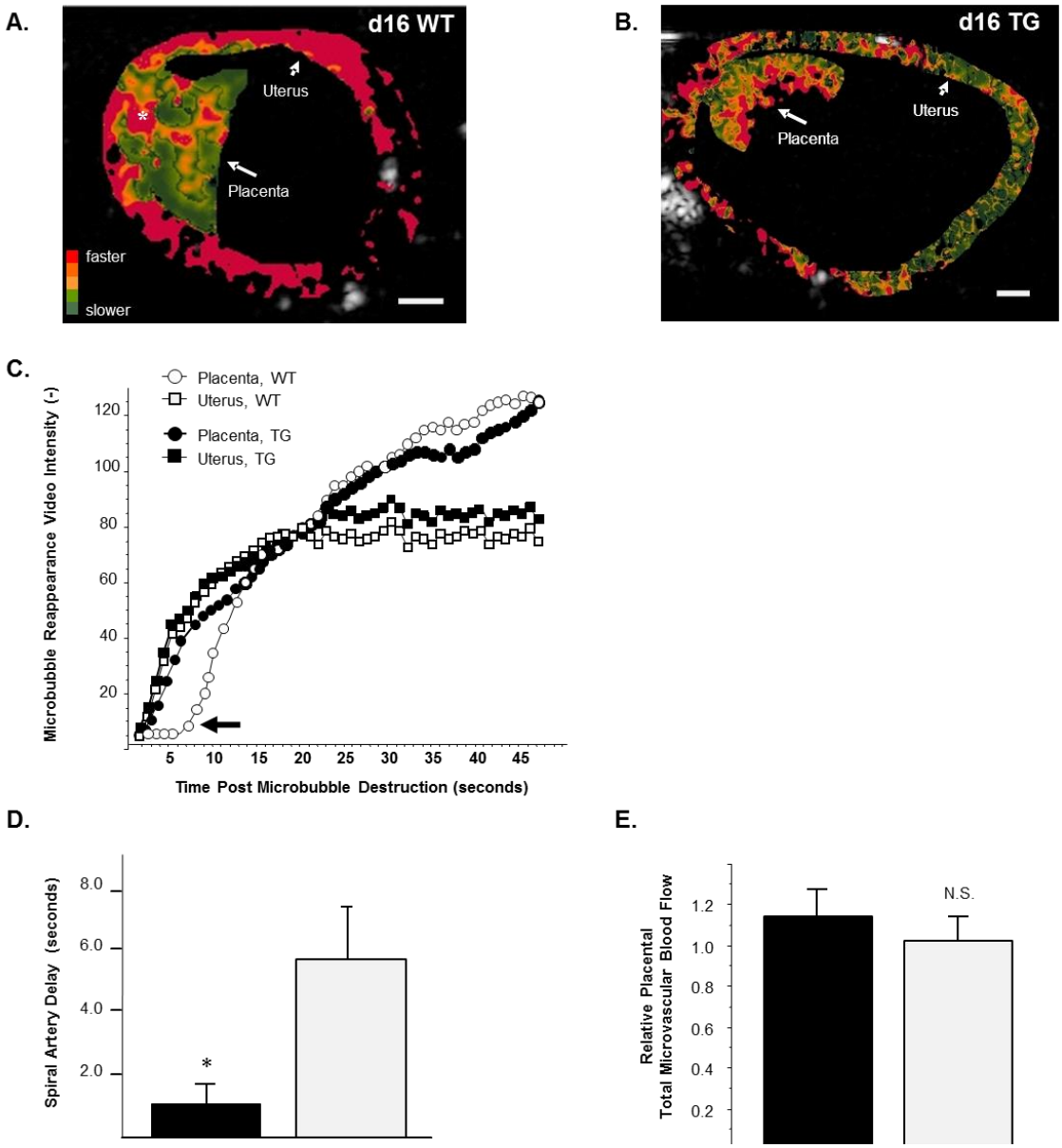

<u>Figure 2.3.</u> Microbubble-enhanced ultrasound measures uteroplacental blood flow. A) Microbubble reappearance kinetics in the uterine wall are fast (digitally coded as red), which then slow as the bubbles wind their way through the uterine spiral arteries (asterisk), leading to relatively slower filling rates of the placental labyrinth (coded as green) in WT controls. B) In contrast, the placentas in TG dams fill very quickly relative to the uterine wall, with no apparent spiral artery lag time. C) Reappearance kinetics plotted as signal intensity relative to time (seconds) highlights the spiral artery lag time in this day 16 WT uteroplacental unit (arrow), which is absent in the day 16 TG dam. D) Data averaged over six litters per maternal genotype show reproducible lag times in WT dams (4-8 seconds), which are essentially absent in TG mice. E) The maternal component of placental blood flow volume is not significantly different between WT and TG dams. Data are mean +/- SEM of at least three implantation sites/litter. (A-B) scale bar is 2.0 mm. * $P<0.05$; N.S. is not significant.

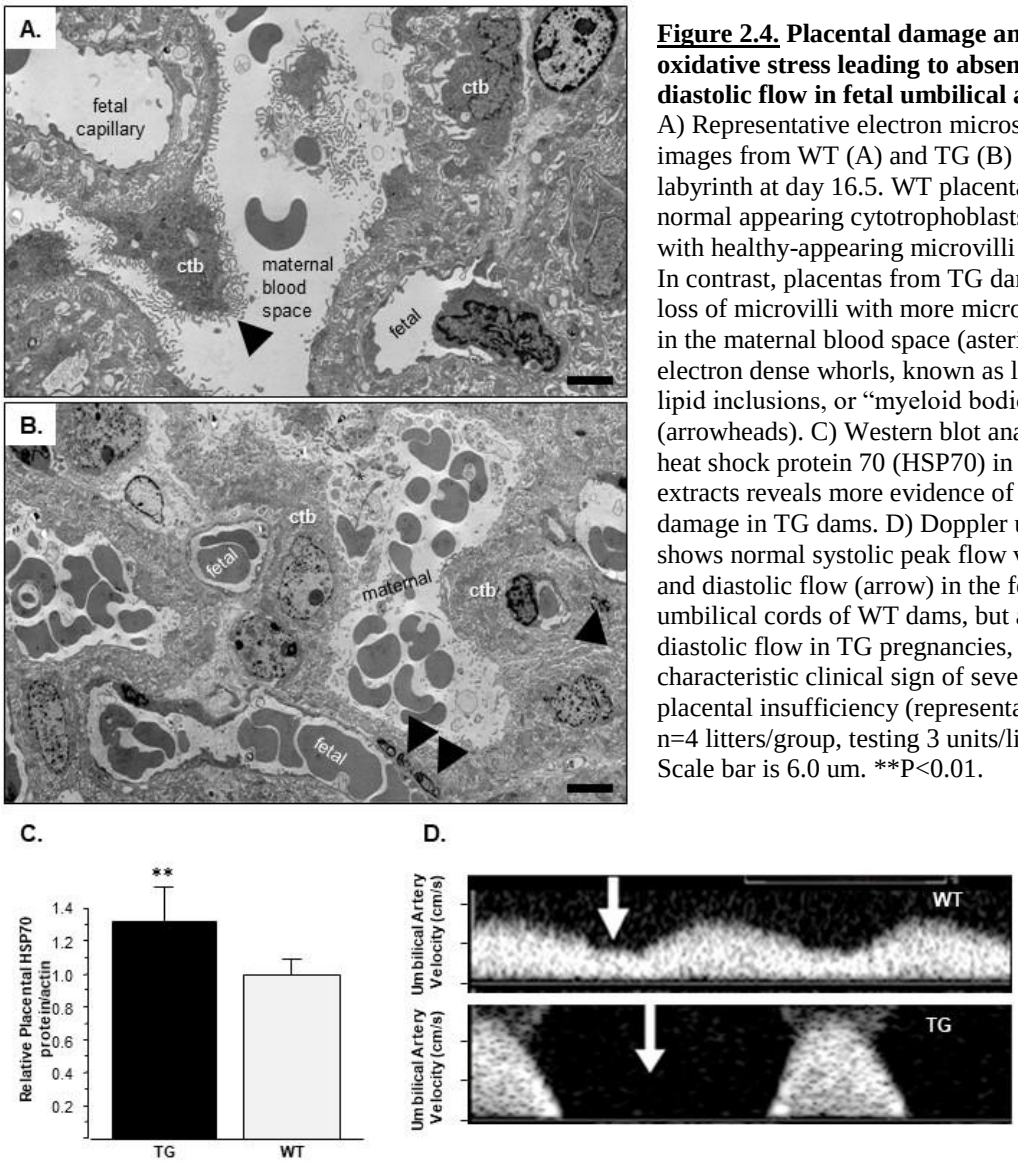

Figure 2.4. Placental damage and oxidative stress leading to absent end diastolic flow in fetal umbilical arteries. A) Representative electron microscopic images from WT (A) and TG (B) placental labyrinth at day 16.5. WT placentas have normal appearing cytotrophoblasts (ctb) with healthy-appearing microvilli (arrow). In contrast, placentas from TG dams show loss of microvilli with more microvesicles in the maternal blood space (asterisk) and electron dense whorls, known as lamellated lipid inclusions, or "myeloid bodies" (arrowheads). C) Western blot analysis for heat shock protein 70 (HSP70) in placental extracts reveals more evidence of placental damage in TG dams. D) Doppler ultrasound shows normal systolic peak flow velocity and diastolic flow (arrow) in the fetal umbilical cords of WT dams, but absent diastolic flow in TG pregnancies, which is a characteristic clinical sign of severe placental insufficiency (representative of n=4 litters/group, testing 3 units/litter). Scale bar is 6.0 um. **P<0.01.

Placental Damage and Absent End-Diastolic Flow in TG Mice

Faster flow velocities may be responsible for placental damage, because the placentas from TG dams showed evidence of ultrastructural damage and their placentas expressed more heat shock protein 70 (HSP70) compared with WT controls (Figure 2.4). In humans, damaged small placentas are associated with umbilical cord Doppler absent end diastolic flow (39), which was seen in all 12 cords examined from TG dams, but none of the WT controls (0/12; Fishers Exact p-value<0.001).

Uterine VEGF Transfection Rescues Spiral Artery Angiogenesis and Fetal Growth

Uterine vascular targeted transfections we performed in WT and TG virgin mice using VEGF and/or firefly Luciferase plasmid conjugated to cationic microbubbles according to our group's previously published methods (31). Expression time course studies were first performed in non-mated WT mice to confirm hVEGF165 expression in uterine tissues, which peaked at 3-7 days post transfection (Figure 2.5).

Uterine luciferase expression was monitored daily by intraperitoneal luciferin injection and bioluminescence (Figure 2.5 C). Ex vivo resected organs (uterus, bladder, liver, lungs) were also examined by bioluminescence and expression was localized in formalin fixed sections by immunohistochemistry as described (31). We observed strong Luciferase signal in the uterus and bladder, but not lung or liver and transfection localized to endothelial cells as expected (data not shown).

Transfected mice were mated with WT males and timed pregnancies (from vaginal plug and transfection date) were used for uteroplacental arterial 3DmicroCT imaging at e16.5, or allowed to deliver at term (e19.5). Notably, not all uteroplacental units in TG dams transfected with VEGF showed full spiral artery architectural recovery (Figure 2.6A), but efficiency was sufficient to increase spiral artery angiogenesis and rescue birthweight. Luciferase transfection (control) did not increase birthweight.

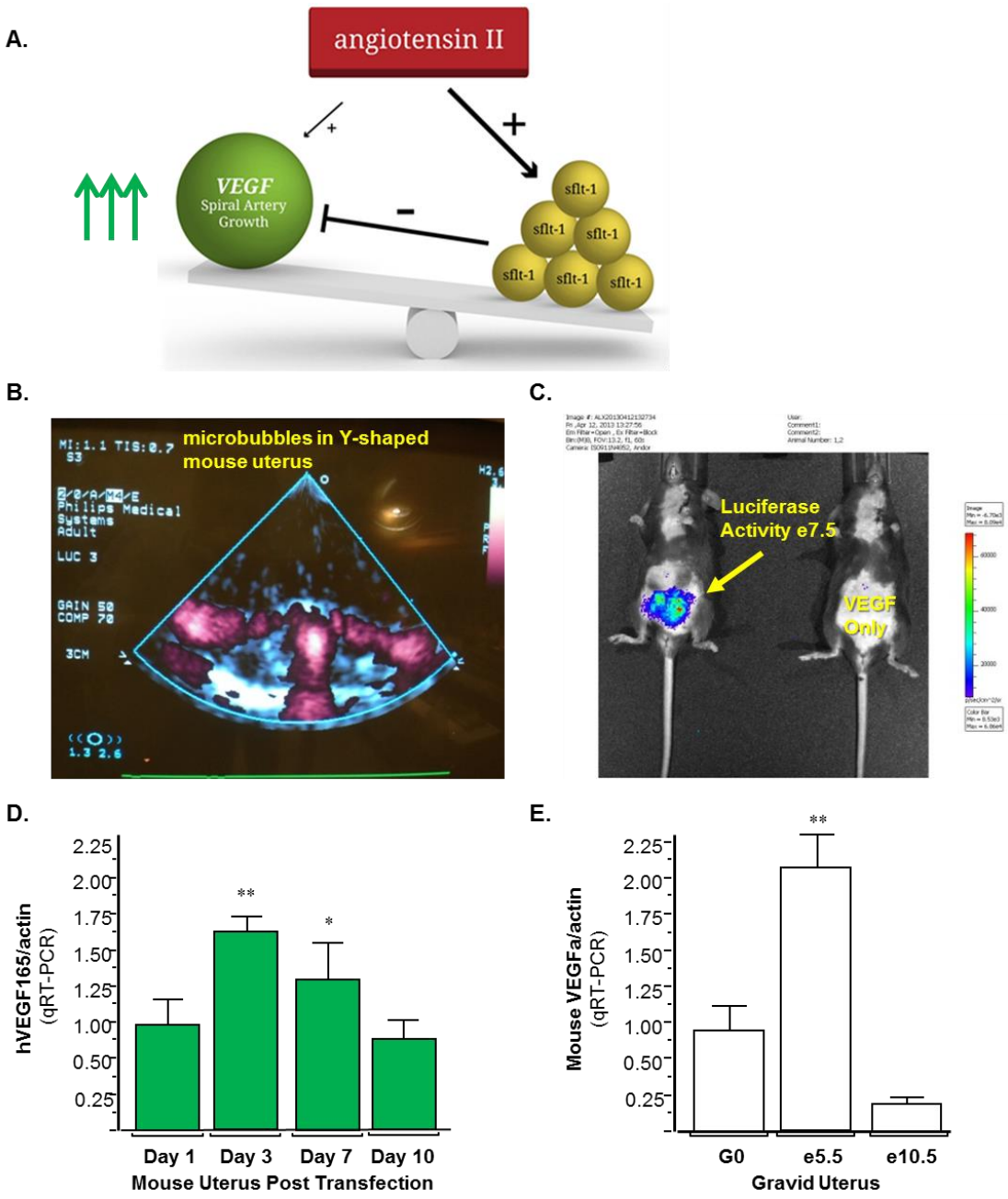

Figure 2.5. Microbubble Conjugated VEGF/Luciferase Plasmid DNA Transfection of Mouse Uterine Vasculature. (A) Working hypothesis is increased VEGF expression by uterine spiral artery endothelial cells will rescue the elevated angiotensin II maternal TG phenotype. B) Microbubble conjugated plasmid DNA was delivered to the uterine vasculature by popping the bubbles with targeted pulse delivering VEGF and/or luciferase to uterine endothelial cells as previously described by our group (31). C) Firefly luciferase reporter activity was localized and monitored in pregnant mice. Time course for uterine VEGF expression by delivered hVEGF plasmid (D) or endogenous murine VEGF (E) measured by qRT-PCR. Delivered VEGF spike correlated with endogenous VEGF expression spike in the gravid mouse uterus (n=4-6 litters per group); * $P<0.05$; ** $P<0.01$.

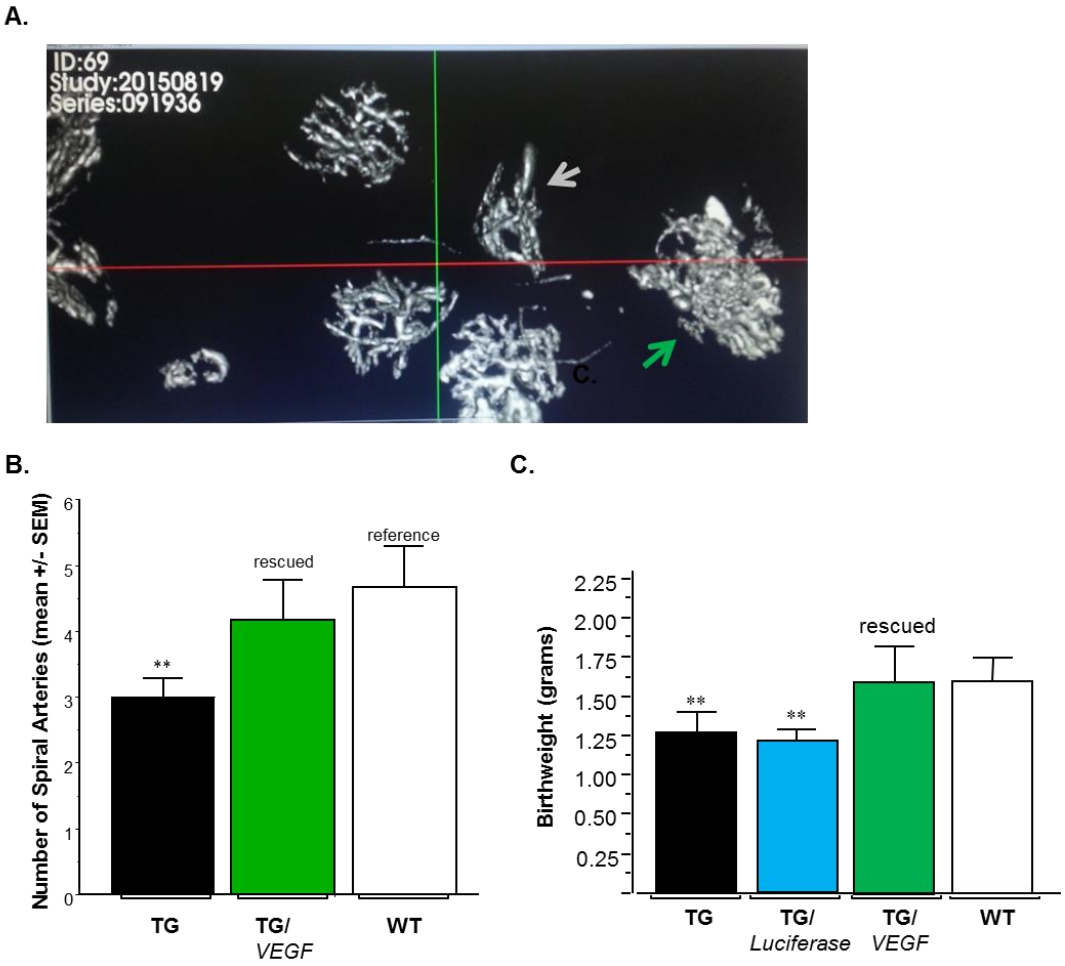

<u>Figure 2.6.</u> Microbubble Conjugated VEGF Delivery Rescued Spiral Artery Angiogenesis and Fetal Birthweight. (A) Representative 3DmicroCT image of 7 uteroplacental units within a VEGF transfected TG gravid uterus at day 16.5. Some of the units showed normal appearing spiral artery branching, lengthening, and coiling (green arrow), while others di d not (grey arrow). B) Overall the number of spiral artery branches per unit were rescued in VEGF treated TG dams compare with untreated TG dams. C) Luciferase transfection did not rescue birthweight, but VEGF delivery yielded litters with birthweights very similar to WT controls (n=4-6 litters/group); **P<0.01.

Discussion

Transgenic mice expressing 20% more systemic AGT than C57BL/6J controls develop gestational hypertension and have growth restricted progeny, similar to women with the A(-6) promoter variant associated with preeclampsia and FGR (17, 22). These TG dams have characteristic features of placental insufficiency, including elevated serum sflt-1 and absent end-diastolic flow in fetal umbilical arteries. They have fewer and less

coiled spiral arteries, which is associated with increased uteroplacental blood flow velocities and significant placental damage.

Renin-Angiotensin System and Spiral Artery Remodeling

The systemic renin-angiotensin system (RAS) is upregulated during pregnancy and is known to play a major role in regulating blood pressure and blood volume (44, 27). Tissue-specific RAS systems, including the spiral artery RAS, are also upregulated and have local effects (19, 24, 27). Since AGT is at the K_m of the renin-angiotensinogen reaction (20), abnormally elevated AGT expression is expected to lead to increased angiotensin II activity and potential pathology, including abnormal spiral artery remodeling (7, 19, 23, 24). The significance of the TG mouse model is it isolates the effects of elevated AGT expression. Our results demonstrate that abnormally increased maternal AGT expression leads to less spiral artery growth and less branching, which may be interpreted as abnormal pregnancy-induced remodeling (29). Elevated angiotensin II activity may also affect vascular tone (44), which may account for increased blood pressure and reduced blood volume (27) in this model.

Although systemic levels may not reflect local tissue-specific systems (44), it is reasonable to hypothesize that elevated AGT expression may abnormally stimulate placental sflt-1 production (25). We did observe significantly increased maternal serum sflt-1 levels by mid-gestation and their placentas produced slightly more sflt-1 at term. This increase in sflt-1 production, however, was not sufficient to cause glomerular damage or proteinuria (1). This may be because sflt-1 levels were about 10-fold less than those used to induce glomerular damage in rats (1); although they were nearly 10-fold more than elevated levels observed in women with preeclampsia (1). Whether circulating

sflt-1 levels were sufficient to sequester spiral artery VEGF (14, 15) and reduce pregnancy-induced spiral artery growth requires further study, but we have now shown that delivering VEGF to uterine endothelial cells is sufficient to rescue the phenotype in our mouse model.

Abnormal Spiral Artery Remodeling, Faster Flow Velocities, and Placental Damage

Pregnancy-induced spiral artery growth is important. Before pregnancy, mice do not have spiral arteries (45), but from early to mid-gestation the spiral arteries branch and elongate from the uterine radial arteries into coiled conduits regulating blood flow to the placenta (46). This is similar to spiral artery growth and remodeling observed in women each month during the secretory phase of their cycle and during the early stages of pregnancy (45, 46). This remodeling appears to vary within and between individuals, which may play a role in pregnancy complication risk (6, 7), but we suspect spiral artery growth variation may also be involved in regulating normal uteroplacental blood flow. For example, our group has recently reported there is significant variance in flow rates (12-45 ml/min) between cotyledons within each rhesus macaque placenta tested by contrast-enhanced imaging (47). Perhaps differences in spiral artery length and dilation play a critical role in regulating the pulsatile delivery of maternal blood to the placenta. Perhaps a common underlying cause of placental insufficiency is a shift in this normal variance (6, 7).

Maternal blood pressure may also affect flow rates, but it is important to point out that uteroplacental vascular resistance is not well understood. It may be more likely that the proximal radial arteries, which show less branching, have smaller luminal diameters,

and have active smooth muscle cells, are more important regulators of driving pressure than spiral arteries (11, 38). Regardless, the consequence was placental damage.

Placental damage in our model was not caused by reduced uteroplacental blood flow volume, but may have been caused by the observed increased flow velocity in TG dams. Fewer spiral arteries in parallel under greater driving pressures would be expected to increase shear stress effects. The loss of trophoblast microvilli in TG dams may reflect this increased stress similar to what is seen in women with preeclampsia (40). Indeed, shear stress is proportional to the flow velocity and inversely related to vessel radius. TG dams have higher uteroplacental flow velocities and smaller radii due to fewer spiral arteries per metrial triangle. Modeling shear stress is very complicated, however, and this prediction may not be correct despite the surprising correlations we observed between our modeled transit times and empirical microbubble enhanced imaging studies. The problem is shear stress estimates are based on *straight* vessels (not coiled) and laminar flow. The problem becomes even more complicated when considering the turbulence in the placental labyrinth or intervillous space of a human.

Placental Invasion and uNK cell Activation

A limitation of this study is we did not investigate the role of placental invasion or differences in uNK cell activation, which are known regulators of spiral artery angiogenesis and remodeling (48-50). Placental proximity seems to be important for spiral artery angiogenesis in the mouse, but invasion into the walls of these vessels is less important in these brief gestational periods than what seems necessary in women (45, 46). Uterine NK cell activation plays a key role in murine spiral artery angiogenesis and likely plays an important role in women [our investigation into uNK cell

activity/maternal genotype and its role in uterine VEGF production is covered in Chapter 3 of this doctoral thesis].

Nonetheless, it is important to point out that effects of placental invasion and/or uNK cell activation impacting spiral artery angiogenesis in TG mice would be *secondary* to the maternal AGT genotype. Elevated maternal AGT expression and metrial angiotensin II production seem to be sufficient to lead to be the primary cause of abnormal spiral artery angiogenesis, abnormal blood flow to the placenta, placental damage, and fetal growth restriction. This process can be essentially rescued by increasing VEGF expression in the uterine vascular network during early pregnancy.

Vascular Endothelial Growth Factor and Spiral Artery Angiogenesis

An important strength of this study is the demonstration that plasmid-conjugated microbubbles may be used to target increased expression of candidate genes in endothelial cells during pregnancy. We have previously used this technology to increase VEGF expression in an ischemic limb murine model (31) and have shown that targeting by microbubble cavitation does not lead to hemorrhage, but it does transfect endothelial cells at relatively high efficiency. Expression last about 1 week post transfection, although luciferase activity may be detected weeks after transfection in our experience. This is important because uterine VEGF peaks around e5.5-6.5 in the mouse uterus during the early period of spiral artery angiogenesis (50) and before pruning of the arterial network into well-formed spiral arteries. Our data suggest that sufficiently available ***endothelial*** VEGF is required for normal spiral artery angiogenesis. Endothelial availability is essential because VEGF receptors on endothelial cells (VEGFR1) stimulate

different angiogenic/anti-angiogenic pathways than receptors in the vessel wall and surrounding decidua (VEGFR2) (51).

A difference in VEGF availability (intravascular/endothelial versus decidual/endometrial stromal) may therefore explain why artificially increasing ***decidual*** VEGF availability rather than restricting the increase to endothelial cells could lead to different outcomes in transgenic mice. For example, Fan et al (2014) showed that increasing VEGF expression in uterine decidual cells in transgenic mice led to poor pregnancy outcomes (52). Spiral artery angiogenesis studies were not performed in that study, but one may speculate that increased VEGFR2 stimulation may lead to excessive vasculogenesis and less well formed spiral arteries to provide normal blood flow to the placenta (blood flow studies were also not performed in that study).

Sources of Funding:

This study was funded by the *Preeclampsia Foundation*, the *Society of Reproductive Investigation*, the *National Institute of Child Health and Human Development* (1R21HD068896-01A1) and the *Office of Women's Health Research*: Oregon K12 BIRCWH (HD043488-08), and the *Oregon Medical Research Foundation*.

Chapter 3

Fetal Sex Affects Uteroplacental Angiogenesis in Mouse Model of Fetal Growth Restriction

Abstract

Elevated maternal angiotensinogen (AGT) expression (20% increase in AGT transgenic (TG) dams vs. wild-type (WT) controls) reduces spiral artery branching and coiling by gestational day (GD) 16.5. The consequence is abnormal uteroplacental blood flow, placental damage, and fetal growth restriction that disproportionately affects male offspring. We hypothesized that, in addition to maternal genotype, male fetal sex will impact uteroplacental vascular structure, uterine natural killer cell (uNK) activity, and uteroplacental expression profiles affecting pregnancy-induced angiogenesis. Uteri from WT and TG dams were harvested during early gestation (GD6.5 and GD8.5) to measure uNK activity via whole mounts using fluorescent Ly49 (inactive uNKs), DBA (active uNKs), and CD31 (developing blood vessels) staining to examine the role of early angiogenesis affecting later spiral artery remodeling. At day 16.5 we measured spiral artery architecture by 3D microCT. We calculated placental capillary density, measured placental nutrient transport, and compared placental transcriptomic profiles at day 16.5. We observed that males from TG dams were associated with decreased maternal uNK activity, reduced pro-angiogenic expression in the metrial triangle, reduced angiogenesis at days 6.5, 8.5, and fewer spiral arteries per placental unit at day 16.5. Male placentas from TG dams also had reduced placental capillary density compared with their female siblings and WT controls. Surprisingly, transcriptomic analysis revealed upregulation of

nutrient transporters in male placentas from TG dams, which was confirmed by lipid and amino acid transport studies performed at day 16.5. We conclude that male fetal sex compounds the impact of maternal genetic risk in this mouse model. Our data suggest the mechanism may be related to less placental pro-angiogenic signaling, reduced uNK cell activation, and significantly fewer spiral arteries per placental unit in males from TG dams.

Introduction

Fetal growth restriction (FGR) is a common and potentially life-threatening complication, occurring in 5-10% of all human pregnancies (1). It is a multifactorial disorder characterized by constrained growth during pregnancy, resulting in fetal weight below the 10th percentile for gestational age relative to the average population (2). Negative health outcomes associated with FGR include increased perinatal mortality and a three-fold increased risk of adult onset diabetes and cardiovascular disease (3, 4). Male fetuses are more negatively affected by FGR than females: they are more likely to be stillborn, born earlier with poorer survival outcomes, and they have a greater risk for developmental programming of adult onset diseases (5–8).

Small for gestational age newborns come from small placentas with gross and histologic features of maternal malperfusion (placental insufficiency), including infarctions and accelerated villous maturation (9). Placental insufficiency implies that the mother or the placenta have an impaired ability to supply fetal nutrient demands (10–14). This may be related to insufficient maternal nutrition (e.g. low protein diet), insufficient delivery of nutrients (e.g. pathologic changes in the uteroplacental arterial network),

and/or increased fetoplacental demand (e.g. twin gestations) (4, 15–18). The reason why males do more poorly than female growth restricted babies is unknown, but a leading hypothesis is that males do not sufficiently invest maternal derived nutrients into placental growth compared with females (8) and/or they may have relatively increased metabolic demands (19).

Maternal nutrition to the fetoplacental unit is supplied via the uteroplacental arterial network. Maternal uterine angiogenesis and pregnancy-induced remodeling are essential for a normal pregnancy outcome in both mice and humans (9, 20, 21). In humans, the endometrial spiral arteries grow, coil, and dilate in a process related to a combination of placental invasion and vascular angiogenic growth factors (e.g. placental growth factor [PLGF], vascular endothelial growth factor [VEGF]) (22–24). Mouse uterine arterial angiogenesis and vascular remodeling mimic human pregnancy-induced changes with the exception that in mice the uterine spiral arteries grow *de novo* for pregnancy (25).

The mouse placenta is different than humans in that it is composed of a labyrinth of interdigitating maternal capillary-like spaces lined by placental trophoblasts encasing fetoplacental capillaries. In contrast, in humans, the spiral arteries open into the intervillous space, which then drains into the decidual veins (25). The placental bed of mice and humans, however, is very similar composed of decidual cells, macrophages, dendritic cells, and uterine natural killer cells (uNK) that are thought to play a key role in regulating proper spiral artery angiogenesis and remodeling during pregnancy (22–26). Uteroplacental angiogenic factors like VEGF are released by activated uNK cells and they are made by placental cells to stimulate angiogenesis in the uterus and in the placenta (27). Indeed, vascular growth in the both the uterus and placenta seem to rely on

similar angiogenic/anti-angiogenic pathways involved in vasculogenesis to grow capillary-like networks and angiogenesis to prune them into arteries and capillary beds for nutrient exchange (28, 29).

We hypothesized that uteroplacental angiogenesis may be different in males compared with their female siblings. We studied a murine angiotensinogen gene titration over-expression model (1.2-fold wild-type levels), which was originally designed to mimic a common human promoter variant associated with chronic hypertension, pregnancy-induced hypertension, and fetal growth restriction (30, 31). Our group has shown that TG mice have reduced spiral artery angiogenesis, abnormal blood flow to their placentas, develop placental damage and FGR (see Chapter 2). This mouse model was selected in part because mice have multiple pups per litter and fetal sex could then be compared within each litter and between litters relative to maternal genotype.

Methods

Transgenic Mouse Model: Experimental procedures were approved by the Institutional Animal Care and Use Committee of Oregon Health and Science University. Angiotensinogen (AGT) 3-copy transgenic (TG) dams (B6.129P2-Agt^{tm1Unc}/J (30)) were purchased from The Jackson Laboratory (Bar Harbor, Maine) and backcrossed with wild-type (WT) C57/BL6 mice from Charles River Laboratories (Wilmington, MA) for more than ten generations before experimentation. Adult (11-13 weeks old) TG and WT females were bred with WT males and matings were timed from vaginal plug (GD0.5). Fetal sex (SRY) and genotype (AGTdup) were determined by PCR. Briefly, DNA from fetal liver tissue or adult tail snips was extracted using DNeasy (QIAgen; Valencia, CA)

or REDExtract-n-Amp PCR Reaction Mix (Sigma-Aldrich; St. Louis, MO), respectively. AGT genotype and fetal sex were determined by PCR using specific primer sets [Supplemental Table 3.1] that yielded products of expected size and DNA sequence. Both PCR reactions used the following cycling parameters: initial melting at 94C for 2 min; followed by 40 cycles of 94C for 20 s, 65C for 30 s, 72C for 30 s; followed by a final 72C extension for 5 min. All samples have the endogenous AGT genetic PCR product (160 bp), which served as an internal positive control for the PCR reaction. WT genotypes had only the 160 bp band; whereas, AGT 3-copy mice (TG) showed both a 160 bp band and a 189 bp band for the AGTdup transgene. In the SRY reaction, a 249 bp band indicated male fetal sex; females lacked the SRY band, but retained the WT AGT product. Note: only WT fetal genotypes from TG dams were used for these analyses; TG pups from TG dams introduced an additional potential confounder (3-copies of AGT gene) excluded in these analyses.

Tissue Samples for Expression Analysis: Maternal blood, uterine decidua (metrial triangle), placentas, and corresponding fetal livers (to determine fetal sex and genotype corresponding to its placenta and maternal metrial triangle) were isolated from TG and WT mice (4-6 litters/group) at mid-gestation (GD12.5) and late gestation (GD16.5) for qRT-PCR, ELISA, HPLC, and RNASeq (GD16.5 only) experiments. Maternal blood was collected in heparin tubes and centrifuged and plasma banked at -80C. Maternal metrial triangles from the placenta bed and fetal placentas were microdissected at GD12.5 using a published protocol (23). Placentas at GD16.5 from TG and WT dams were flash frozen and RNA and protein were extracted using commercially available kits.

Three Dimensional MicroCT Measurements of Uterine Arterial Networks: TG and WT dams (n=4 litters each) were euthanized and perfused for microCT imaging at GD16.5 (per vaginal plug after timed mating) as previously described by Dr. Rennie in our group (32). Spiral artery number, branching, and coiling in each uteroplacental unit were measured independently by two reviewers (MR and JH) blinded to maternal genotype and fetal sex. The average values from each reviewer for each uteroplacental unit were used to generate mean values +/- SEM per fetal sex for each litter.

Placental Stereometry: Placentas obtained from the microCT harvest were weighed, measured, and paraffin-embedded for histologic analysis. Fetoplacental capillary number and density for each placenta was determined using a standard stereometric approach (33, 34). Briefly, randomly oriented and sectioned placental slices (5 μm thick) were immunostained for CD31 to highlight endothelial cells in fetoplacental capillaries. The placental labyrinth within each section was outlined using Stereo Investigator and software (MBF Bioscience; Williston, VT). The number of capillaries within each placenta's labyrinth area calculated and compared within groups (e.g. fetal sex and maternal genotype).

Angiogenic/Anti-angiogenic Protein Expression Analysis*:* 10ug of protein from each sample determined by BCA (Thermo Fisher; Waltham, MA) were analyzed using commercially available ELISAs (R&D Systems; Minneapolis, MN) for sFlt1, VEGF, and PLGF according to manufacturer's instructions. Protein expression levels in each sample were generated by comparison with the standard curve generated by kit internal standards. Each experiment was performed in triplicate and values were within the dynamic range of each ELISA assay.

Placental Nutrient Transport Assay: Placental transport of radiolabeled fatty acids and amino acids were measured in vivo in four TG and four WT dams at GD16.5 (near term) using previously described methods (35–37). Briefly, ^{14}C-radiolabeled C-DHA (2uCi/kg) (lipid transport) or ^{14}C-methylaminoisobutyric acid (MeAIB) (50 uCi/kg) (amino acid transport) were administered in a 100ul PBS bolus via maternal jugular catheterization. The mice were euthanized at 90 or 3 minutes, respectively; maternal blood, placentas, and fetuses were collected and solubilized with Solvable/Biosol (PerkinElmer; Waltham, MA) to determine radioactivity in each fraction relative to weight. Maternal-placental-fetal unidirectional clearance (K) for each tracer was calculated by dividing fetal counts (N) by the area under the maternal isotope concentration curve (AUC) from time 0 to sacrifice (dpm*min*ul-1) multiplied by placental weight (W): K=N/[AUC*W]. Experiments were performed in triplicate and reported as the means per fetal sex per maternal genotype.

Placental Transcriptomics: cDNA libraries were prepared from placentas known to be from male or female pups from TG and WT dams (representative of 4 litters per group) using the TruSeq RNA Sample Preparation Kit (Illumina; San Diego, CA). Poly-A containing mRNA was extracted using magnetic poly-T oligonucleotide containing beads, then fragmented and copied into first strand cDNA followed by second strand cDNA synthesis. cDNA fragments were ligated to adapters, purified, and enriched via PCR to create final cDNA libraries with hexamer barcodes to facilitate sample multiplexing. Purified libraries were quantified on a Bioanalyzer 2100 (Agilent; Santa Clara, CA) using a DNA 1000 chip and sequenced using Illumina HiSeq™ 2000. *CLC-workbench* (version 9.0; CLCbio) was used for analysis on reads compiled for *de novo*

assembly. Differential gene expression was calculated using Empirical analysis of DGE in *CLC-workbench*, controlling FDR at 0.05. GO terms were found using Database for Annotation, Visualization and Integrated Discovery (DAVID) and the GO FAT filter. GO-term enrichment tests were also performed (38, 39)

qRT-PCR Validation of RNASeq: RNA from each sample was converted to cDNA using SuperScript III First-Strand Synthesis System and amplified using TaqMan probes (Life Technologies; Carlsbad, CA) to measure expression of several significant genes from key gene ontologies identified by RNASeq relative to *Gapdh* base-line expression: *Fabp1, Fabp4, Acox2, Cox1, Cox2, Clec2d, Klrb1b* [Primers in Supplemental Table 3.2]. Amplification was conducted using a Roche LightCycler as follows: 1 cycle at 95C for 5 minutes, 40 cycles of 95C for 15 seconds and 65C for 60 seconds (with acquisition at 65C). Cycle point crossings were compared with a standard curve for each marker to quantify the relative starting amount of mRNA expressed in each sample.

uNK Cell Activation and Angiogenesis in Whole Mounts*:* Uterine natural killer cell activation and metrial triangle angiogenesis whole mount experiments were performed in collaboration with Dr. Anne Croy's laboratory as described by their group (23, 40). Briefly, immunofluorescence assays were performed at GD6.5 and 8.5 using *in situ* whole mounts from TG and WT dams (4-6 litters/group). when the populations of uNK cells have been reported to be changing most dramatically (23). GD8.5 is also when vasculogenesis/angiogenesis is reportedly at its peak (40). First, the mesometrial uterine walls were bisected on the midsagittal line of the mesometrial-antimesometrial axis. It was then stained with FITC-conjugated *Dolichos biflorus* agglutinin (DBA) lectin (Vector Laboratories; Burlingame, CA), which when positive indicates activated uNK

cells; and PE-conjugated Ly49C/I (BD Pharmigen; Franklin Lakes, NJ), which when positive indicates inactive uNK cells. Anti-CD31 (Biolegend; San Diego, CA) staining highlighted endothelial cells in the metrial triangle to quantify blood vessel number, branching, and so-called "blebbing" (41) in each whole mount. The embryo was then digested for DNA and genotyping.

Statistical Analysis: Fetal sex per maternal genotype was the primary variable for analysis using the mean from at least four litters per maternal genotype. Data were analyzed by two-way ANOVA with Tukey's multiple-comparison post hoc correction.

Results

Male Fetal Sex Affects Maternal Uterine Angiogenesis in TG Dams

Representative 3D microCT images from males and females from WT dams and TG dams are shown in Figure 3.1A. Fetal sex in WT dams did not appear to affect maternal uterine angiogenesis. However, male fetal sex in TG dams was associated with fewer spiral arteries per placental unit ($p<0.01$). Maternal spiral arteries were also shorter and did not coil as often when the pup was a male in TG dams ($p< 0.05$).

Angiogenic/Anti-Angiogenic Levels in Maternal Metrial Triangle at Mid-Gestation

Concentrations of VEGF, PLGF, and sFlt1 were impacted by maternal genotype and fetal sex in the metrial triangles sampled at mid-gestation (Figure 3.2). Gestational age GD12.5 was suboptimal to evaluate the angiogenic milieu provided peak angiogenesis occurs around GD8.5 (40), but specific microdissection of the metrial triangle away from the fetoplacental unit was not possible in our hands before GD12.5 (confirmed by histologic analysis of microdissected tissues). Nonetheless, at GD12.5 the

metrial triangles in the placental beds of male pups from TG dams showed significantly less PLGF ($p<0.05$) and more sFlt1 ($p<0.01$) compared with males from WT dams. Females from TG dams showed no difference in VEGF or PLGF levels vs WT, but they too showed slightly more sFlt1 ($p<0.05$). Overall, the ratio of sFlt-1 (anti-angiogenic) over angiogenic factors like VEGF and PLGF was significantly greater in males from TG dams compared with all other groups ($p<0.001$).

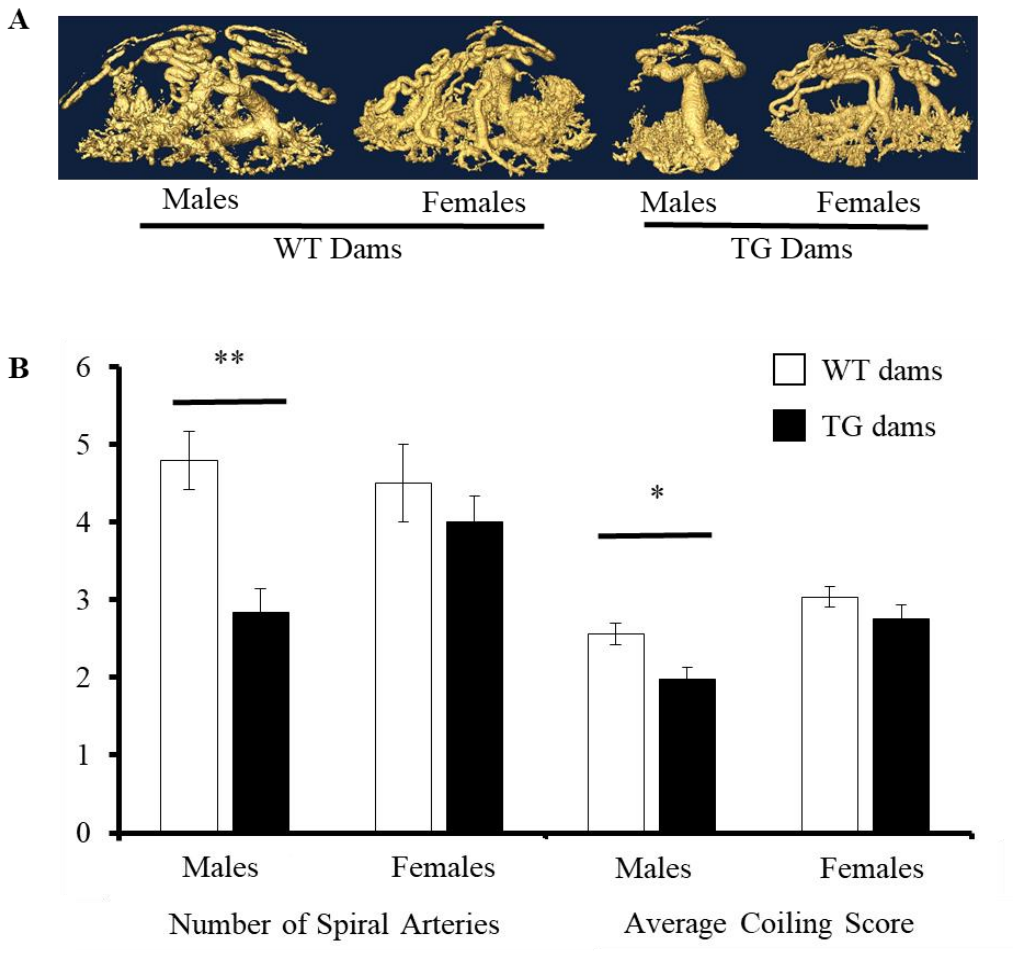

Figure 3.1. Uteroplacental 3D microCT perfusion to assess spiral artery structure. A) Representative microCT images of uterine spiral arteries at day 16.5 metrial triangles from WT and TG dams divided by fetal sex. B) Quantification of spiral artery number and average coiling score (mean ± SEM). Asterisks indicate significant differences between sex-matched placentas from WT and TG dams within each metric by student t-test (*: $p<0.05$, **: $p<0.01$, ***: $p<0.001$).

uNK Cell Activity and Angiogenesis in Metrial Triangle at Gestational Days 6.5 and 8.5

Activation of decidual uNK cells in early gestation were measured as a ratio of Ly49 (inactive) to DBA (active) as previously published by the Croy laboratory (23). Females from both WT and TG dams reduced their ratio of Ly49 to DBA positive cells, indicating uNK cell activation, from GD6.5 to GD8.5 (Figure 3.3). Compared to Dr.

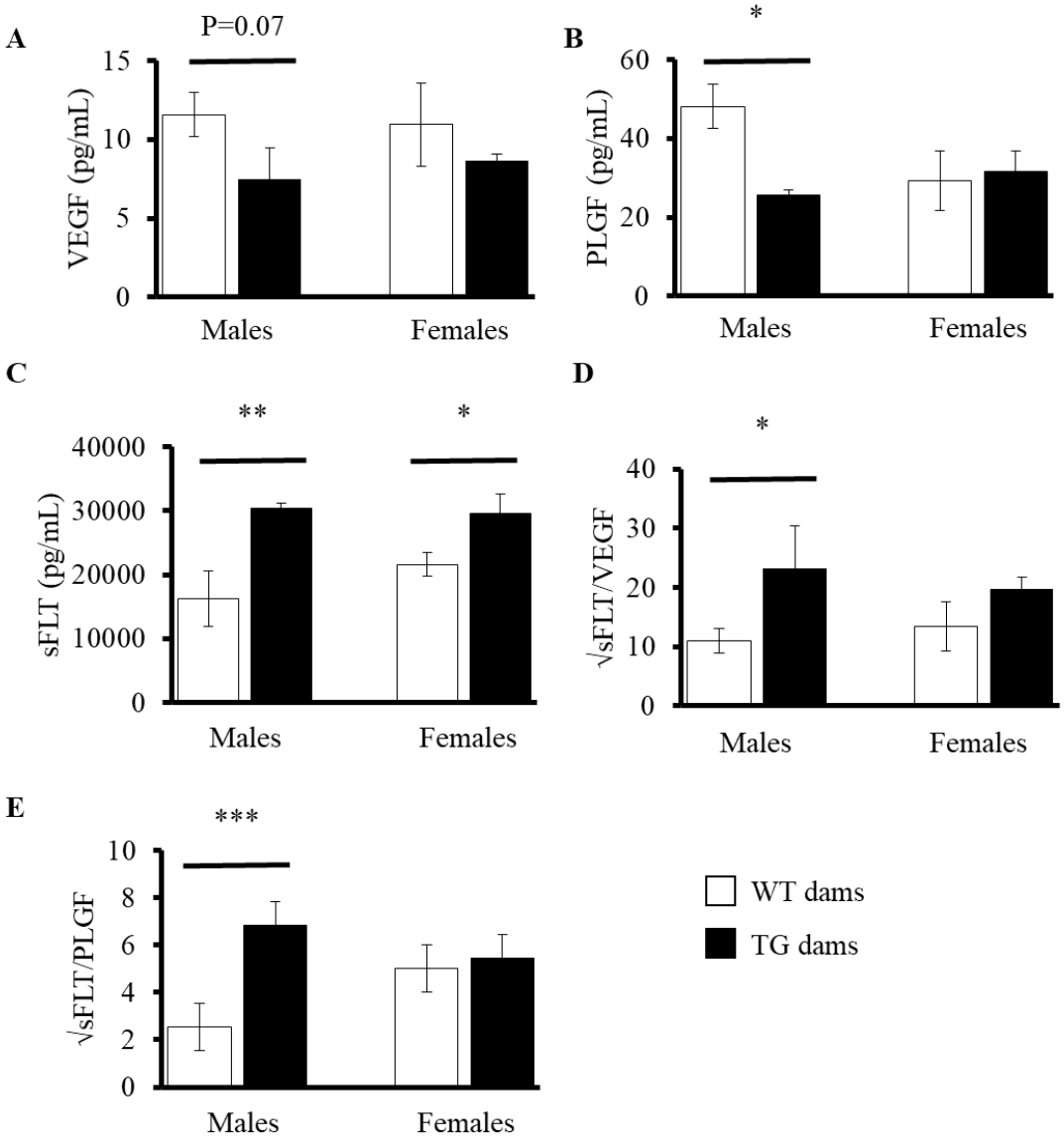

Figure 3.2. Angiogenic and anti-angiogenic factors concentrations in GD13 metrial triangle. All panels are mean ± SEM. A) VEGF and B) PLGF (angiogenic). C) sFLT (anti-angiogenic). D) Anti-angiogenic to angiogenic ratio with angiogenic factor VEGF and E) PLGF. Asterisks indicate a significant difference between sex-matched WT and TG mice (*: $p<0.05$, **: $p<0.01$, ***: $p<0.001$).

Croy's previously published values in mice, data from WT mice in our study compared favorably (Figure 3.3A, B). Overall, pups from TG dams showed less uNK cell activation compared to WT, but this was largely a function of failure to activate uNK cells in metrial triangles related to male pups (Figure 3.3A—no change from GD6.5 to 8.5). Females from TG dams were relatively more activated compared with WT controls (Figure 3.3B), but not significantly different than published Croy expected values (23).

The potential impact of differences in metrial uNK cell activation and angiogenic/anti-angiogenic composition on spiral artery architecture was measured by 3D microCT at GD16.5 (late term). To investigate the potential impacts of fetal sex on early vasculogenesis and angiogenic pruning in the metrial triangle, we stained whole mounts at GD6.5 and GD8.5 for CD31 to highlight the vascular networks in the metrial triangle and measure vasculogenic "blebbing" as defined by Dr. Anne Croy's group (41) and vascular branching/area. There was reproducibly less vascular blebbing in the metrial triangles of TG dams compared to WT controls independent of fetal sex (Figure 3.3C). Fetal sex differences arose when analyzing the branches/area, which is a measure of vascular pruning to create proper arterial networks (41). Pruning occurs after GD6.5 yielding fewer total vascular branches per unit area (Figure 3.3D). Males from TG dams showed pruning results similar to those from WT dams, but females from TG dams did not prune their vascular networks as readily (Figure 3.3D). We suspect less pruning in females from TG dams could be a compensatory response to the relatively reduced vasculogenic blebbing driven by the TG phenotype. The consequence could be relatively normal spiral artery architecture in females from TG dams by GD16.5, which is clearly absent in males from TG dams whose corresponding metrial triangles continued pruning

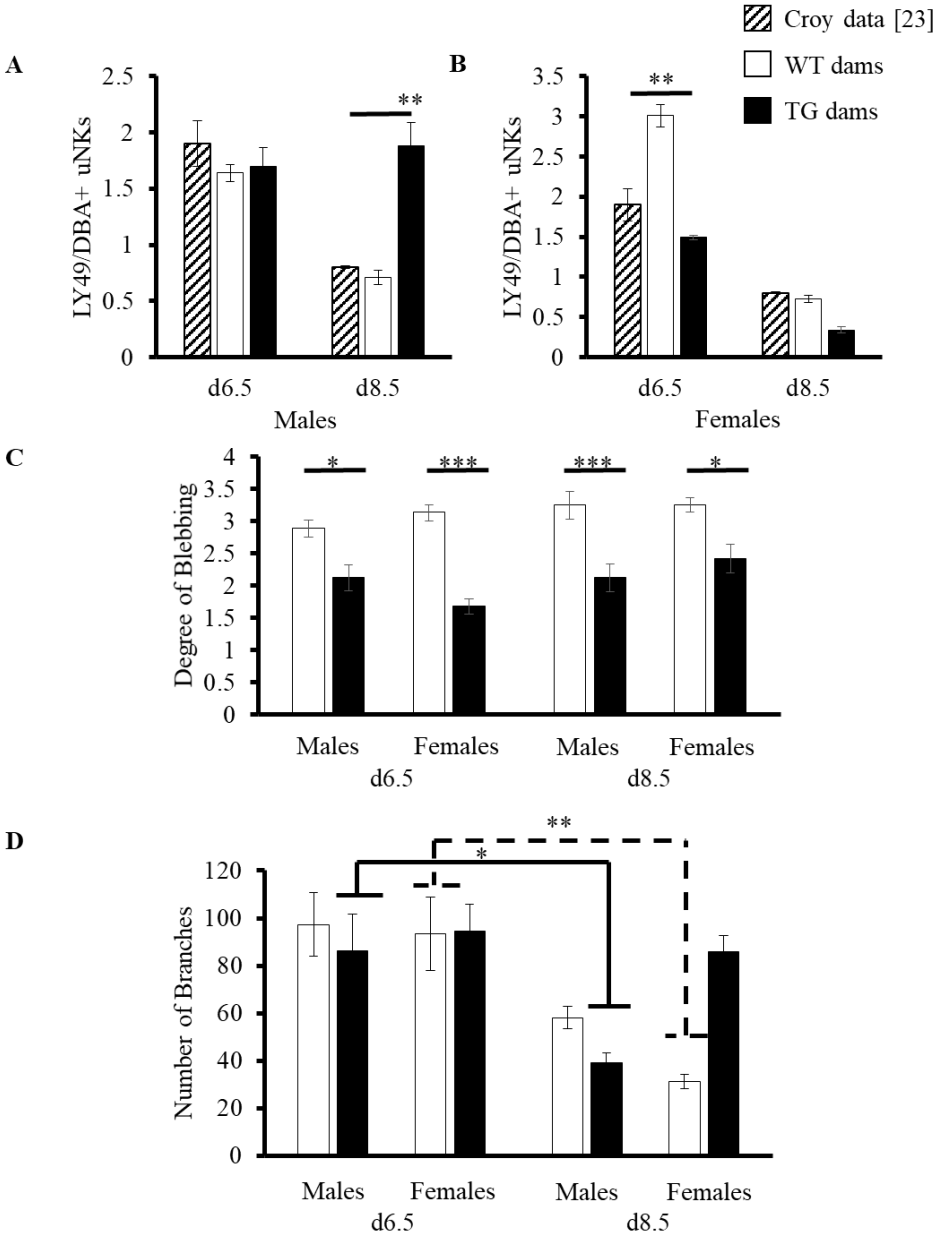

Figure 3.3. Early gestation comparisons of TG vs. WT, GD6.5 vs. GD8.5. A & B) uNK cell activation expressed as ratios (Ly49/DBA+) divided by fetal sex (A) Males, B) Females). An increase in DBA+ cells indicates uNK activation. Ly49 positive cells are inactive uNK cells. Asterisks indicate significant differences between sex-matched WT and TG mice by two-way ANOVA (*: $p<0.05$, **: $p<0.01$, *8*: $p<0.001$). Significance of interest between groups (*: $p<0.05$; **: $p<0.01$; ***: $p<0.001$): WT 6.5 F and TG 6.5 F: ***; WT 6.5 M and WT 6.5 F: **; WT 6.5 F and WT 8.5 F: ***; TG 8.5 M and TG 8.5 F: *. Trending of interest: TG 6.5 F and TG 8.5 F: 0.0969. C & D) Vascular changes divided by fetal sex. CD31 was used as a vascular endothelial marker. Number of branches and vascular blebbing were all considered as markers of angiogenesis. Asterisks indicate significant differences between sex-matched WT and TG mice by two-way ANOVA (*: $p<0.05$, **: $p<0.01$, ***: $p<0.001$). C) Degree of blebbing. Increased blebbing metric indicates increased "blurriness," an indicator of branching angiogenesis. D) Number of branches as compared by fetal sex.

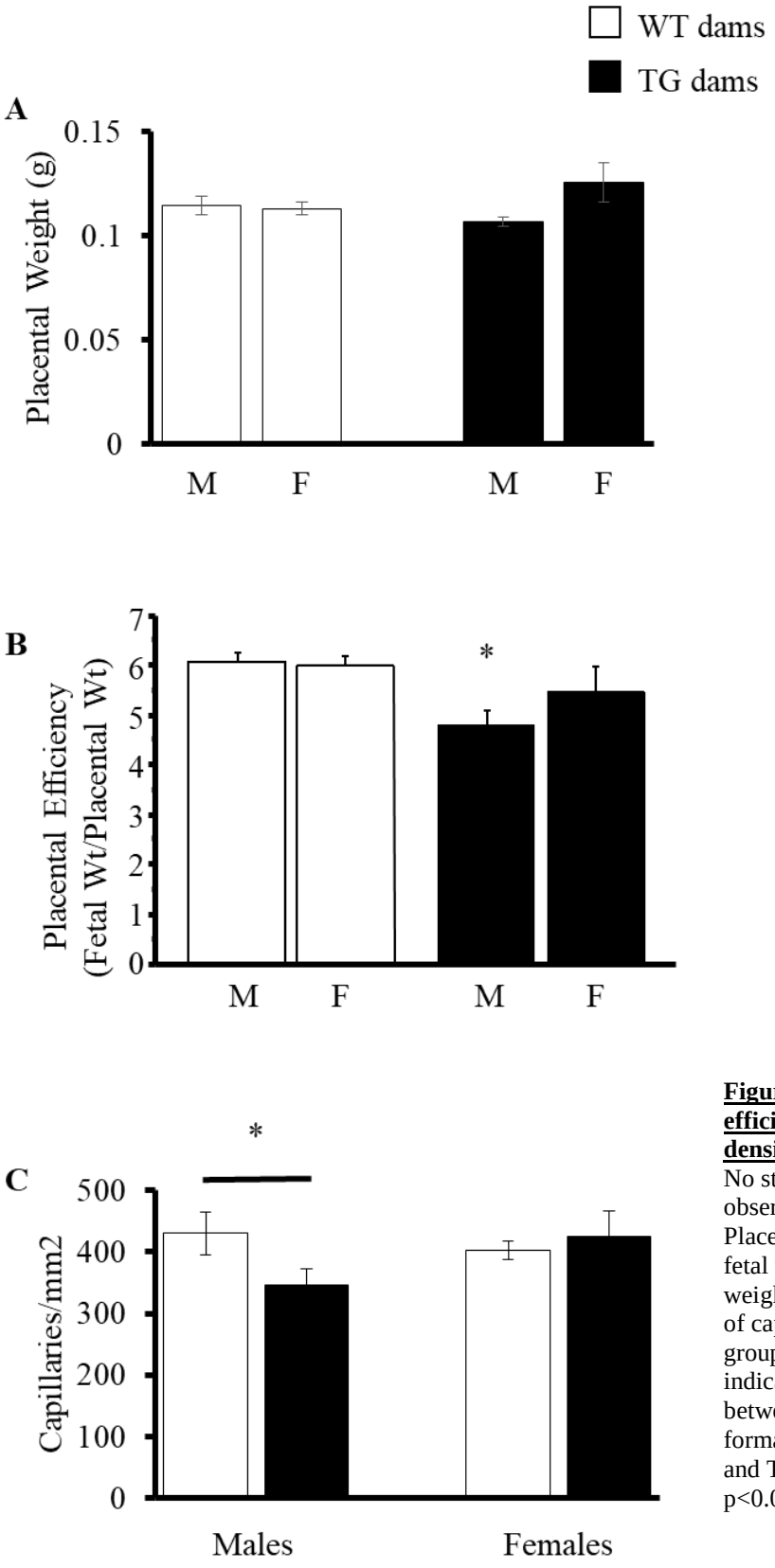

Figure 3.4. Placental weight, efficiency, and capillary density. A) Placental weights. No statistical difference was observed between groups. B) Placental efficiency (ratio of fetal weight over placental weight). C) Statistical analysis of capillary density between groups (mean ± SEM). Asterisk indicates significant difference between labyrinth capillary formation in sex-matched WT and TG mice. *: $p<0.05$, **: $p<0.01$, ***: $p<0.001$.

vascular networks despite depressed vasculogenesis. We hypothesize that uNK cell activation leads to less pruning with females from TG dams showing the most uNK cell activation at GD8.5 (Figure 3.3B) and least amount of pruning (Figure 3.3D). In contrast, males from TG dams show the least amount of uNK activation and most pruning.

Placental Histopathology, Nutrient Transport, and Transcriptomic Analysis

Males from TG dams were smaller than males from WT dams both at GD16.5 (0.48 +/- 0.03g vs. 0.55 +/- 0.02g (p=0.05)) and at birth (1.29 +/- 0.02g vs. 1.46 +/- 0.04g (p=0.02)), but females only showed a difference at birth (GD16.5 0.48 +/- 0.04g vs. 0.52 +/- 0.02g (NS), birth 1.23 +/- 0.01g vs. 1.37 +/- 0.02g ($p<0.001$)). Placental weights were similar between groups. Males from TG dams had a significantly lower fetal:placental weight ratio (placental efficiency) compared with their female siblings (p=0 05, Figure 3.4). Placental histopathologic stereometric analysis revealed fewer capillaries per unit areas in the placental labyrinths of males from TG dams compared with their female siblings and WT controls (Figure 3.4). Surprisingly, lipid and amino acid transport tended to be increased not decreased by the placentas of TG dams compared with WT controls, which was more pronounced in females from TG dams (Figure 3.5).

We elected to take both a candidate gene and more global transcriptomic approach to investigating why placentas from TG dams may have less angiogenesis and greater nutrient transport at GD16.5. First, transcriptomic analysis of microdissected placental tissue samples revealed that placentas from males from TG dams expressed far more genes than males from WT controls. There were minimal differences between females from TG and WT mice (Figure 3.6). 132 genes were similarly different in both males and females from TG dams compared with WT controls; gene ontology analysis

via DAVID revealed the most striking differences between TG and WT placental expression were related to upregulation of lipid transport pathways, upregulation of oxidation-reduction processes, and downregulation of negative regulators of the innate immune response, which implies an increase in placental inflammation. qRT-PCR

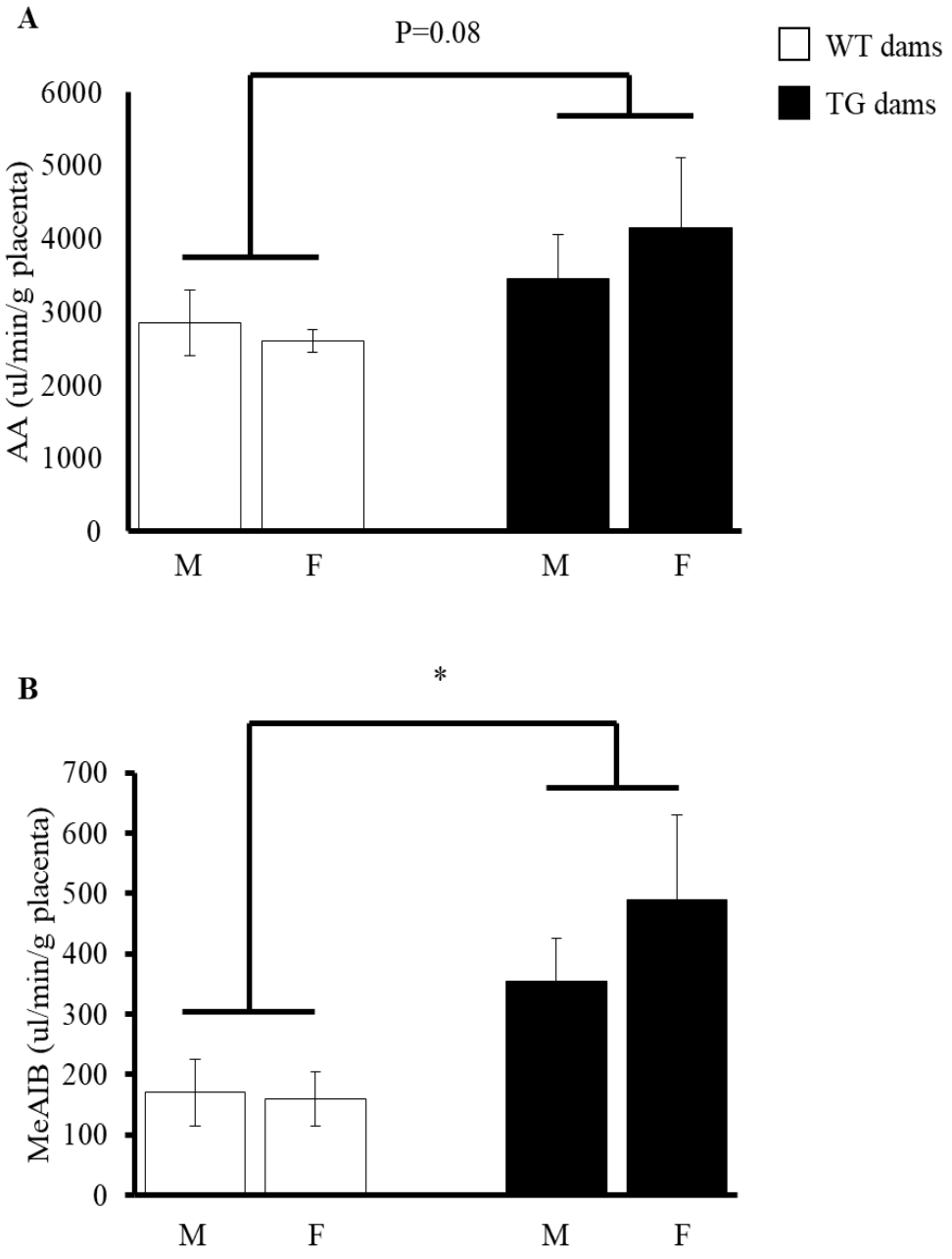

Figure 3.5. Placental nutrient transport at day 16.5 gestation. A) Lipid transport measured by labeled arachidonic acid (AA). B) Amino acid transport measured by labeled methylaminoisobutyrate (MeAIB, highly selective for Amino Acid transport system in the placentas of males (M) and females (F).

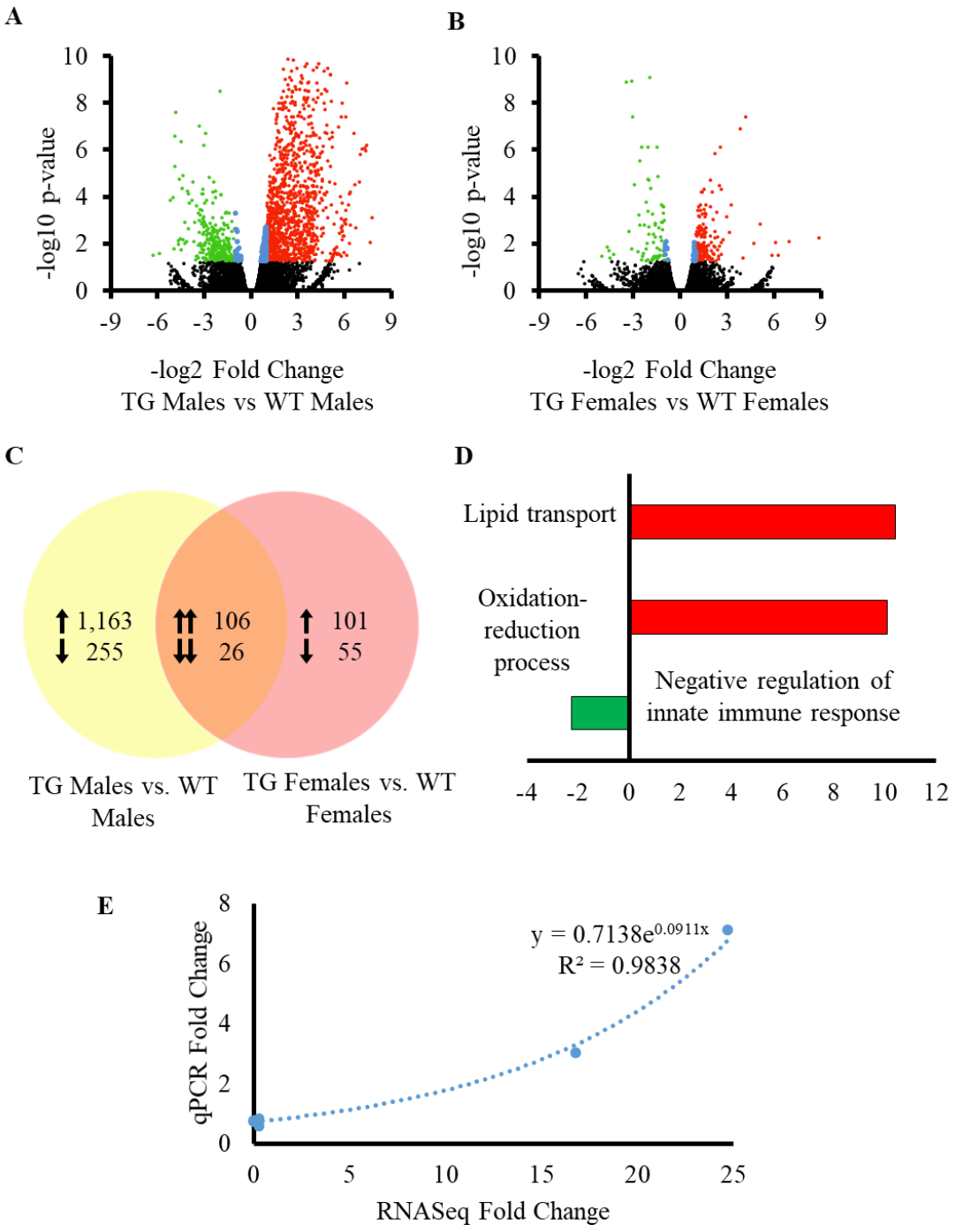

Figure 3.6. Fetal sex and maternal transgene effect on global expression analysis. Volcano plots of distribution differences, comparing expression between A) males (top), B) or females (bottom) from different maternal genotypes. C) Venn diagram quantifying up versus downregulation of genes. D) Comparison of key gene ontology group of males from transgenic vs. wild-type dams as classified by DAVID. Red indicates overexpression of gene groups in transgenic males and includes groups involved in lipid metabolism and oxidative stress. Green indicates downregulation of the negative regulation of innate immune response in transgenic males. E) Correlation of RNASeq gene expression versus qRT-PCR.

validation of candidate genes within these pathways [Supplemental Table 3.1] correlated well with fold-changes observed in RNASeq data (Figure 3.6E).

Discussion

Our data suggest that the combination of maternal genetic predisposition and male fetal sex abnormally impacts maternal uNK cell activation, uteroplacental angiogenesis, placental gene expression, and placental nutrient transport compared with controls. These observations advance the field by showing for the first time that the placentas from males may interact and communicate differently with maternal uterine tissue than the placentas from females, which appear more resistant to the maternal AGT genetic risk factor.

Maternal Genetic Predisposition for Fetal Growth Restriction

Several factors have been linked to increased likelihood of FGR, including maternal diet and maternal genetic factors. Angiotensinogen promoter variants have been associated with FGR in humans (42–44) and are the pretext for the TG mouse model used in our study. The A-6 promoter variant associated with FGR in humans is a common allele present in approximately 14% of Caucasians and imparts a 20-fold increased risk of having pregnancy complications compared with the G-6 allele. Similar risk has been reported in studies of Japanese women (45, 46). Several other maternal genes have also been shown to increase risk. For example, the single nucleotide polymorphism G-308A of *TNF-α* is associated with FGR, preterm birth, and increased infant mortality (47–49). Placentas with this *TNF-α* mutation were also more sensitive to increased Angiotensin II and released more inflammatory cytokines (50). Additionally, the 14-bp insertion into the 3’-untranslated region of *HLA-G* coupled with an increased G*0106 allele frequency has

been reported to be more common in pregnancies complicated by preeclampsia and miscarriage (51).

To better understand the underlying pathophysiology of FGR, several mouse models have been developed to mimic the human condition. We used the AGT 3-copy transgenic mouse originally made by Dr. Oliver Smithies (52) backcrossed into our WT controls. This construct expresses 20% more systemic AGT than WT and presents with gestational hypertension and FGR, similar to women with the A(-6) promoter variant (31, 45, 53). *TNF-α* knockout mice have been studied by others, which seems to protect against placental pathology caused by infection (54). More relevant to the placental insufficiency model, the endothelial nitric oxide synthase (*eNOS*) knockout model also demonstrates reduced uterine spiral artery angiogenesis and reduced placental nutrient transport (55). *eNOS* knockouts also show elevated superoxide production, which can affect metabolic function similar to what we observed in our model (56, 57).

Angiogenic/Anti-angiogenic Axis

Males from TG dams increase release of anti-angiogenic sFlt1 without a corresponding increase of pro-angiogenic VEGF or PLGF. The pro- and anti-angiogenic ratios appeal to be critical hallmarks of FGR in our model. Both males and females from TG dams showed increased anti-angiogenic sFlt1 production detected in maternal blood and in metrial triangle tissue samples. However, only males from TG dams were associated with reduced VEGF and PLGF levels in the metrial triangles. This may explain why males were associated with less spiral artery and placental angiogenesis.

VEGF binds cell-surface tyrosine kinase VEGFRs for vascular and endothelial growth (58). PLGF, a member of the VEGF family, is structurally similar to VEGF and

shares a receptor, VEGFR-1. VEGFR-1 activation stimulates angiogenesis, but the location of VEGFR-1 activation is also important (60). Endothelial-mediated activation may have entirely different effects on angiogenesis than VEGFR-2 or VEGFR-1 activation in the surrounding uterine decidua or vascular media. sFlt1 is the soluble splice variant of receptor VEGFR-1 and acts as an anti-angiogenic decoy molecule, binding and sequestering pro-angiogenic PLGF and VEGF. Notably, increasing Angiotensin II enhances release of sFlt1 by placental trophoblasts, leading to excessive sequestering of critical growth factors (61–63).

Impact of Maternal Genotype and Male Fetal Sex on Spiral Artery Architecture

Male fetal sex in TG dams, but not WT dams affected uteroplacental angiogenesis. Importantly, we excluded TG (3-copy) progeny from TG dams in our analyses. We only included 2-copy (WT) progeny from TG dams to control for this potential covariate. The additional confounding element of fetal AGT genotype is a subject of future studies by our group. Nonetheless, the "WT" (2-copy) genetic male progeny from TG dams affected maternal uNK cell activation, maternal uterine angiogenesis, and the final structure of maternal spiral artery architecture.

The maternal uterine spiral arteries did not branch and coil in the placental beds of males from TG dams as much as their female siblings or WT controls. Spiral artery remodeling begins early in pregnancy and is complete by mid-gestation in mice (64). We tested for differences during the period when uNK cells begin to be activated (65, 66) and observed less uNK cell activation in the metrial triangles of males from TG dams, but not in their female siblings compared with WT controls. Notably, there were no significant

differences in uNK cell activation in males versus females from WT dams, suggesting the combination of maternal genetic risk and male fetal sex led to the abnormal phenotype.

Uterine NK cells are thought to play a key role in modulating early angiogenesis and pruning to create proper spiral arteries for normal uteroplacental blood flow and nutrient delivery to the fetus (67). When activated, they release VEGF and stimulate angiogenesis, which we measured by the degree of blebbing (41) in whole mounts of the metrial triangle. They are then inactivated by mid-gestation as the angiogenic network is pruned into functional spiral arteries. Uterine NK cell activation begins early in pregnancy (GD6.5) and they are inactivated by mid-gestation (66). Our data suggest that male fetal sex somehow inhibits normal maternal uNK cell activation leading to less angiogenesis. Their female siblings also showed less angiogenic blebbing compared with WT controls, but they seemed to compensate by reducing the degree of vascular pruning at GD8.5, which may explain why these females had relatively normal spiral artery architecture after mid-gestation (GD16.5 measured by 3D microCT). We and others suspect that activated uNK cells may not only play a role in stimulating angiogenesis, but they may also modulate pruning (24, 68, 69). Poor uNK activation related to male fetal sex in TG dams may be the reason why we observe less angiogenesis and more pruning in males from TG dams.

How the placenta communicates with maternal uNK cells is not entirely clear. In humans this may be through direct interaction or via T-cells and dendritic cells. Trophoblast invasion occurs near the end of first trimester human gestation and may allow for direct recognition of HLA class I molecules by uNKs to influence spiral artery remodeling and function (70). CD56+ uNKs interact with T cells to release interferon

gamma to protect against infection (71), or with dendritic cells via HLA-G and TNF-α antigens (54). In early gestation, uNKs are thought to partner via antigen presentation to T cells (predominantly CD8+) (66). In mice, however, uterine spiral arteries remodel before trophoblast invasion, so a paracrine signaling mechanism is more likely than a direct contact model. We are currently exploring this new concept by assessing both trophoblast invasion depth in murine spiral arteries and paracrine signaling by extracellular vesicles (EVs) released by the placenta targeting maternal uNK cells, endothelial cells, or other cells potentially involved in spiral artery angiogenesis. EVs may regulate maternal angiogenesis and immune functions by carrying placental signals to target maternal tissues (72). We hypothesize that proteins and small RNAs (microRNAs) are delivered by EVs to maternal cells. To test this, we have recently begun experiments on a Cre-*loxP* mouse dam expressing ubiquitous tdTomato and a placenta-specific Cre sire. Cre recombination in a LoxP host cell will induce GFP expression in the placenta, released placental EVs, and transformed maternal tissues (73).

Fetal Sex Affects Placental Gene Expression

The main differences between placentas from males compared with females were related to upregulation of genes involved in nutrient transport and downregulation if immune response genes. There is little known about fetal sex effects on placental gene expression (19, 74). Our RNASeq data revealed a few expected fetal sex differences related to the expression of genes on X and Y sex chromosomes. Males from TG dams had lower expression of X chromosome genes linked to brain development (*BEX* family (75)), but higher expression of genes part of the infection response and lymphoproliferative pat hways (*Sh2d1* family (76)) compared to sex-matched controls. If

X-linked gene differences play an important role in placental mediation of uteroplacental angiogenesis, relationships between fetal X chromosome aneuploidy and an increased risk for fetal growth restriction would be expected. This would be confounded by the known impact of aneuploidy in general leading to small placentas and small babies with the exception of Turner's Syndrome (X0) (77–79).

There were differences in fetal sex hormone production revealed by our RNASeq data. For example, male placentas from TG dams upregulate the gene *HSD3B1,* which encodes for 3-beta-hydroxysteroid dehydrogenase isomerase, an enzyme in the steroid synthesis pathway, and increased *HSD3B1* increases progesterone and androgen levels (80–82). Progesterone blocks estrogen receptor 1 (*ESR1*) expression, which was notably reduced in male placentas from TG dams. This may be significant because *ESR1* encodes for estrogen receptor alpha (ERα); knocking out ERα is known to reduce angiogenesis in mouse models (83, 84). In humans, males from gestational diabetic pregnancies also have decreased *ESR1* (85). *ESR1* likely regulates angiogenesis via the VEGF pathway, which is downregulated with reduced estrogen reception activity (86–88).

Consequences of Abnormal Maternal Spiral Artery Architecture

In Chapter 2 we showed that differences in spiral artery architecture lead to differences in uteroplacental blood flow and placental damage. We could not control for fetal sex in those blood flow studies performed *in vivo* because of the limitations of ultrasound imaging resolution in mice at day 16.5. This is because we cannot accurately discriminate the precise location of each uteroplacental unit within the right and left uterine horns by ultrasound imaging. In the current study, however, we could precisely measure nutrient transfer by each placenta and relate these metrics to fetal sex. We made

these measurements late in gestation (GD16.5) to correlate with documented uteroplacental vascular architecture, uteroplacental blood flow, and known fetoplacental growth restriction at this gestational age in our mouse model. Provided that the placentas from TG dams are relatively smaller and more damaged than WT controls, we were surprised to observe significantly more lipid and amino acid transfer by placentas in TG dams. Placental transcriptomic data was also obtained from placentas at GD16.5 and predicted increased lipid and amino acid nutrient delivery at GD16.5.

We suspect that increased nutrient delivery in the placentas of TG dams late in gestation may be a compensatory mechanism rather than an underlying cause of FGR in this model. We did not test placentas earlier in gestation, but it is well known that other FGR models also show increased uteroplacental nutrient delivery later in gestation (89–91). Future studies will test whether placental RNA expression and nutrient delivery are different in those from TG dams and related to fetal sex when examined at GD12.5; this is the earliest gestational age for reliable placental micro-dissection in our experience.

Study Limitations

These observations are intriguing and may lead to a better understanding of why human males seem to be more likely to be stillborn, growth restricted, and why they are more likely to have developmental programming of adult onset diseases (8). A potential limitation of our study, however, is the assumption that humans and mice may share pathogenic mechanisms. Since mouse placentas are different than human placentas, it may not be a good model and the underlying mechanisms may be entirely different (92). It is true that human placentation and murine placentation differ in a number of ways, from overall structure to the criticality of trophoblast invasion (26, 93). However, both

animals grow uterine spiral arteries and both may share similar placental:maternal uterine interactions regulating this essential process (22, 26). The advantage of using a mouse model is the power of transgenics to mimic human maternal genotypes and the power of comparing males and female siblings from the same litters. Most importantly, animal models are required to sample uteroplacental tissues throughout gestation—an advantage not possible for human studies until better “liquid biopsies” of the uteroplacental environment are available.

This work provides new insights into the combined effects of maternal genetic risk and fetal sex. Our observations suggest that male fetal sex in high risk pregnancies may compound maternal pathology, perhaps due to differences in uNK cell activation and early differences in uterine vascular remodeling.

Supplemental Table 3.1. Primer sequences for AGT and SRY PCR. PCR for AGTdup was used to determine copy number and differentiate between 2-copy and 3-copy AGT mice. SRY was used to determine male fetal sex.

Primer Name	Sequence
AGT oIMR0750	5'-ACACTCAGAGACCATGAGTACACC-3'
AGT oIMR0751	5'-GAGTTCACTACCCACAAGTCTCC-3'
SRY Forward	5'-AGAGATCAGCAAGCAGCTGG-3'
SRY Reverse	5'-TCTTGCCTGTATGTGATGGC-3'

Supplemental Table 3.2. Genes identified from gene ontologies for verification.

Gene Name	Selected Related Gene Ontology Groups p<0.05	RefSeq
Fabp1	GO:0008289	NM_017399.4
Fabp4	GO:0050727	NM_024406.2
Acox2	GO:0016042, GO:0005777, GO:0055114, GO:0006631, GO:0016054	NM_001161667.1, NM_053115.2
Cox1	GO:0020037, GO:0009055, GO:0055114	NCBI Gene ID: 17708
Cox2	GO:0020037, GO:0009055, GO:0055114	NCBI Gene ID: 17709
Clec2d	GO:0045824, GO:0045088, GO:0002697,GO:0002716, GO:0031342, GO:0006952, GO:0031341	NM_053109.3
Klrb1b	GO:0045824, GO:0031342, GO:0031341	NM_030599.4
Gapdh	Control	NM_001289726.1, NM_008084.3

Chapter 4

Renal DNA Methylation and the Developmental Programming of Stress-Induced Hypertension in Male Mice

Abstract

Fetal growth restriction is associated with developmental programming of adult onset hypertension, which may be related to differences in kidney nephron development. Prior studies have shown that maternal protein restriction is associated with reduced fetal nephrogenesis in rodent models. We hypothesized that a transgenic (TG) mouse model of fetal growth restriction may similarly affect fetal kidney development leading to adult onset hypertension. We employed a previously described murine angiotensinogen (AGT) gene titration model known to develop stress-induced hypertension in male mice with 3 copies of AGT compared with 2 copies of the gene. In this study, we investigated whether fetal growth restriction in 2-copy mice from 3-copy TG dams (designated pTG) leads to developmental programming differences in kidney development and blood pressure compared with age- and sex-matched wild-type (WT) mice from WT dams. Progeny were tested at birth, as 2 week old "neonates," and as adults (12 weeks old). We measured weights, tested for renal oxidative stress using the Hydroxyprobe assay, tested for renal DNA methylation differences, quantitated the number of nephrons/kidney by stereology, and measured adult blood pressure by radio-telemetry +/- stress induction. Our results show that progeny from TG dams were born about 10% smaller, they showed signs of fetal renal oxidative stress, and there were renal DNA methylation differences in their male pups, but the number of nephrons was not different at 2 weeks of age

compared with WT controls. By 12 weeks of age, however, 2-copy male progeny from TG dams had relatively smaller adult kidneys with fewer total nephrons and they developed stress-induced hypertension like their 3-copy male siblings. We conclude that developmental programming of hypertension may involve differences in post-natal kidney DNA methylation and subsequent growth, rather than reduced nephrogenesis.

Introduction

Fetal growth restriction is associated with developmental programming of adult onset hypertension and cardiovascular disease (1-8). Although hypertension is a multifactorial disease, many studies have shown developmental programming related to the *in utero* environment is also a major contributor to the variance in adult blood pressure in humans (6-10) and in animal models (11-14). Animal models employed to investigate the underlying mechanisms typically use differences in maternal diet (macronutrient profile alteration), uteroplacental insufficiency generated by placental embolization (15), or surgical ligation of major vessels feeding the placenta (13, 16). These studies have yielded important insights into the relationship between placental insufficiency caused by differences in maternal nutrition or differences in blood flow to the placenta. However, severely restricted low protein maternal diets, or significantly decreasing blood flow to the placenta, are manipulations with known limitations that may not be applicable to most human pregnancies, especially in developed nations.

In contrast, our group employs a mouse model designed to mimic a common human angiotensinogen (AGT) genetic variant associated with chronic hypertension and obstetric complications of placental insufficiency in women (17-19). The murine AGT

gene duplication (*3-copy*) transgenic (TG) mouse model was originally generated and characterized by Smithies et al (19) to mimic the 20% increase in circulating plasma AGT levels observed in humans with the common A(-6)G promoter variant (17, 18). Smithies demonstrated that these 3-copy mice develop elevated blood pressure compare with controls by employing tail-cuff plethysmography (19). This blood pressure result has been challenging to reproduce with more recent radio-telemetry technology, however, suggesting that a relative "stress-induced hypertension" may be a more accurate phenotype of the 3-copy TG model.

We hypothesize that wild-type (WT) progeny from TG dams crossed with WT males may similarly develop "stress-induced hypertension" like their 3-copy siblings. In addition, since the progeny of TG dams are born relatively smaller than controls, we suspect that they may have fewer nephrons similar to other rodent growth restriction models (11). This would be important because reduced nephron number is associated with chronic hypertension in adult humans (20). Reduced nephron number also seems to be a consequence of placental insufficiency in adult rats (11, 21) and sheep (22). Notably, in rats, the kidney's nephron number is established by post-natal day 10 (23). Maternal protein restriction in rats seems to affect nephrogenesis, rather than post-natal kidney development (21), but this is not entirely clear. Increased fetal oxidative stress could also play a role in this process (24). Therefore, our objective was to test whether placental insufficiency and fetal growth restriction in TG dams leads to elevated fetal renal oxidative stress, reduced nephrogenesis, and adult onset stress-induced hypertension.

Methods

Transgenic Mouse Model of Placental Insufficiency: Transgenic mice with 3 copies (*AGT*dup) of the murine *Agt* gene on a C57Bl/6J background (strain number B6.129P2-Tg(*AGT*dup)1Unc/J), as well as control C57Bl/6J mice (WT) with the normal 2 copies of *Agt*, were obtained from The Jackson Laboratory (Bar Harbor, ME) and back-crossed into C57Bl/6J for at least 10 generations before performing the described experiments. Our group has previously published pregnancy-related experiments using this model (25). The colony is maintained under an IACUC-approved protocol # B11130 with free access to food and water. They are housed under standard temperature-controlled 12:12hr light:dark conditions. TG dams were generated *de novo* for each breeding experiment by using 3-copy females from WT dams bred with TG males. We had previously discovered that using TG females from TG dams caused significant generational effects (miscarriage, infertility, very small litter sizes) as a confounding variable. Therefore, for the purposes of these experiments, all TG females used for breeding were progeny from WT dams. At least 4 litters per maternal genotype were used for all experiments. 2-copy (WT) progeny from TG and WT dams were used for all analyses with the exception of 3-copy male siblings used as positive controls for blood pressure studies (19).

Genotype and Sex: AGT genotype and fetal sex were determined by PCR using specific primer sets that yielded products of expected size and DNA sequence:

Agt oIMR0750 (from The Jackson Laboratory genotyping protocol)

5’-ACACTCAGAGACCATGAGTACACC-3’ and

Agt oIMR0751 5’-GAGTTCACTACCCACAAGTCTCC-3’); or

Sry Fwd 5’-AGAGATCAGCAAGCAGCTGG-3’ and

Sry Rev 5'-TCTTGCCTGTATGTGATGGC-3'. Briefly, fetal livers were digested in Proteinase K overnight, then genomic DNA was isolated using the QIAgen DNeasy kit with the spin-column protocol (QIAgen, Inc., Valencia, CA). PCR was performed on the genomic DNA, in separate reactions, to determine 1) *Agt* genotype and 2) sex by presence or absence of the *SRY* gene. Both PCR reactions used the following cycling parameters: initial melting at 94C for 2 min; followed by 40 cycles of 94C for 20 s, 65C for 30 s, 72C for 30 s; followed by a final 72C extension for 5 min. All samples have the endogenous AGT genetic PCR product (160 bp), which served as an internal positive control for the PCR reaction. WT genotypes had only the 160 bp band; whereas, AGT 3-copy mice (TG) showed both a 160 bp band and a 189 bp band for the AGTdup transgene. In the SRY reaction, a 249 bp band indicated male fetal sex; females lacked the SRY band, but retained the AGT product.

Blood Pressure Measured by Radio-Telemetry +/- Stress Induction: At 12 weeks of age, progeny from TG (5 litters) and WT (5 litters) dams (litters used for birthweight studies, blood pressure studies, renal stereology) underwent surgical placement of carotid telemetric blood pressure transducers (Data Sciences, Intl., St. Paul, MN). Briefly, surgery was performed under anesthesia using inhaled isoflurane (O_2 flow rate of 1.5L/min & 4% isoflurane for induction; O_2 0.5L/min and 1.5% isoflurane during surgery). Radio transmitters were placed in a subdermal pouch at the ventral abdominal area and then the probe was tunneled under the skin into the neck. The blood pressure transducer (Chronic Use TA11PA-C10 Implant, DSI) was then placed into the left carotid artery and secured with a suture. Animals were allowed to recover 7 days. The mean arterial blood pressures (BP) were measured each day beginning at 10 am for 4

consecutive days using PhysioTel telemetry receivers (model RPC-1, DSI) placed under each cage. Mean arterial pressure was recorded for 2 hrs using DataQuest Advanced Research Technology Gold Acquisition software (Version 2.20, DSI) with data points recorded as 15-second averages. The final 30 min of this 2-hr recording was reported as the BP at "REST." After this rest period, mice were spontaneously STRESSED by briefly shaking the cage followed by loud music torture (*Led Zeppelin*) for a 30-minute recording period. The average values from 4 days of data collection were reported for each mouse as the REST or STRESS mean arterial pressures. Heart rate, systolic, and diastolic pressure were not measured in this experiment. Male 3-copy siblings from the TG litters served as blood pressure positive controls.

Nephron Counting by Stereometry: After the completion of blood pressure studies, these 12 week old mice were euthanized and their kidneys were harvested for analysis. They were each weighed, measured, cut in 2-mm thick transverse slices, fixed, paraffin-embedded. Randomly sampled slices were embedded in Technovit (Heracus Kulzer GMBH, Wehrheim, Germany), and 3 sections (15-μm thick) were cut from the middle of the embedded slices; sections were stained with periodic acid-Schiff stain and hematoxylin, the 1st and 3rd stained sections were used for nephron counting as described previously (11). A separate section was stained with hematoxylin and eosin and analyzed for evidence of glomerulosclerosis by a pathologist (TKM) blinded to the experimental condition of the animal. In addition, to determine whether differences in nephrogenesis occur during development or after the post-natal period, we included a cohort of "neonatal" progeny harvested two weeks after delivery (day 14) from 5 WT and 5 TG litters. This timeframe was chosen to ensure complete development (23) without allowing

for the initiation of nephron dropout with increasing age. The area of the renal cortex in neonates was outlined and measured using *ImageJ* to provide a nephron density metric.

Fetal Renal Hypoxia Analysis*:* To study the potential role of oxidative stress in fetal kidneys leading to nephron loss, we employed the commercially available *Hydroxyprobe* kit (Hypoxyprobe, Inc., Burlington, MA) injecting dams (n=4-6 litters per maternal genotype: TG, WT) intraperitoneally at e18.5 with 60mg/kg. After two hours, dams were anesthetized with isoflurane and one maternal kidney was transiently ligated as a positive control tissue for histologic analysis. Placentas were removed and fixed in formalin for paraffin-embedding and Hydroxprobe analysis. Fetal kidneys and livers were removed as described below for similar analysis. Tissue sections were immunostained in batch and in duplicate for 1) tissue hypoxia using the Hypoxyprobe kit (Hypoxyprobe, Inc.); 2) cell proliferation using Ki-67; and 3) evidence of apoptosis using an ApopTag kit (Sigma-Aldrich, St. Louis, MO). Ligated maternal kidney served as a positive control for Hydroxyprobe studies; human endometrium was the positive control for Ki-67 and apoptosis. Sections were scored by an anatomic pathologist (tkm) and student who were both blinded to maternal phenotype as negative (0), weakly positive (1), or strongly positive (2). Discrepancies between reviewers were adjudicated and consensus scores were reported as the mean per fetal sex per litter.

Fetal Kidney DNA Methylation Analysis: Genomic DNA was isolated from whole fetal kidneys (e18.5), then cut with restriction enzyme *MseI*, and enriched for methylated DNA using an anti-5-methyl cytidine antibody for DNA methylation analysis using a *NimbleGen DNA Methylation Array* performed by Roche-Nimblegen (Roche Sequencing Solutions, Madison, WI). CpG-specific log2-ratios were obtained from Roche-Nimblegen

(RNG) as PAIR files and processed by RNG's Detect_DMR algorithm (with "high-sensitivity" setting and 750bp window). For each CpG, the algorithm pools of all probes within 750bp in either direction were applied to a linear mixed effects model with random intercepts representing probe effects and a fixed effects model representing progeny of Tg vs. controls log-fold-change. Using the *qvalue* package in R, nominal CpG-specific p-values were subsequently converted to q-values do derive false discovery rates. As a global comparison of sex-specific effects, the sex-specific array-wide distributions of fixed regression coefficients representing CpG-specific effects of progeny of Tg vs. controls, i.e. log-fold-changes were compared using the Kolmogorov-Smirnov test. All nominal p-values were Bonferroni-adjusted. In addition, using a published approach, values were adjusted to compensate for potential differences in cell composition in kidneys (26). This is important because unlike methylation studies using cell lines, whole organ analysis is confounded by mixed tissue composition and compensation must be made for potential differences between the contributions of metabolically active proximal tubes compared with interstitial stromal cells. Statistical adjustments for expected numbers of cell types and relative composition (provided by relative nephron density stereology studies in this case—see below) were used to generate volcano plots and unsupervised heat maps to compare groups.

Statistical Methods: Weights, nephron number, and BP means were compared using two-way ANOVA with Bonferroni post hoc analysis, using Maternal Genotype and Sex as factors. If significant interactions were found ($P_{INT}<0.05$), sexes were analyzed separately using unpaired t-test with or without Welch’s correction for different variances as appropriate. For nonparametric measures (Hypoxyprobe, Ki-67, ApopTag), Mann

Whitney U tests were used to test effects of Maternal Genotype and Sex separately. For all tests, $P<0.05$ was considered significant. Data are presented as means ± SEM.

Results

Sex Differences in Fetal Growth Restriction and Adult Catch-Up Growth

The progeny of TG dams were growth restricted at birth (male (1.29 ± 0.04g; $P<0.03$) and female (1.23 ± 0.01g; $P<0.0001$)) compared with age- and sex-matched WT controls (1.46 ± 0.05g and 1.37 ± 0.02g, respectively). Interestingly, both sexes showed a relative drop in weight compared with matched WT controls at 1 week of age (Figure 4.1). Following weaning at 3 weeks of age, body weights remained reduced in the TG progeny ($P<0.0001$ for males, $P=0.0006$ for females). They then showed catch-up growth with females slightly exceeding WT females by 12 weeks; however, males did not catch-up (pTG males 29.75 ± 0.63g versus pWT males 32.17 ± 0.48g; $P<0.02$).

Fetal Growth Restriction Leads to Stress-Induced Hypertension

There was no difference in mean arterial pressure at rest between any of the adult mice, including 3-copy male "positive controls" and progeny from TG and WT dams (Figure 4.2). However, similar to the likely stressor of tail-cuff plethysmography employed by Smithies' group in his original characterization of this TG model (19, 27), we observed a statistically significant increase in BP in stressed 3-copy male controls (Figure 4.2A). Their 2-copy male siblings showed a less robust stress response, but they too demonstrated an increase in BP ($P<0.05$) compared with WT males exposed to the same stressors and measured at the same time. Females from TG dams did not have stress-induced hypertension, unlike their male siblings (Figure 4.2B).

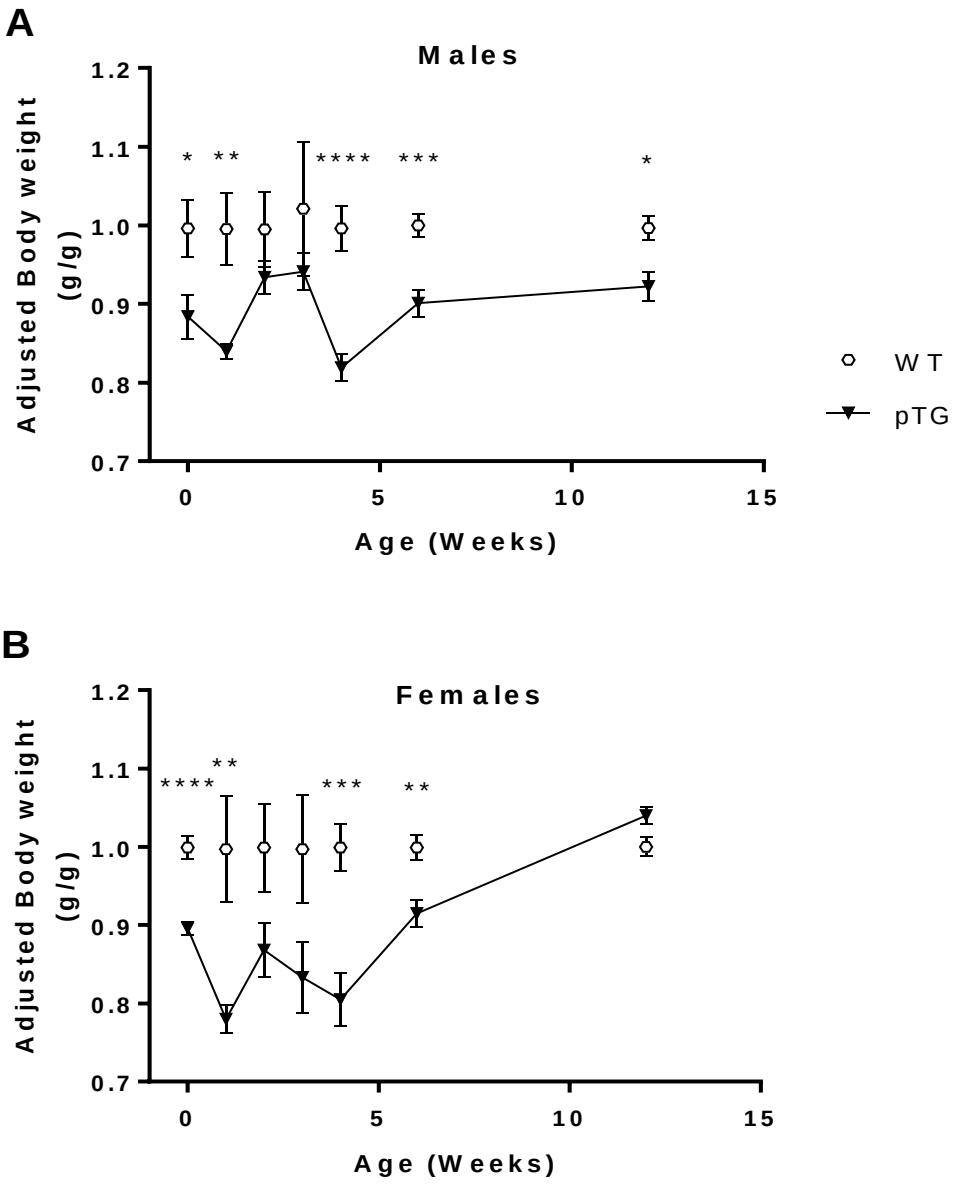

Figure 4.1: Birthweight and Catch-Up Growth of Progeny from TG and WT Dams. The sex-specific mean body weight for 10 litters was averaged and presented as means ± SEM from birth through 12 weeks for the progeny of TG dams (closed triangles) relative to the body weight of age-matched WT controls (open circles). Data are separated by fetal sex (A and B). *P<0.05; **P<0.01; ***P<0.001; ****P<0.0001.

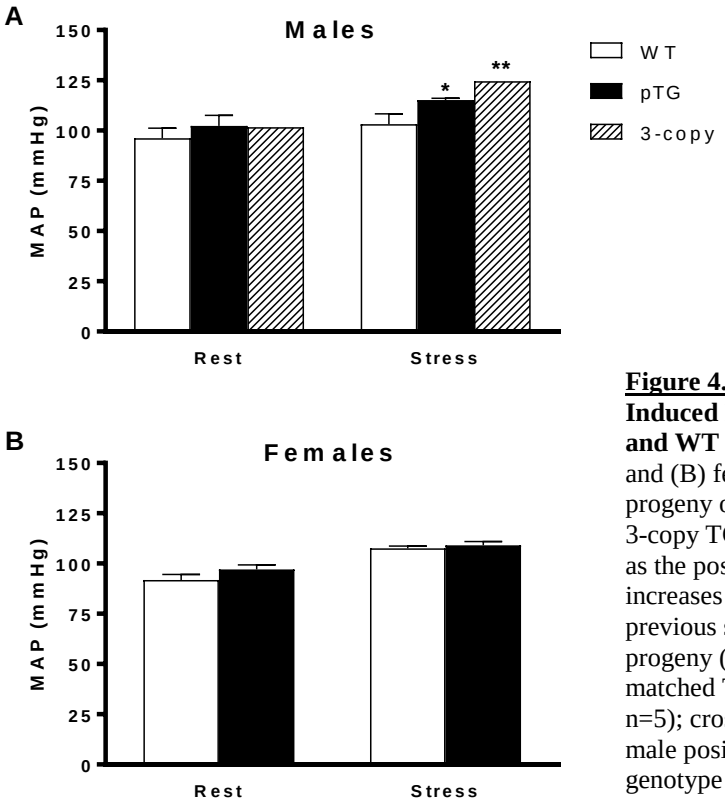

Figure 4.2: Adult Resting and Stressed-Induced Blood Pressure in Progeny of TG and WT Dams. Blood pressure for (A) males and (B) females shown as means ± SEM for progeny of TG dams (pTG) and WT controls. 3-copy TG male progeny of WT dams served as the positive control for stress-induced increases in blood pressure for comparison to previous studies (19). Data are from adult WT progeny (males, n=5; females, n=6); age-matched TG progeny (males, n=6; females, n=5); cross-hatched bar is data from 3-copy male positive controls (n=6). *Maternal genotype effect, $P<0.05$.

Neonatal Renal Morphometry and Nephron Number

At 2 weeks of age, neonatal nephron density within the renal cortex was very similar in males and females from TG and WT dams (Figure 4.3A). However, by 12 weeks, their adult relations clearly showed fewer glomeruli/kidney in male progeny from TG dams (Figure 4.3B). We suspect this may be related to differences in post-natal kidney growth into adulthood, because kidney weights were very similar between groups in 2 week old neonates (pTG males 42.3 ± 1.8 mg versus WT males 44.3 ± 1.2 mg) but significantly less in adult pTG males compared with age-matched male WT controls Figure 4.3C). Interestingly, females from TG dams seem to have slightly larger kidneys with slightly more nephrons/kidney than WT females, but this was not statistically

significant. Renal function was not compared between groups, but histologic examination of kidney sections by a renal pathologist revealed no diagnostic pathology (e.g. negative for glomerular sclerosis, arteriopathy, interstitial inflammation).

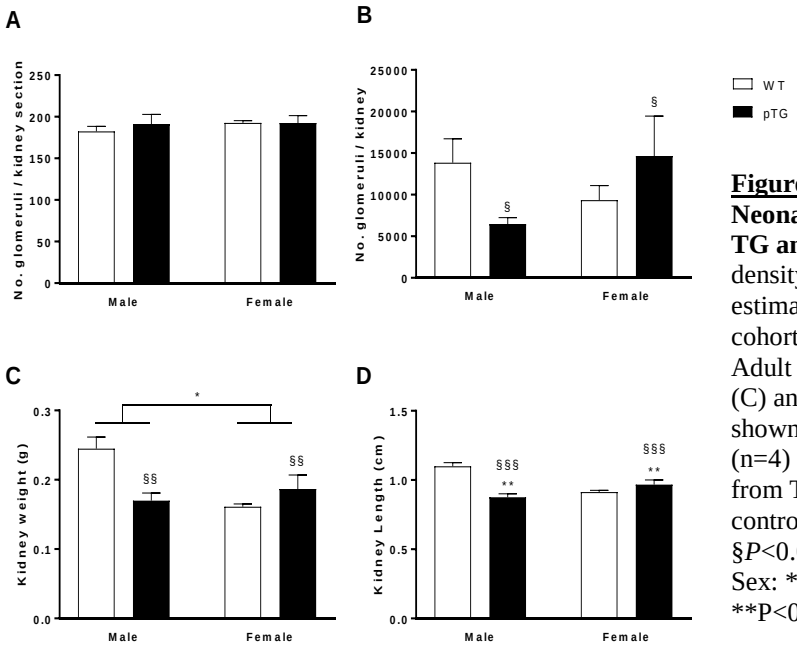

Figure 4.3: Glomerular Number in Neonatal and Adult Progeny of TG and WT Dams. A) Nephron density in neonatal cohort . B) Total estimated nephron number in adult cohort determined by stereology. Adult kidney weight in grams (g) (C) and length (cm) (D). Data are shown as means ± SEM for male (n=4) and female (n=4) progeny from TG dams (pTG) and WT controls (male, n=6; female, n=8). §*P*<0.05, §§P<0.005, §§§P<0.0001; Sex: *P<0.05; Maternal genotype: **P<0.005.

Fetal Renal Oxidative Stress in Growth Restricted Progeny from TG Dams

Hypoxyprobe is an *in vivo* assay used to label relatively hypoxic tissues with a marker than can then be detected *ex vivo* by immunohistochemistry. Partially ligated maternal kidneys served as a positive control for the Hydroxyprobe assay and they reproducibly showed positive immunostaining in the proximal tubule cells, which were negative in the contralateral maternal kidney (data not shown). In TG dams, this control was not actually necessary because the placentas in these litters were strongly positive for Hydroxyprobe immunostaining. In contrast, none of the placentas from WT litters were positive. Fetal kidneys from TG dams similarly showed reproducible staining in their proximal tubules (Figure 4.4A), independent of fetal sex, which was absent in WT

controls (Figure 4.4A, B). To determine whether oxidative stress led to different compensatory responses in male and female fetal kidneys we immunostained serial sections for Ki-67 (proliferation marker) and ApopTag (apoptosis marker). Provided our stereology results from adults, we hypothesized that males from TG dams would have less Ki-67 and/or more tubular apoptosis compared with their female siblings. This hypothesis was incorrect. There was not statistically significant difference in tubular proliferation index, or apoptosis, between groups (Figure 4.4C, D).

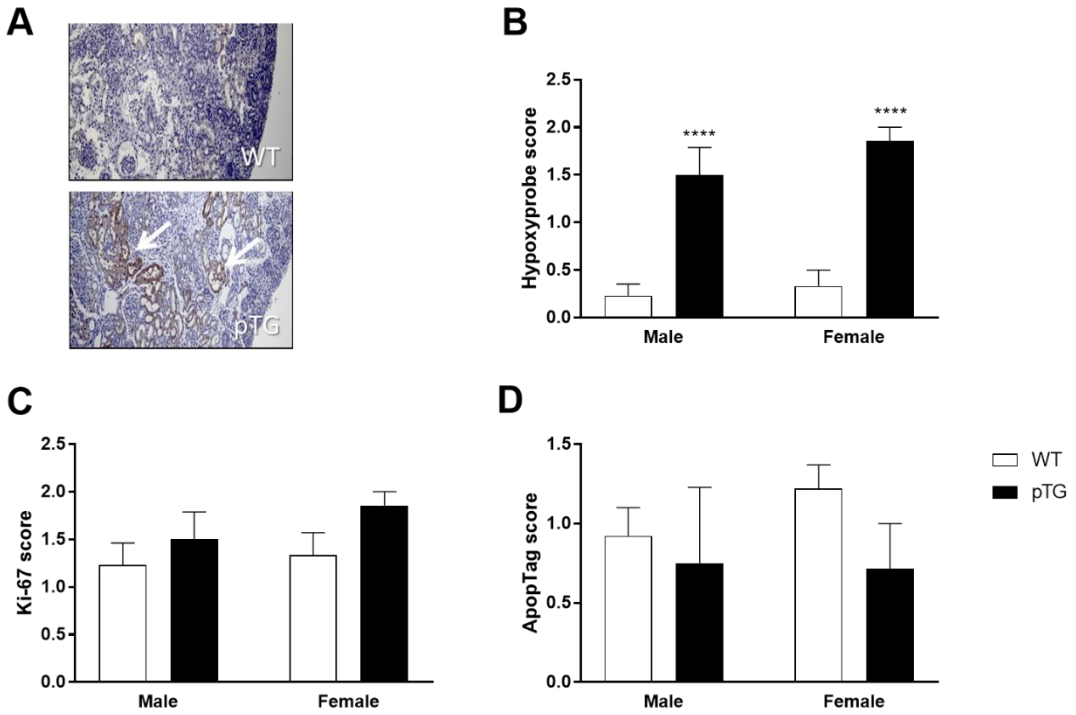

Figure 4.4: Fetal Kidney Oxidative Stress, Cell Proliferation and Apoptosis in Progeny of TG and WT Dams. Immunohistochemical staining levels for Hypoxyprobe (A) in fetal kidneys of WT and TG dams reveals positive signs of oxidative stress in the proximal tubules of both males and females from TG dams (B). There is no difference in the Ki-67 proliferation index (C) or renal tubular apoptosis by ApopTag (D) between groups. Data are shown as means ± SEM for male and female progeny. Data from 5 litters per group with (WT: male, n=13; female, n=9); (TG: male, n=4; female, n=7).
***Maternal genotype effect, P<0.0001.

Fetal Kidney DNA Hypermethylation in Males from TG Dams

Since we did not observe differences in fetal kidney oxidative stress or nephron density in the neonatal cohort, we elected to screen flash frozen archived fetal kidney samples for potential epigenetic effects. We tested for differences in fetal renal DNA methylation using Roche NimbleGen DNA Methylation Microarrays. Dr. E. Andres Houseman (Biostatistician at Oregon State University) performed the analysis employing his published strategy (26) to compensate for the confounding effects of using mixed tissue samples (e.g. whole kidney rather than isolated proximal tubule cell line). The problem with mixed tissue DNA methylation analysis is they vary by cell composition.

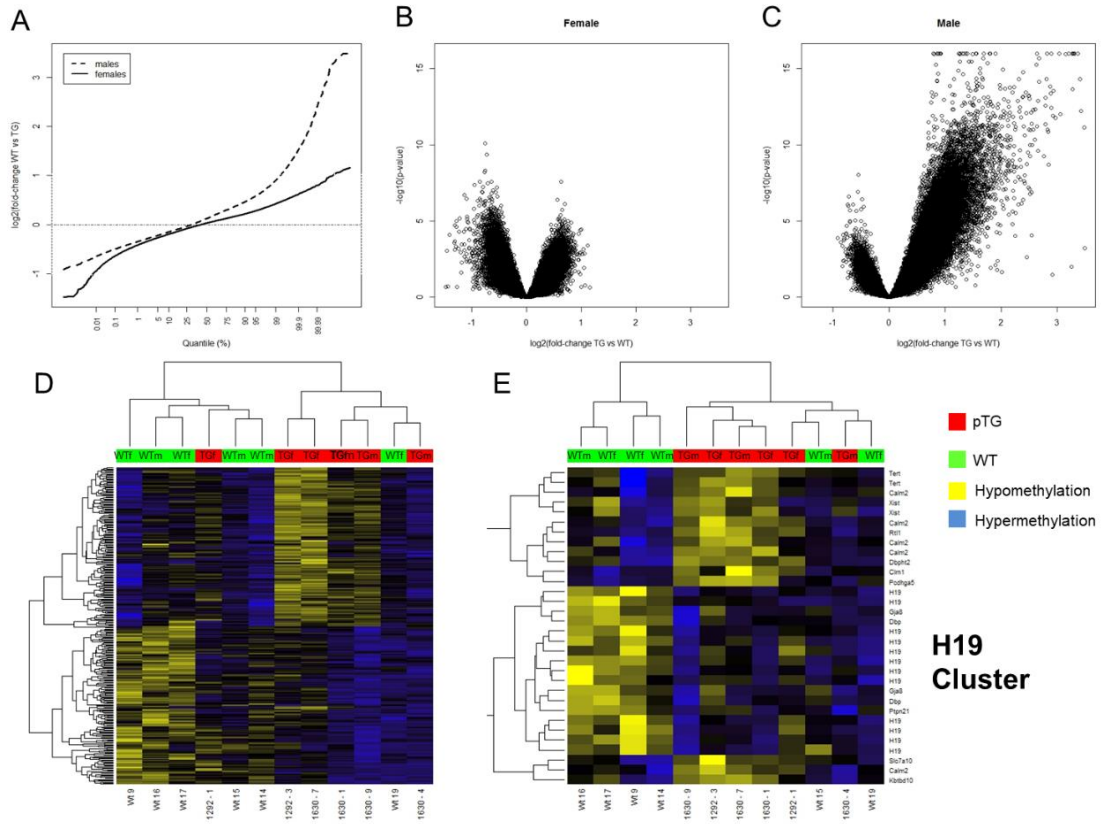

Figure 4.5: Global Promoter Methylation in Fetal Kidney in Progeny of TG and WT Dams. Distribution of log2-fold-changes in promoter methylation in males (dotted line) and females (solid line) from TG dams compared with age- and sex-matched WT controls. Volcano plots show no significant difference in fetal renal DNA methylation between female groups, but marked hypermethylation in males from TG dams. Unsupervised cluster analysis using global DNA methylation data or rank ordered data show relatively good separation between groups with accentuation of the H19 locus.

The analysis revealed that the distribution of global DNA methylation in fetal kidneys from WT controls compared with TG dams (reported as the log2-fold-change) varied between male and female mice (Figure 4.5A; Kolmogorov-Smirnov $P<10^{-15}$). It also showed that males had a much higher proportion of extremely large values – loci for which progeny of TG dams were hypermethylated relative to controls – than females. Volcano plots (Figures 4.5B and C) reinforced the point that males had a large number of nominally significant, large positive, hypermethylated loci relative to WT males and their female siblings from TG dams.

Unsupervised clustering of fetal DNA methylation profiles revealed relatively good separation of profiles from WT and TG progeny (Figures 4.5D, E). Data suggest H19 loci may be more hypermethylated in the progeny from TG dams compared with WT controls. However, our investigation into the distribution of log2-fold-change values between CpGs mapped to insulin-like growth factor genes thought to be involved in

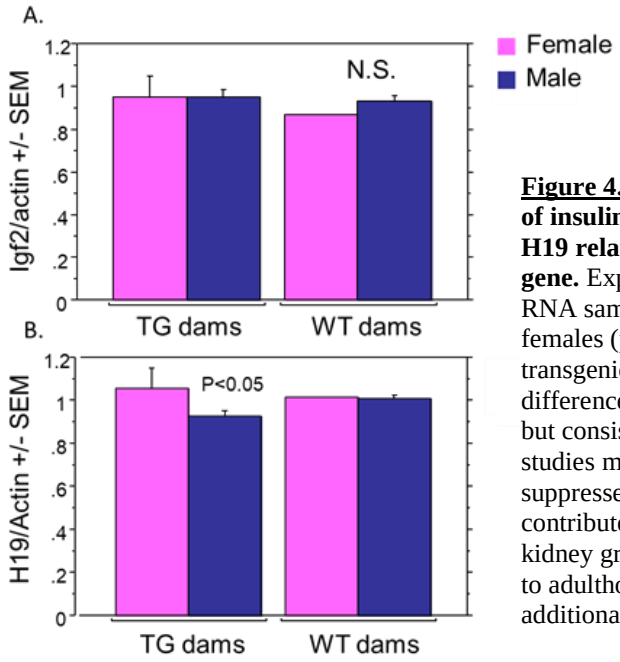

Figure 4.6. Targeted qRT-PCR analysis of insulin-like growth factor 2 (Igf2) and H19 relative to beta-actin housekeeping gene. Expression levels in fetal kidney RNA samples from males (blue) and females (pink) from wild-type (WT) and transgenic (TG) dams. We observed no differences in Igf2 levels between groups, but consistent with H19 DNA methylation studies males from TG dams had relatively suppressed H19 expression. Whether this contributes to their relatively decreased kidney growth from the post-natal period to adulthood is uncertain and requires additional studies.

nephrogenesis (Igf1, Igf1r, Igf2, Igf2r) were not statistically different by fetal sex (there may be trend, q=0.08). Pilot studies using qRT-PCR semi-quantitative expression analysis for Igf2 and H19 levels in fetal kidneys did not show any differences in insulin-like growth factor 2 between groups, but there was less H19 expression in the fetal kidneys of males from TG dams (Figure 4.6).

Discussion

Our data suggest that fetal growth restriction in this "physiologic" gene titration model of placental insufficiency is sufficient to affect fetal kidney DNA methylation, nephron number in adults, and the developmental programming of adult onset stress-induced hypertension. This type of "hypertension" is not chronic hypertension and was insufficient in our model to lead to diagnostic kidney pathology. However, this type of "white-coat" hypertension (named for patients' stress-induced elevations in blood pressure measured at doctors' offices) is a well-recognized clinical risk factor for chronic hypertension and kidney damage (27).

The murine *Agtdup* 3-copy mouse model we employed was originally developed by Nobel Laureate Dr. Oliver Smithies (19, 27) to mimic a common human AGT promoter variant A(-6)G (17, 18) that is associated with a 1.2-fold increase in circulating AGT levels. Since AGT is the rate limiting substrate in the renin-angiotensin reaction, this elevation is thought to increase angiotensin II levels and shift the Guytonian volume:pressure distribution to a more vasoconstrictive phenotype (19). Women with this common human AGT genetic variant are also at an increased risk for developing placental insufficiency and obstetric complications (19), including fetal growth

restriction. We have previously studied this 3-copy mouse during pregnancy and found that it has a number of features similar to women with placental insufficiency (25). We now show that these mice also have fetal growth restriction. Moreover, the growth restricted mice have very similar post-natal growth curves to growth restricted humans who later develop cardiovascular disease (1, 2), including the post-natal "dip" in weight observed at 1 week in our mouse model in at 1 year of age in human studies.

The key finding in this study is developmental programming of stress-induced hypertension in male, but not female adults from TG dams. The genotype and sex of the progeny were strictly controlled and compared with age- and sex-matched WT controls from the same genetic background (C57Bl/6J). 2-copy progeny from TG dams do not have elevated AGT expression (19, 27) and they do not have elevated blood pressure when at rest. However, these mice did show stress-induced increases in mean arterial pressure similar to their 3-copy male siblings (19). It is important to point out that 3-copy male "positive controls" did not have elevated blood pressures measured by telemetry at rest. We explain this finding by suggesting that radio-telemetry may ameliorate the stress likely arising with tail-cuff constriction.

We only observed a stress-induced increase in blood pressure in our model. It did not persist and was ameliorated within 24 hours in all of our animals. Other developmental programming models of adult-onset hypertension have reported *sustained hypertension* rather than stress-dependent hypertension. A potential anatomic correlation with those models is relatively fewer nephrons in the malnourished or growth restricted progeny. It was Langley-Evans who first showed that rat offspring exposed to maternal protein restriction in various periods of gestation developed programmed hypertension

(29) and these adult rats had reduced nephron numbers (21). Woods et al. published very similar results in her rat model (11, 30, 31) and also demonstrated that uninephrectomy shortly after birth led to hypertension in adults (32). Their work supported the idea that reduced nephron development may cause hypertension.

We also observed fewer numbers of nephrons in adult males in our model, but not in our neonatal cohort and we did not appreciate a difference in the proliferation index or apoptotic frequency in fetal kidneys from cases and controls. We did observe evidence of increased oxidative stress in the proximal tubules of fetal kidneys from TG dams, but there were no fetal sex differences to explain the adult sex differences seen in this model. Despite the fewer numbers of glomeruli in adult males from TG dams, and their predilection for stress-induced hypertension, we did not identify renal pathology in their kidneys. Nonetheless, this is consistent with the observation secondary glomerular sclerosis is thought to require at least a 50% reduction in nephron number to develop this pathology (33). It may therefore not be surprising that the relatively young male adults (12 weeks of age) in our study did not have histologic evidence of renal pathology and they did not develop chronic hypertension.

Investigations into the impact of these programming effects on older male and female mice from this model needs to be explored, but for now we emphasize the significance of the neonatal cohort and fetal renal hypermethylation studies. The neonatal cohort data suggest this model may not affect nephrogenesis. Instead, we suspect it may affect the overall growth of the kidney in male offspring, or lead to increased nephron dropout with aging. We now hypothesize that differences in renal DNA methylation may

play a role in this process, but more work is needed, including more targeted candidate gene methylation and expression studies.

Why do male mice in this model have more DNA methylation and how could that lead to fewer nephrons/kidney without evidence of reduced nephrogenesis or glomerular pathology? The male fetus may respond to placental insufficiency by shunting blood away from less-vital organs (kidney, liver, etc.) to spare the growth of more-vital organs like the brain and heart (1, 2). Relatively hypoxic tissues paradoxically produce more reactive oxygen species via mitochondrial respiratory complex function (34). In turn, they are more prone to additional oxidative stress and epigenetic changes. Maternal hypoxia has been shown to increase reactive oxygen species production in the placenta (35) like we also observed in our model and we did observe evidence of oxidative stress in fetal kidneys. Perhaps males respond differently than females to this developmental stress? Loss of nephrons in adults does occur without diagnostic evidence of glomerular damage. For example, a recent study by Denic et al., using a combination of renal biopsies and serial imaging studies, showed that a substantial loss of nephrons through adult life in humans does occur without diagnostic glomerular sclerosis, or other clinical signs usually associated with nephron dropout (36). Therefore, our current working hypothesis is males from TG dams respond to oxidative stress with differences in renal DNA methylation that may predispose them to nephron dropout as they mature from neonates to adults. This hypothesis needs to be further explored in future studies.

Alternative explanations should also be considered. For example, Bagby et al. showed there is microvascular hypersensitivity to norepinephrine in nutritionally-programmed microswine offspring with stress-dependent hypertension (37). Indeed,

several laboratories have shown vascular hyperactivity to phenylephrine and other pressor effects in various programming models, including reduced uteroplacental perfusion (38) and in the progeny of eNOS knockout mice that do not properly grow and dilate uterine spiral arteries during pregnancy (39). We did not test for differences in sympathetic activity in our model, but this should be done.

Finally, the clinical significance of white-coat hypertension should not be underestimated. It has been shown that repeated bouts of stress-dependent hypertension can progress to sustained hypertension (34)—like what commonly occurs in patients with sleep apnea (a growing clinical problem associated with the current obesity epidemic). Therefore, this mouse model may provide important insights into the pathologic mechanisms involved in developmental programming and the early signs of clinically significant cardiovascular disease.

Chapter 5

Concluding Remarks and Future Directions

In this dissertation, we presented data supporting an overarching hypothesis that placental insufficiency leading to fetal growth restriction is a multifactorial process, which involves both maternal genetic risk factors and fetal sex. Chapter 1 defines the known pathophysiology of fetal growth restriction and divides this primary hypothesis into the three parts which became the focus of each data chapter of this dissertation: the maternal phenotype in FGR, the fetal phenotypes in FGR, and long-term health impacts of FGR on offspring.

In Chapter 2, we tested whether a maternal genotype mimicking a common human angiotensinogen variant associated with fetal growth restriction affects uterine angiogenesis and pregnancy outcome. We demonstrated that this genotype leads to increased tissue-specific angiotensin II production and is associated with aberrant increases in the anti-angiogenic factor sFlt1, which sequesters available VEGF and may be responsible for reduced uterine spiral artery number and coiling in this model compared with wild-type controls. The consequence of abnormal uterine vascular remodeling was placental damage and fetal growth restriction. Notably, the phenotype could be rescued by transfecting uterine blood vessels with VEGF, which suggests the angiotensin/sFlt1/VEGF pathway plays a key role in pregnancy-induced uterine angiogenesis, supporting our hypothesis (Figure 5.1).

Because males are more likely to have significant pregnancy complications compared with their female siblings, in Chapter 3 we hypothesized that male fetal sex may somehow affect uteroplacental angiogenesis and nutrient transfer. By employing micro-dissection techniques we could compare fetal sex with placental architecture and maternal placental bed tissue (metrial triangle) expression levels. We observed that males in our mouse model were associated with an increased antiangiogenic sFlt1 level both in their placentas and in metrial triangle tissue samples. They also had less pro-angiogenic VEGF and PLGF expression. Their female siblings in this model also increased sFlt1 levels, but did not appreciably change their levels of VEGF or PLGF. This imbalanced ratio seen in males may be one reason maternal uterine spiral artery angiogenesis and placental capillary labyrinth angiogenesis are relatively suppressed. This is an entirely novel finding and required further investigation into potential mechanisms that could be involved in this process.

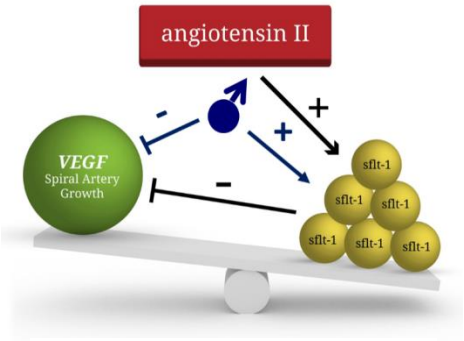

Figure 5.1. Working hypothesis.

In Chapter 4, we address the DOHAD consequences of FGR, particularly in terms of cardiovascular control as measured by blood pressure and renal development. We found adult males from our transgenic mouse model had elevated blood pressure in response to environmental stress and fewer nephrons in their kidneys compared to controls. Despite renal hypermethylation and elevated oxidative stress evident in the proximal renal tubules of GD18.5 FGR male mice, no reduction in nephrons were observed until adulthood. Females from TG dams showed increased fetal renal oxidative

stress compared to sex-matched controls. Although nephron density was not different at 2 weeks postpartum, as adults these FGR females had an increased nephron density. Blood pressures from adult females from TG dams were the same as WT controls.

uNKs and Angiogenic Impact

We have postulated several mechanisms affecting the imbalance of antiangiogenic:pro-angiogenic factors seen in FGR midgestation. One such mechanism could be differences in maternal uterine NK cell activation, which is known to play a key role in the metrial triangle (and human decidua) to modulate local VEGF levels and mediate pregnancy-induced spiral artery angiogenesis. Males from TG dams had less activation of uNK cells during the critical GD6.5 to 8.5 uteroplacental vascular developmental window. During this same time period of development, maternal vasculogenesis (measured by scoring whole mount sections for vascular "blebbing") was depressed in males in this model and by GD8.5 they had fewer vascular branches, which suggest either reduced angiogenesis or an over-active vasculogenesis "pruning" process. This important observation fits with what is known about uNK cell function during pregnancy. That is to say, uNK cells are the principal agents of spiral artery angiogenesis because they activate pruning in relatively low VEGF conditions, resulting in decreased vessel number (1, 2).

In our data, this "pruning" process turns out to be an important potential mechanism to explain our findings. It is a necessary physiologic adaptation to increase vasculogenesis in response to hypoxia and to organize these networks into functional arteries and capillary beds (3–5). In fact, others have also reported relatively deficient spiral artery growth in mice lacking uNK cells in the presence of low vascular growth

factor levels (6). A reduction in maternal uterine angiogenesis affects uteroplacental blood flow and maternal-fetal nutrient exchange (7). The sex difference may not only be limitations in males, but perhaps better compensation in females in our mouse model. Females from TG dams showed reduced "blebbing" compared with WT controls, but they seemed to compensate by differences in uNK cell activation and differences in pruning by GD8.5. They did not prune angiogenic networks as much as males did, which may be why females from TG dams did not have fewer or less coiled spiral arteries than WT controls. This may be related to the lower sFlt1/VEGF or PLGF ratio observed in female placentas. They did not show a reduction in VEGF in the metrial triangle the way males did, so it is possible that the lack of low VEGF signaling together with differences in uNK activation helped to "rescue" females from TG dams.

Hormonal Regulation of Uteroplacental Vascular Growth

Another indication of possible compensatory responses by female placentas to the TG maternal uterine environment is the expression differences we observed in female placentas compared with their male siblings. Our RNASeq data point to potential differences in sex hormone production by these placentas. As discussed at the end of Chapter 3, male placentas from TG dams upregulate the gene *HSD3B1*, which encodes for 3-beta-hydroxysteroid dehydrogenase isomerase that drives production of placental progesterone and androgens (8–10). Progesterone blocks estrogen receptor 1 (*ESR1*) expression and we reproducibly observed reduced *ESR1* levels in male placentas from TG dams (Figure 5.2). This may be significant because ER is known regulator of angiogenesis. The mechanism is likely complex, however, because decreased VEGF is also associated with reduced estrogen reception activity (11–13). Interestingly, males

from human gestational diabetic pregnancies, another form of placental insufficiency, also have decreased *ESR1* (14). Increased *HSD3B1* is also linked to increased testosterone (15). Increasing maternal testosterone was recently found in another study to reduce uterine blood flow and spiral artery remodeling; moreover, the magnitude of these changes were greater in males than females (16).

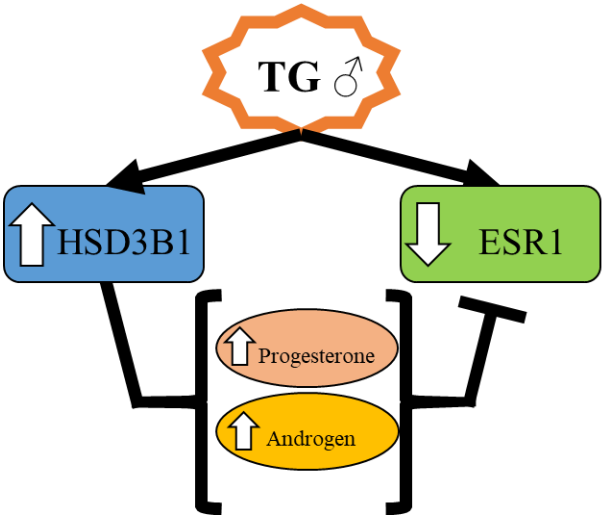

Figure 5.2. Influence of maternal angiotensinogen and male fetal sex on expression of *HSD3B1* and *ESR1*, as potential drivers of reduced uteroplacental angiogenesis in early gestation.

Placental Extracellular Vesicle Release and Maternal Response

In mice, uterine spiral arteries remodel before trophoblast invasion, so a direct contact model is unlikely, but placental paracrine signaling may be the mechanism. We are currently investigating this new concept by validating both murine invasion, where we expect to see no difference, and paracrine signaling by extracellular vesicles (EVs). EVs have been shown to target specific cells and affect their function via delivery of proteins and RNA (17–19). Fetal placentas may be using EVs to regulate maternal angiogenesis and immune functions similar to how neoplasms (i.e. cancers, tumors) may regulate their microenvironments (20, 21). EVs are thought to regulate maternal

angiogenesis and immune functions by carrying placental signaling cargo to target tissues (20). To test the action of EVs, our laboratory has recently begun experiments employing a Cre-*loxP* mouse transgenic model with tdTomato expression in the dam and a placenta-specific Cre sire. Crossing the two causes Cre recombination at *loxP* flanking sites and allows Cre-mediated removal of DsRed-stop, changing expression from DsRed+ to eGFP+ in placental cells (while allowing DsRed+ cells to serve as a positive control), including EVs released by the placenta and any cells transformed by EV products (22, 23). Our preliminary data indicate that the placenta releases EVs continuously over the course of pregnancy, and by late gestation, the maternal kidney proximal tubules express eGFP instead of DsRed (Figure 5.3). This may be indicative of transformation by placental EVs, which we plan to assess by testing for the presence of Cre mRNA to verify expression and transformation of the kidney. The purpose of the placenta for

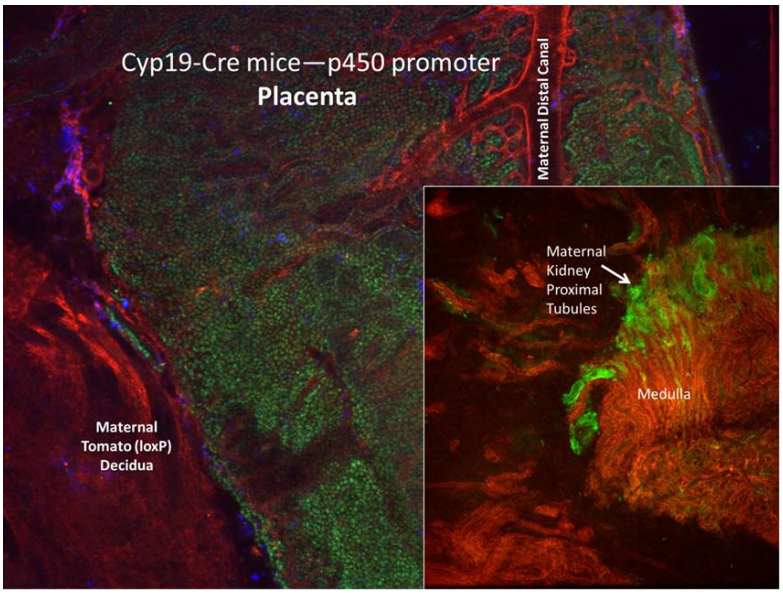

Figure 5.3. Maternal tomato *loxP* mouse crossed with placental driven Cre male creates GFP positive fetal placentas that over-express Cre. Placental EVs released into the maternal blood appear to interact with the maternal kidney leading to GFP upregulation in proximal tubules.

releasing EVs and influencing other cells is currently unknown, but could play a role in controlling vascular tone.

DOHAD Implications of Placental Insufficiency

Developmental programming of stress-induced hypertension affected male, but not female adults from TG dams, by reducing the number of adult nephrons and causing increased blood pressure. Our lab previously found that 2-copy mice expressed increased angiotensinogen in the proximal renal tubules compared to 3-copy mice, which led to situational hypervolemia (24). As we only considered 2-copy male mice from 3-copy dams for analysis, it is possible that reduced nephron counts as a result of FGR combined with hypervolemia could lead to the observed increased hypertension and hyperfiltration (25). Males have higher morbidity and mortality associated with chronic kidney disease and renal issues, and early evidence indicates testosterone may be a detrimental factor dividing male and female renal pathology (26). Experiencing later acute renal injury such as exposure to heavy metals, Hepatitis C or HIV infection, or malignancy would further exacerbate this condition (27).

This work has explored the links between FGR and maternal factors, fetal sex, and developmental programming of disease. Many studies still do not separate data by fetal sex despite being long recognized as a data confounder. The research presented in this dissertation strongly supports consideration for the impact of fetal factors on gestational maternal response, postnatal outcomes, and adult disease. Potential mechanisms addressed in this chapter provide ample future directions for this promising research in an effort to better address improving the state of maternal and fetal health.

References by Chapter

Chapter 1 References

1. Bamfo, JEAK and Odibo, AO. Diagnosis and management of fetal growth restriction. J Pregnancy. 2011;2011:1–15.

2. Peleg, D, Kennedy, CM, and Hunter, SK. Intrauterine Growth Restriction: Identification and Management. Am Fam Physician. 1998;453–460.

3. Kulandavelu, S, Whiteley, KJ, Bainbridge, SA, Qu, D, and Adamson, SL. Endothelial NO synthase augments fetoplacental blood flow, placental vascularization, and fetal growth in mice. Hypertension. 2013;61:259–66.

4. Louey, S, Cock, ML, Stevenson, KM, and Harding, R. Placental Insufficiency and Fetal Growth Restriction Lead to Postnatal Hypotension and Altered Postnatal Growth in Sheep. Pediatr Res. 2000;48:808–814.

5. Hayward, CE, Lean, S, Sibley, CP, Jones, RL, Wareing, M, Greenwood, SL, et al. Placental Adaptation: What Can We Learn from Birthweight:Placental Weight Ratio? Front Physiol. 2016;7:28.

6. Hendrix, N and Berghella, V. Non-placental causes of intrauterine growth restriction. Semin Perinatol. 2008;32:161–5.

7. Salafia, CM, Zhang, J, Charles, AK, Bresnahan, M, Shrout, P, Sun, W, et al. Placental characteristics and birthweight. Paediatr Perinat Epidemiol. 2008;22:229–239.

8. Gagnon, R. Placental insufficiency and its consequences. Eur J Obstet Gynecol Reprod Biol. 2003;110:S99–S107.

9. Gude, NM, Roberts, CT, Kalionis, B, King, RG, Loke, YW, King, A, et al. Growth and function of the normal human placenta. Thromb Res. 2004;114:397–407.

10. Maynard, SE, Min, J, Merchan, J, Lim, K, Li, J, Mondal, S, et al. Excess placental soluble fms-like tyrosine kinase 1 (sFlt1) may contribute to endothelial dysfunction , hypertension, and proteinuria in preeclampsia. J Clin Invest. 2003;111:649–658.

11. Newnham, JP. The developmental origins of health and disease (DOHaD) – why it is so important to those who work in fetal medicine. Ultrasound Obs Gynecol. 2007;29:121–123.

12. Barker, DJ., Osmond, C, Winter, P., Margetts, B, and Simmonds, S. Weight in Infancy and Death From Ischaemic Heart Disease. Lancet. 1989;334:577–580.

13. La Maestra, S, Kisby, GE, Micale, RT, Johnson, J, Kow, YW, Bao, G, et al. Cigarette smoke induces DNA damage and alters base-excision repair and tau levels in the brain of neonatal mice. Toxicol Sci. 2011;123:471–9.

14. Ravelli, G-P, Stein, ZA, and Susser, MW. Obesity in Young Men after Famine Exposure in Utero and Early Infancy. N Engl J Med. 1976;295:349–353.

15. Lackland, DT, Bendall, HE, Osmond, C, Egan, BM, and Barker, DJP. Low Birth Weights Contribute to the High Rates of Early-Onset Chronic Renal Failure in the Southeastern United States. Arch Intern Med. 2000;160:1472.

16. Osmond, C, Barker, DJ, Winter, PD, Fall, CH, and Simmonds, SJ. Early growth and death from cardiovascular disease in women. BMJ. 1993;307:1519–24.

17. Barker, DJ, Osmond, C, Golding, J, Kuh, D, and Wadsworth, ME. Growth in utero, blood pressure in childhood and adult life, and mortality from cardiovascular disease. BMJ. 1989;298:564–7.

18. Briscoe, TA, Rehn, AE, Dieni, S, Duncan, JR, Wlodek, ME, Owens, JA, et al. Cardiovascular and renal disease in the adolescent guinea pig after chronic placental insufficiency. Am J Obstet Gynecol. 2004;191:847–855.

19. Burton, GJ, Woods, AW, Jauniaux, E, and Kingdom, JCP. Rheological and Physiological Consequences of Conversion of the Maternal Spiral Arteries for Uteroplacental Blood Flow during Human Pregnancy. Placenta. 2009;30:473–482.

20. Dechend, R and Luft, FC. Angiogenesis factors and preeclampsia. Nat Med. 2008;14:1187–8.

21. Zygmunt, M, Herr, F, Münstedt, K, Lang, U, Liang, OD, Kerbel, RS, et al. Angiogenesis and vasculogenesis in pregnancy. Eur J Obstet Gynecol Reprod Biol. 2003;110 Suppl 1:S10-8.

22. Charnock-Jones, DS, Kaufmann, P, Mayhew, TM, Clark, D., Licence, D., Charnock-Jones, D., et al. Aspects of human fetoplacental vasculogenesis and angiogenesis. I. Molecular regulation. Placenta. 2004;25:103–13.

23. Maulik, D, Frances Evans, J, and Ragolia, L. Fetal growth restriction: pathogenic mechanisms. Clin Obstet Gynecol. 2006;49:219–27.

24. Risau, W and Flamme, I. Vasculogenesis. Annu Rev Cell Dev Biol. 1995;11:73–91.

25. Demir, R, Seval, Y, and Huppertz, B. Vasculogenesis and angiogenesis in the early human placenta. Acta Histochem. 2007;109:257–265.

26. Kingdom, JCP and Kaufmann, P. Oxygen and placental villous development: Origins of fetal hypoxia. Placenta. 1997;18:613–621.

27. Geva, E, Ginzinger, DG, Zaloudek, CJ, Moore, DH, Byrne, A, and Jaffe, RB. Human Placental Vascular Development: Vasculogenic and Angiogenic (Branching and Nonbranching) Transformation Is Regulated by Vascular Endothelial Growth Factor-A, Angiopoietin-1, and Angiopoietin-2. J Clin Endocrinol Metab. 2002;87:4213–4224.

28. Detmar, M, Brown, LF, Schön, MP, Elicker, BM, Velasco, P, Richard, L, et al. Increased Microvascular Density and Enhanced Leukocyte Rolling and Adhesion in the Skin of VEGF Transgenic Mice. J Invest Dermatol. 1998;111:1–6.

29. Odorisio, T, Schietroma, C, Zaccaria, ML, Cianfarani, F, Tiveron, C, Tatangelo, L, et al. Mice overexpressing placenta growth factor exhibit increased vascularization and vessel permeability. J Cell Sci, 2002;115.

30. Rennie, MY, Whiteley, KJ, Kulandavelu, S, Adamson, SL, Sled, JG, Sapin, V, et al. 3D visualisation and quantification by microcomputed tomography of late gestational changes in the arterial and venous feto-placental vasculature of the mouse. Placenta. 2001;28:833–40.

31. Roberts, VHJ, Lo, JO, Salati, JA, Lewandowski, KS, Lindner, JR, Morgan, TK, et al. Quantitative assessment of placental perfusion by contrast-enhanced ultrasound in macaques and human subjects. Am J Obstet Gynecol. 2016;214:369.e1-369.e8.

32. Malassiné, A, Frendo, JL, and Evain-Brion, D. A comparison of placental development and endocrine functions between the human and mouse model. Hum Reprod Update. 2003;9:531–9.

33. Adamson, SL, Lu, Y, Whiteley, KJ, Holmyard, D, Hemberger, M, Pfarrer, C, et al. Interactions between Trophoblast Cells and the Maternal and Fetal Circulation in the Mouse Placenta. Dev Biol. 2002;250:358–373.

34. Croy, BA, Burke, SD, Barrette, VF, Zhang, J, Hatta, K, Smith, GN, et al. Identification of the primary outcomes that result from deficient spiral arterial modification in pregnant mice. Pregnancy Hypertens. 2011;1:87–94.

35. Jauniaux, E, Poston, L, and Burton, GJ. Placental-related diseases of pregnancy: involvement of oxidative stress and implications in human evolution. Hum Reprod Update. 2006;12:747–755.

36. Croy, BA, Zhang, J, Tayade, C, Colucci, F, Yadi, H, and Yamada, AT. Analysis of uterine natural killer cells in mice. Methods Mol Biol. 2010;612:465–503.

37. Moffett-King, A. Natural killer cells and pregnancy. Nat Rev Immunol. 2002;2:656–663.

38. Croy, BA, He, H, Esadeg, S, Wei, Q, Mccartney, D, Zhang, J, et al. Uterine natural killer cells: insights into their cellular and molecular biology from mouse modelling. Reproduction. 2003;149–160.

39. Lash, GE, Schiessl, B, Kirkley, M, Innes, BA, Cooper, A, Searle, RF, et al. Expression of angiogenic growth factors by uterine natural killer cells during early pregnancy. J Leukoc Biol. 2006;80:572–80.

40. Seshadri, S and Sunkara, SK. Natural killer cells in female infertility and recurrent miscarriage: a systematic review and meta-analysis. Hum Reprod Update. 2014;20:429–38.

41. Oh, M-J, Lee, JK, Lee, NW, Shin, J-H, Yeo, MK, Kim, A, et al. Vascular endothelial growth factor expression is unaltered in placentae and myometrial resistance arteries from pre-eclamptic patients. Acta Obstet Gynecol Scand. 2006;85:545–50.

42. Kim, M, Park, HJ, Seol, JW, Jang, JY, Cho, Y-S, Kim, KR, et al. VEGF-A regulated by progesterone governs uterine angiogenesis and vascular remodelling during pregnancy. EMBO Mol Med. 2013;5:1415–30.

43. Ni, Y, May, V, Braas, K, Osol, G, Celia, G, Gokina, N, et al. Pregnancy augments uteroplacental vascular growth factor gene expression and vasodilator endothelial effects. Am J Physiol - Hear Circ Physiol. 1997;273:H938–H944.

44. Landgren, E, Schiller, P, Cao, Y, and Claesson-Welsh, L. Placenta growth factor stimulates MAP kinase and mitogenicity but not phospholipase C-γ and migration of endothelial cells expressing Flt 1. Oncogene. 1998;16:359–367.

45. Foidart, JM, Schaaps, JP, Chantraine, F, Munaut, C, and Lorquet, S. Dysregulation of anti-angiogenic agents (sFlt-1, PLGF, and sEndoglin) in preeclampsia--a step forward but not the definitive answer. J Reprod Immunol. 2009;82:106–11.

46. He, Y, Smith, SK, Day, KA, Clark, DE, Licence, DR, and Charnock-Jones, DS. Alternative Splicing of Vascular Endothelial Growth Factor (VEGF)-R1 (FLT-1) pre-mRNA Is Important for the Regulation of VEGF Activity. Mol Endocrinol. 2013:NP.

47. Kulandavelu, S, Whiteley, KJ, Qu, D, Mu, J, Bainbridge, SA, and Adamson, SL. Endothelial nitric oxide synthase deficiency reduces uterine blood flow, spiral artery elongation, and placental oxygenation in pregnant mice. Hypertension. 2012;60:231–8.

48. Laresgoiti-Servitje, E and Gomez-Lopez, N. The pathophysiology of preeclampsia involves altered levels of angiogenic factors promoted by hypoxia and autoantibody-mediated mechanisms. Biol Reprod. 2012;87:36.

49. Lucey, DR, Clerici, M, and Shearer, GM. Type 1 and type 2 cytokine dysregulation in human infectious, neoplastic, and inflammatory diseases. Clin Microbiol Rev. 1996;9:532–62.

50. James, JL, Whitley, GS, and Cartwright, JE. Shear stress and spiral artery remodelling: the effects of low shear stress on trophoblast-induced endothelial cell apoptosis. Cardiovasc Res. 2011;90:130–9.

51. Li, M and Liu, B. Epithelial to mesenchymal transition in the progression of tubulointerstitial fibrosis. Chin Med J (Engl). 2007;120:1925–1930.

52. Dosiou, C and Giudice, LC. Natural Killer Cells in Pregnancy and Recurrent Pregnancy Loss: Endocrine and Immunologic Perspectives. Endocr Rev. 2005;26:44–62.

53. Soong, L. Dysregulated Th1 Immune and Vascular Responses in Scrub Typhus Pathogenesis. J Immunol. 2018;200:1233–1240.

54. Saito, S and Sakai, M. Th1/Th2 balance in preeclampsia. J Reprod Immunol. 2003;59:161–173.

55. Whitley, GSJ and Cartwright, JE. Cellular and molecular regulation of spiral artery remodelling: lessons from the cardiovascular field. Placenta. 2010;31:465–74.

56. Chaouat, G, Ledee-Bataille, N, Zourbas, S, Ostojic, S, Dubanchet, S, Martal, J, et al. Cytokines, implantation and early abortion: re-examining the Th1/Th2 paradigm leads to question the single pathway, single therapy concept. Am J Reprod Immunol. 2003;50:177–186.

57. Harris, LK. IFPA Gabor Than Award lecture: Transformation of the spiral arteries in human pregnancy: key events in the remodelling timeline. Placenta. 2011;32 Suppl 2:S154-8.

58. Felker, AM and Croy, BA. Uterine natural killer cell partnerships in early mouse decidua basalis. J Leukoc Biol. 2016;100:645–655.

59. Murphy, SP, Fast, LD, Hanna, NN, and Sharma, S. Uterine NK Cells Mediate Inflammation-Induced Fetal Demise in IL-10-Null Mice. J Immunol. 2005;175:4084–4090.

60. Ingemarsson, I. Gender aspects of preterm birth. BJOG An Int J Obstet Gynaecol. 2003;110:34–38.

61. Mondal, D, Galloway, TS, Bailey, TC, and Mathews, F. Elevated risk of stillbirth in males: systematic review and meta-analysis of more than 30 million births. BMC Med. 2014;12:220.

62. Di Renzo, GC, Rosati, A, Sarti, RD, Cruciani, L, and Cutuli, AM. Does fetal sex affect pregnancy outcome? Gend Med. 2007;4:19–30.

63. Eriksson, JG, Kajantie, E, Osmond, C, Thornburg, K, and Barker, DJP. Boys live dangerously in the womb. Am J Hum Biol. 2010;22:330–5.

64. Zaren, B, Lindmark, G, and Bakketeig, L. Maternal smoking affects fetal growth more in the male fetus. Paediatr Perinat Epidemiol. 2000;14:118–126.

65. Ravelli, AC, van der Meulen, JH, Osmond, C, Barker, DJ, and Bleker, OP. Obesity at the age of 50 y in men and women exposed to famine prenatally. Am J Clin Nutr. 1999;70:811–816.

66. Eriksson, JG, Forsén, T, Tuomilehto, J, Jaddoe, VW V., Osmond, C, and Barker, DJP. Effects of size at birth and childhood growth on the insulin resistance syndrome in elderly individuals. Diabetologia. 2002;45:342–348.

67. Fall, CH, Vijayakumar, M, Barker, DJ, Osmond, C, and Duggleby, S. Weight in infancy and prevalence of coronary heart disease in adult life. BMJ. 1995;310:17–9

68. Barker, DJ, Osmond, C, Golding, J, Kuh, D, and Wadsworth, ME. Growth in utero, blood pressure in childhood and adult life, and mortality from cardiovascular disease. BMJ. 1989;298:564–7.

69. Barker, DJ, Bull, AR, Osmond, C, and Simmonds, SJ. Fetal and placental size and risk of hypertension in adult life. BMJ. 1990;301:259–62.

70. Lu, H, Cassis, LA, Kooi, CW, and Daugherty, A. Structure and functions of angiotensinogen. Hypertens Res. 2016;39:492–500.

71. Nielsen, AH, Schauser, KH, and Poulsen, K. Current topic: the uteroplacental renin-angiotensin system. Placenta. 2000;21:468–77.

72. Streatfeild-James, RM., Williamson, D, Pike, RN, Tewksbury, D, Carrell, RW, and Coughlin, PB. Angiotensinogen cleavage by renin: importance of a structurally constrained N-terminus. FEBS Lett. 1998;436:267–270.

73. Irani, RA and Xia, Y. The functional role of the renin-angiotensin system in pregnancy and preeclampsia. Placenta. 2008;29:763–71.

74. Hall, JE, Guyton, AC, Jackson, TE, Coleman, TG, Lohmeier, TE, and Trippodo, NC. Control of glomerular filtration rate by renin-angiotensin system. Am J Physiol. 1977;233:F366-72.

75. Sigmon, DH, Carretero, OA, and Beierwaltes, WH. Angiotensin dependence of endothelium-mediated renal hemodynamics. Hypertension. 1992;20:643–50.

76. Kingdom, JC, McQueen, J, Connell, JM, and Whittle, MJ. Fetal angiotensin II levels and vascular (type I) angiotensin receptors in pregnancies complicated by intrauterine growth retardation. Br J Obstet Gynaecol. 1993;100:476–82.

77. Poisner, AM. The human placental renin-angiotensin system. Front Neuroendocrinol. 1998;19:232–52.

78. Haller, H, Hempel, A, Homuth, V, Mandelkow, A, Busjahn, A, Maasch, C, et al. Endothelial-cell permeability and protein kinase C in pre-eclampsia. Lancet. 1998;351:945–9.

79. Shesely, EG, Maeda, N, Kim, HS, Desai, KM, Krege, JH, Laubach, VE, et al. Elevated blood pressures in mice lacking endothelial nitric oxide synthase. Proc Natl Acad Sci U S A. 1996;93:13176–81.

80. Morgan, T, Craven, C, Lalouel, JM, and Ward, K. Angiotensinogen Thr235 variant is associated with abnormal physiologic change of the uterine spiral arteries in first-trimester decidua. Am J Obstet Gynecol. 1999;180:95–102.

81. Ishigami, T, Tamura, K, Fujita, T, Kobayashi, I, Hibi, K, Kihara, M, et al. Angiotensinogen Gene Polymorphism Near Transcription Start Site and Blood Pressure Role of a T-to-C Transition at Intron I. Hypertension. 1999;34:430–434.

82. Zhang, EG, Smith, SK, Baker, PN, and Charnock-Jones, DS. The regulation and localization of angiopoietin-1, -2, and their receptor Tie2 in normal and pathologic human placentae. Mol Med. 2001;7:624–35.

83. Okada, H. A look at transactivation of the EGF receptor by angiotensin II. J Am Soc Nephrol. 2012;23:183–5.

84. Saito, Y and Berk, BC. Transactivation: a novel signaling pathway from angiotensin II to tyrosine kinase receptors. J Mol Cell Cardiol. 2001;33:3–7.

85. Izevbigie, EB, Gutkind, JS, and Ray, PE. Angiotensin II and basic fibroblast growth factor mitogenic pathways in human fetal mesangial cells. Pediatr Res. 2000;47:614–21.

86. Wu, G, Bazer, FW, Cudd, TA, Meininger, CJ, and Spencer, TE. Maternal Nutrition and Fetal Development. J Nutr. 2004;134:2169–2172.

87. Kristensen, J, Vestergaard, M, Wisborg, K, Kesmodel, U, and Secher, NJ. Pre-pregnancy weight and the risk of stillbirth and neonatal death. BJOG An Int J Obstet Gynaecol. 2005;112:403–408.

88. O'Brien, TE, Ray, JG, and Chan, W-S. Maternal Body Mass Index and the Risk of Preeclampsia: A Systematic Overview. Epidemiology. 2003;14:368–374.

89. Zamudio, S, Palmer, SK, Droma, T, Stamm, E, Coffin, C, and Moore, LG. Effect of altitude on uterine artery blood flow during normal pregnancy. J Appl Physiol. 1995;79:7–14.

90. Shah, PS and Balkhair, T. Air pollution and birth outcomes: a systematic review. Environ Int. 2011;37:498–516.

91. Zhou, Y, Damsky, CH, and Fisher, SJ. Preeclampsia is associated with failure of human cytotrophoblasts to mimic a vascular adhesion phenotype. One cause of defective endovascular invasion in this syndrome? J Clin Invest. 1997;99:2152–64.

92. Chambers, JC, Fusi, L, Malik, IS, Haskard, DO, Swiet, M De, and Kooner, JS. Association of Maternal Endothelial Dysfunction With Preeclampsia. JAMA. 2001;285:1607.

93. Goulopoulou, S and Davidge, ST. Molecular mechanisms of maternal vascular dysfunction in preeclampsia. Trends Mol Med. 2015;21:88–97.

94. Inoue, I, Nakajima, T, Williams, CS, Quackenbush, J, Puryear, R, Powers, M, et al. A nucleotide substitution in the promoter of human angiotensinogen is associated with essential hypertension and affects basal transcription in vitro. J Clin Invest. 1997;99:1786–97.

95. Schunkert, H, Hense, HW, Gimenez-Roqueplo, AP, Stieber, J, Keil, U, Riegger, GA, et al. The angiotensinogen T235 variant and the use of antihypertensive drugs in a population-based cohort. Hypertension. 1997;29:628–33.

96. Lalouel, J-M and Rohrwasser, A. Genetic susceptibility to essential hypertension: insight from angiotensinogen. Hypertension. 2007;49:597–603.

97. Ward, K, Hata, A, Jeunemaitre, X, Helin, C, Nelson, L, Namikawa, C, et al. A molecular variant of angiotensinogen associated with preeclampsia. Nat Genet. 1993;4:59–61.

98. Morgan, T, Craven, C, Nelson, L, Lalouel, JM, and Ward, K. Angiotensinogen T235 expression is elevated in decidual spiral arteries. J Clin Invest. 1997;100:1406–15.

99. Kim, HS, Krege, JH, Kluckman, KD, Hagaman, JR, Hodgin, JB, Best, CF, et al. Genetic control of blood pressure and the angiotensinogen locus. Proc Natl Acad Sci U S A. 1995;92:2735–9.

100. Morgan, TK, Montgomery, K, Mason, V, West, RB, Wang, L, van de Rijn, M, et al. Upregulation of histidine decarboxylase expression in superficial cortical nephrons during pregnancy in mice and women. Kidney Int. 2006;70:306–14.

101. Gu, W, Liu, J, Niu, Q, Wang, H, Lou, Y, Liu, K, et al. A-6G and A-20C polymorphisms in the angiotensinogen promoter and hypertension risk in Chinese: a meta-analysis. PLoS One. 2011;6:e29489.

102. Langley-Evans, SC, Welham SJ, Jackson AA. Fetal exposure to a maternal low protein diet impairs nephrogenesis and promotes hypertension in the rat. Life Sci. 1999;64:965-974.

103. Curhan, GC, et al. Birth weight and adult hypertension and obesity in women. Circulation. 1996;94:1310-5.

104. Woods, LL. Maternal Nutrition and Predisposition to Later Kidney Disease. Curr. Drug Targets. 2007;8:906-913.

105. Larsson, L, Aperia, A, Wilton, P. Effect of normal development on compensatory renal growth. Kidney Int. 1980;18:29-35.

Chapter 2 References

1. Maynard S, Min J, Merchan J, Lim K, Li J, Mondal S, Libermann T, Morgan J, Sellke F, Stillman I, Epstein F, Sukhatme V, Karumanchi S. Excess placental soluble fms-like tyrosine kinase 1 (sFlt1) may contribute to endothelial dysfunction, hypertension, and proteinuria in preeclampsia. J Clin Invest. 2003;111(5):649-658.

2. Silasi M, Cohen B, Karumanchi S, Rana S. Abnormal placentation, angiogenic factors, and the pathogenesis of preeclampsia. Obstet Gynecol Clin North Am. 2010;37(2):239-253.

3. Guttmacher A, Maddox, Y, Spong C. The Human Placental Project: Placental structure, development, and function in real time. Placenta. 2014;35:303-304.

4. Thornburg K, O'Tierney P, Louey S. The placenta is a programming agent for cardiovascular disease. Placenta. 2010;31 Suppl:S54-59.

5. Khong T. Acute atherosis in pregnancies complicated by hypertension, small-for-gestational-age infants, and diabetes mellitus. Arch Pathol Lab Med. 1991;115:722-725.

6. Starzyk K, Salafia C, Pezzullo J, et al. Quantitative differences in arterial morphometry define the placental bed in preeclampsia. Hum Pathol. 1997;28:353-358.

7. Morgan T, Craven C, Lalouel J-M, Ward K. Angiotensinogen Thr235 variant is associated with abnormal physiologic change of the uterine spiral arteries in first-trimester decidua. Am J Obstet Gynecol. 1999;180:95-102.

8. Craven C, Morgan T, Ward K. Decidual spiral artery remodeling begins before cellular interaction with trophoblasts. Placenta. 1998;19:241-252.

9. Fisher SJ. The placental problem: linking abnormal cytotrophoblast differentiation to the maternal symptoms of preeclampsia. Reprod Biol Endocrinol. 2004;2:53.

10. Morgan T, Tolosa J, Mele L, and the MFM network. Placental villous hypermaturation is associated with idiopathic preterm birth. J Matern Fetal Neonatal Med. 2013;26(7):647-653.

11. Moll W. Structure adaptation and blood flow control in the uterine arterial system after hemochorial placentation. Eur J Obstet & Gynecol Reprod Biol. 2003;110:S19-27.

12. Erez O, Romero R., Espinoza J, et al. The change in concentrations of angiogenic and anti-angiogenic factors in maternal plasma between the first and second trimesters in risk assessment for the subsequent development of preeclampsia and small-for-gestational age. J Matern Fetal Neonatal Med. 2008;21(5):279-87.

13. Myatt L, Clifton R, Roberts J, et al. Can changes in angiogenic biomarkers between the first and second trimesters of pregnancy predict development of pre-eclampsia in a low risk nulliparous patient population? BJOG. 2013;120(10):1183-1191.

14. Andraweera P, Dekker G, Laurence J, Roberts C. Placental expression of VEGF family mRNA in adverse pregnancy outcomes. Placenta. 2012;33:467-472.

15. Kim M, Park H, Seol J, et al. VEGF-A regulated by progesterone governs uterine angiogenesis and vascular remodeling during pregnancy. EMBO Mol Med. 2013;5:1415-1430.

16. James J, Cartwright J, Whitley G, et al. The regulation of trophoblast migration across endothelial cells by low shear stress: consequences for vascular remodeling in pregnancy. Cardiovascular Res. 2012;93:152-161.

17. Ward K, Hata A, Jeunemaitre X, et al. A molecular variant of angiotensinogen associated with preeclampsia. Nat Genet. 1993;4:59-61.

18. Inoue I, Nakajima T, Williams C, et al. A nucleotide substitution in the promoter of human angiotensinogen is associated with essential hypertension and affects basal transcription in vitro. J Clin Invest. 1997;99:1786-1797.

19. Morgan T, Craven C, Nelson L, et al. Angiotensinogen T235 expression is elevated in decidual spiral arteries. J Clin Invest 1997;100:1406-1415.

20. Poulsen, K. Kinetics of the renin system. The basis for determination of the different components of the system. Scand. J. Clin. Lab. Invest. 1973;31:1-86.

21. Inoue I, Rohrwasser A, Helin C, et al. A mutation of angiotensinogen in a patient with preeclampsia leads to altered kinetics of the renin-angiotensin system. J Biol Chem. 1995;270(19):11430-6.

22. Zhang X, Varner M, Dizon-Townson D, et al. A molecular variant of angiotensinogen is associated with idiopathic intrauterine growth restriction. Obstet Gynecol. 2003;101(2):237-42.

23. Walther T, Wallukat G, Jank A, et al. Angiotensin II type 1 receptor agonistic antibodies reflect fundamental alterations in the uteroplacental vasculature. Hypertension. 2005;46(6):1275-1279.

24. Morgan T, Craven C, Ward K. Human spiral artery renin-angiotensin system. Hypertension.1998;32:683-687.

25. Zhou C, Ahmad S, MI T, et al. Angiotensin II induces soluble fms-like tyrosine kinase-1 release via calcineurin signaling pathway in pregnancy. Circ Res. 2007;100:88-95.

26. Kim H-S, Lee G, John SW, et al. Molecular phenotyping for analyzing subtle genetic effects in mice: Application to an angiotensinogen gene titration. Proc Natl Acad Sci. 2002;99(7):4602-4607.

27. Morgan T, Rohrwasser A, Zhao L, et al. Hypervolemia of pregnancy is not maintained in mice chronically overexpressing angiotensinogen. Am J Obstet Gynecol. 2006;195:1700-1706.

28. Salas S, Marshall G, Gutiérrez B, and Rosso P. Time course of maternal plasma volume and hormonal changes in women with preeclampsia or fetal growth restriction. Hypertension. 2006;47:203-208.

29. Kulandavelu S, Whiteley K, Qu D, et al. Endothelial nitric oxide synthase deficiency reduces uterine blood blow, spiral artery elongation, and placental oxygenation in pregnant mice. Hypertension. 2012;60:231-238.

30. Falcao S, Stoyanova E, Cloutier G, et al. Mice overexpressing both human angiotensinogen and human renin as a model of superimposed preeclampsia on chronic hypertension. Hypertension. 2009;54(6):1401-1407.

31. Xie A., Belcik T., Qi Y., Morgan T, Champaneri S., Davidson B., Zhao Y., Klibanov A., Ammi A., Lindner J. Ultrasound-mediated vascular gene transfection by cavitation of endothelial-targeted cationic microbubbles. JACC: Cardiovascular Imaging 2012;5(12):1253-62.

32. Fern R, Yesko C, Thornhill B, et al. Reduced angiotensinogen expression attenuates renal interstitial fibrosis in obstructive nephropathy in mice. J Clin Invest.1999;103:39-46.

33. Junwu M and Adamson L. Developmental changes in hemodynamics of uterine artery, utero- and umbilocoplacental, and vitelline circulations in mouse throughout gestation. Am J Physiol Heart Circ Physiol. 2006;291:H1421-1428.

34. Stillman I and Karumanchi A. The glomerular injury of preeclampsia. J Am Soc Nephrol. 2007;18:2281-2284.

35. Dunn S, Qi Z, Bottinger E, et al. Utility of endogenous creatinine clearance as a measure of renal function in mice. Kidney Int. 2004;65(5):1959-1967.

36. Keator C, Lindner J, Belcik J, et al. Contrast-enhanced ultrasound reveals real-time spatial changes in vascular perfusion during early implantation in the macaque uterus. Fertil Steril. 2011;95:1316-1321.

37. Morgan T, Roberts V, Bednarek P, et al. Early first trimester uteroplacental blood flow and the progressive disintegration of spiral artery plugs: New insights from contrast-enhanced ultrasound and tissue histopathology. Hum Reprod. 2017;32(12):2382-2393.

38. Rennie M, Rahman A, Whiteley K, Sled J, Adamson S. Site specific increases in utero- and fetoplacental arterial vascular resistance in eNOS-deficient mice due to impaired arterieal enlargment. Biology of Reproduction. 2015;92(2):1-11.

39. Krebs C, Macara L, Leiser R, et al. Intrauterine growth restriction with absent end-diastolic flow velocity in the umbilical artery is associated with maldevelopment of the placental terminal villous tree. Am J Obstet Gynecol. 1996;175:1534-1542.

40. Gould SF. The ultrastructural demonstration of placental phospholipids in preterm, term, and eclamptic placentas. Placenta. 1983;4(3):241-254.

41. Hnat M, Meadows J, Brockman D, et al. Heat shock protein-70 and 4-hydroxy-2-nonenal adducts in human placental villous tissue of normotensive, preeclamptic and FGR pregnancies. Am J Obstet Gynecol. 2005;193:836-840.

42. Moran P, Lindheimer M, Davison J. The renal response to preeclampsia. Semin Nephrol. 2004;24(6):588-595.

43. Arthuis C, Novell A, Escoffre J, et al. New insights into uteroplacental perfusion: quantitative analysis using Doppler and contrast-enhanced ultrasound imaging. Placenta. 2013;34(5):424-431.

44. Verdonk K, Visser W, Van den Mdieracker A, Jan Danser A. The renin-angiotensin-aldosterone system in preeclampsia: the delicate balance between good and bad. Clinical Science. 2014;126:537-544.

48. Adamson SL, Lu Y, Whiteley K, et al. Interactions between trophoblast cells and the maternal and fetal circulation in the mouse placenta. Dev Biol. 2002;250:358-373.

45. Georgiades P, Ferguson-Smith A, Burton G. Comparative developmental anatomy of the murine and human definitive placentae. Placenta. 2002;23:3-19.

46. Burton G, Woods A, Jauniaux E, Kingdom J. Rheological and physiological consequences of conversion of the maternal spiral arteries for uteroplacental blood flow during human pregnancy. Placenta. 2009;30(6):473-482.

47. Frias A, Schabel M, Roberts V, et al. Using dynamic contrast-enhanced MRI to quantitatively characterize maternal vascular organization in the primate placenta. Magn Reson Med. 2015;73(4):1570-8.

49. Pijnenborg R, Dixon H, Robertson W, Brosens I. Trophoblastic invasion of human decidua from 8 to 18 weeks of pregnancy. Placenta.1980;1:3-19.

50. Hofmann A, Gerber S, Croy A. Uterine natural killer cells pace early development of mouse decidua basalis. Mol Human Reprod. 2014;20(1):66-76.

51. Shibuya M. Differential roles of vascular endothelial growth factor receptor-1 and receptor-2 in angiogenesis. J Biochem Mol Biol. 2006 Sep 30;39(5):469-78.

52. Fan X, Rai A, Kambham N, et al. Endometrial VEGF induces placental sFLT1 and leads to pregnancy complications. J Clin Invest. 2014 Nov;124(11):4941-52.

Chapter 3 References

1. Bamfo, JEAK and Odibo, AO. Diagnosis and management of fetal growth restriction. J Pregnancy. 2011;2011:1–15,

2. Peleg, D, Kennedy, CM, and Hunter, SK. Intrauterine Growth Restriction: Identification and Management. Am Fam Physician. 1998;453–460.

3. Kulandavelu, S, Whiteley, KJ, Bainbridge, SA, Qu, D, and Adamson, SL. Endothelial NO synthase augments fetoplacental blood flow, placental vascularization, and fetal growth in mice. Hypertension. 2013;61:259–66.

4. Barker, DJ and Clark, PM. Fetal undernutrition and disease in later life. Rev Reprod. 1997;2:105–12.

5. Ingemarsson, I. Gender aspects of preterm birth. BJOG An Int J Obstet Gynaecol. 2003;110:34–38.

6. Mondal, D, Galloway, TS, Bailey, TC, and Mathews, F. Elevated risk of stillbirth in males: systematic review and meta-analysis of more than 30 million births. BMC Med. 2014;12:220.

7. Møller, H, James, W, James, W, Sharpe, R, Skakkebaek, N, Carlsen, E, et al. Change in male:female ratio among newborn infants in Denmark. Lancet. 1996;348:828–9.

8. Eriksson, JG, Kajantie, E, Osmond, C, Thornburg, K, and Barker, DJP. Boys live dangerously in the womb. Am J Hum Biol. 2010;22:330–5.

9. Morgan, TK, Tolosa, JE, Mele, L, Wapner, RJ, Spong, CY, Sorokin, Y, et al. Placental villous hypermaturation is associated with idiopathic preterm birth. J Matern Fetal Neonatal Med. 2013;26:647–53.

10. Hayward, CE, Lean, S, Sibley, CP, Jones, RL, Wareing, M, Greenwood, SL, et al. Placental Adaptation: What Can We Learn from Birthweight:Placental Weight Ratio? Front Physiol. 2016;7:28.

11. Hendrix, N and Berghella, V. Non-placental causes of intrauterine growth restriction. Semin Perinatol. 2008;32:161–5.

12. Salafia, CM, Zhang, J, Charles, AK, Bresnahan, M, Shrout, P, Sun, W, et al. Placental characteristics and birthweight. Paediatr Perinat Epidemiol. 2008;22:229–239.

13. Gagnon, R. Placental insufficiency and its consequences. Eur J Obstet Gynecol Reprod Biol. 2003;110:S99–S107.

14. Gude, NM, Roberts, CT, Kalionis, B, King, RG, Loke, YW, King, A, et al. Growth and function of the normal human placenta. Thromb Res. 2004;114:397–407.

15. Woods, LL, Ingelfinger, JR, Nyengaard, JR, and Rasch, R. Maternal Protein Restriction Suppresses the Newborn Renin-Angiotensin System and Programs Adult Hypertension in Rats. Pediatr Res. 2001;49:460–467.

16. Woods, LL. Maternal Nutrition and Predisposition to Later Kidney Disease. Curr Drug Targets. 2007;8:906–913.

17. Croy, BA, Yamada, AT, DeMayo, FJ, and Adamson, SL. The Guide to Investigation of Mouse Pregnancy. 2014, Academic Press.

18. Long, PA and Oats, JN. Preeclampsia in Twin Pregnancy-Severity and Pathogenesis. Aust New Zeal J Obstet Gynaecol. 1987;27:1–5.

19. Clifton, VL. Review: Sex and the Human Placenta: Mediating Differential Strategies of Fetal Growth and Survival. Placenta. 2010;31:S33–S39.

20. Whitley, GSJ and Cartwright, JE. Cellular and molecular regulation of spiral artery remodelling: lessons from the cardiovascular field. Placenta. 31:465–74.

21. Rennie, MY, Detmar, J, Whiteley, KJ, Yang, J, Jurisicova, A, Adamson, SL, et al. Vessel tortuousity and reduced vascularization in the fetoplacental arterial tree after maternal exposure to polycyclic aromatic hydrocarbons. Am J Physiol. 2011;300:H675-84.

22. Croy, BA, Burke, SD, Barrette, VF, Zhang, J, Hatta, K, Smith, GN, et al. Identification of the primary outcomes that result from deficient spiral arterial modification in pregnant mice. Pregnancy Hypertens. 2011;1:87–94.

23. Felker, AM and Croy, BA. Uterine natural killer cell partnerships in early mouse decidua basalis. J Leukoc Biol. 2016;100:645–655.

24. Lash, GE, Schiessl, B, Kirkley, M, Innes, BA, Cooper, A, Searle, RF, et al. Expression of angiogenic growth factors by uterine natural killer cells during early pregnancy. J Leukoc Biol. 2006;80:572–80.

25. Georgiades, P, Ferguson-Smith, AC, and Burton, GJ. Comparative developmental anatomy of the murine and human definitive placentae. Placenta. 2002;23:3–19.

26. Moffett, A and Loke, C. Immunology of placentation in eutherian mammals. Nat Rev Immunol. 2006;6:584–94.

27. Barut, A, Barut, F, Kandemir, NO, Aktunc, E, Arikan, I, Harma, M, et al. Placental chorangiosis: the association with oxidative stress and angiogenesis. Gynecol Obstet Invest. 2012;73:141–51.

28. Zygmunt, M, Herr, F, Münstedt, K, Lang, U, Liang, OD, Kerbel, RS, et al. Angiogenesis and vasculogenesis in pregnancy. Eur J Obstet Gynecol Reprod Biol. 2003;110 Suppl 1:S10-8.

29. Charnock-Jones, DS, Kaufmann, P, Mayhew, TM, Clark, D., Licence, D., Charnock-Jones, D., et al. Aspects of human fetoplacental vasculogenesis and angiogenesis. I. Molecular regulation. Placenta. 2004;25:103–13.

30. Kim, HS, Krege, JH, Kluckman, KD, Hagaman, JR, Hodgin, JB, Best, CF, et al. Genetic control of blood pressure and the angiotensinogen locus. Proc Natl Acad Sci U S A. 1995;92:2735–9.

31. Morgan, TK, Rohrwasser, A, Zhao, L, Hillas, E, Cheng, T, Ward, KJ, et al. Hypervolemia of pregnancy is not maintained in mice chronically overexpressing angiotensinogen. Am J Obstet Gynecol. 2006;195:1700–1706.

32. Rennie, MY, Whiteley, KJ, Kulandavelu, S, Adamson, SL, Sled, JG, Sapin, V, et al. 3D visualisation and quantification by microcomputed tomography of late gestational changes in the arterial and venous feto-placental vasculature of the mouse. Placenta. 2001;28:833–40.

33. Mayhew, TM, Ohadike, C, Baker, PN, Crocker, IP, Mitchell, C, and Ong, SS. Stereological investigation of placental morphology in pregnancies complicated by pre-eclampsia with and without intrauterine growth restriction. Placenta. 2003;24:219–26.

34. Coan, PM, Ferguson-Smith, AC, and Burton, GJ. Developmental dynamics of the definitive mouse placenta assessed by stereology. Biol Reprod. 2004;70:1806–13.

35. Constância, M, Angiolini, E, Sandovici, I, Smith, P, Smith, R, Kelsey, G, et al. Adaptation of nutrient supply to fetal demand in the mouse involves interaction between the Igf2 gene and placental transporter systems. Proc Natl Acad Sci U S A. 2005;102:19219–24.

36. Freeman, TL, Ngo, HQ, and Mailliard, ME. Inhibition of system A amino acid transport and hepatocyte proliferation following partial hepatectomy in the rat. Hepatology. 1999;30:437–444.

37. Haggarty, P, Page, K, Abramovich, D., Ashton, J, and Brown, D. Long-chain polyunsaturated fatty acid transport across the perfused human placenta. Placenta. 1997;18:635–642.

38. Huang, DW, Sherman, BT, and Lempicki, RA. Bioinformatics enrichment tools: paths toward the comprehensive functional analysis of large gene lists. Nucleic Acids Res. 2009;37:1–13.

39. Huang, DW, Sherman, BT, and Lempicki, RA. Systematic and integrative analysis of large gene lists using DAVID bioinformatics resources. Nat Protoc. 2008;4:44–57.

40. Parham, P. NK Cells and Trophoblasts: Partners in Pregnancy. J Exp Med. 2004;200:951–955.

41. Croy, BA, Chen, Z, Hofmann, AP, Lord, EM, Sedlacek, AL, and Gerber, SA. Imaging of vascular development in early mouse decidua and its association with leukocytes and trophoblasts. Biol Reprod. 2012;87:125.

42. Arngrímsson, R, Björnsson, H, and Geirsson, RT. Analysis of Different Inheritance Patterns in Preeclampsia/Eclampsia Syndrome. Hypertens Pregnancy. 1995;14:27–38.

43. Chesley, LC and Cooper, DW. Genetics of hypertension in pregnancy: possible single gene control of pre-eclampsia and eclampsia in the descendants of eclamptic women. Br J Obstet Gynaecol. 1986;93:898–908.

44. Arngrímsson, R, Bjornsson, S, Geirsson, RT, Bjornsson, H, Walker, JJ, and Snaedal, G. Genetic and familial predisposition to eclampsia and pre-eclampsia in a defined population. BJOG An Int J Obstet Gynaecol. 1990;97:762–769.

45. Ward, K, Hata, A, Jeunemaitre, X, Helin, C, Nelson, L, Namikawa, C, et al. A molecular variant of angiotensinogen associated with preeclampsia. Nat Genet. 1993;4:59–61.

46. Jeunemaitre, X, Inoue, I, Williams, C, Charru, A, Tichet, J, Powers, M, et al. Haplotypes of Angiotensinogen in Essential Hypertension. Am J Hum Genet. 1997;60:1448–1460.

47. Molvarec, A, Jermendy, Á, Nagy, B, Kovács, M, Várkonyi, T, Hupuczi, P, et al. Association between tumor necrosis factor (TNF)-α G-308A gene polymorphism and preeclampsia complicated by severe fetal growth restriction. Clin Chim Acta. 2008;392:52–57.

48. Aidoo, M, McElroy, PD, Kolczak, MS, Terlouw, DJ, ter Kuile, FO, Nahlen, B, et al. Tumor necrosis factor-α promoter variant 2 (TNF2) is associated with pre-term delivery, infant mortality, and malaria morbidity in western Kenya: Asembo Bay Cohort Project IX. Genet Epidemiol. 2001;21:201–211.

49. Bartha, JL, Romero-Carmona, R, and Comino-Delgado, R. Inflammatory cytokines in intrauterine growth retardation. Acta Obstet Gynecol Scand. 2003;82:1099–1102.

50. Holcberg, G, Huleihel, M, Sapir, O, Katz, M, Tsadkin, M, Furman, B, et al. Increased production of tumor necrosis factor-alpha TNF-alpha by IUGR human placentae. Eur J Obstet Gynecol Reprod Biol. 2001;94:69–72.

51. Moreau, P, Contu, L, Alba, F, Lai, S, Simoes, R, Orrù, S, et al. HLA-G Gene Polymorphism in Human Placentas: Possible Association of G*0106 Allele with Preeclampsia and Miscarriage. Biol Reprod. 2008;79:459–467.

52. Smithies, O and Kim, H-S. Targeted gene duplication and disruption for analyzing quantitative genetic traits in mice. Proc Natl Acad Sci USA. 1994;91:3612–3615.

53. Zhang, XQ, Varner, M, Dizon-Townson, D, Song, F, and Ward, K. A molecular variant of angiotensinogen is associated with idiopathic intrauterine growth restriction. Obstet Gynecol. 2003;101:237–42.

54. Carpentier, PA, Dingman, AL, and Palmer, TD. Placental TNF-α signaling in illness-induced complications of pregnancy. Am J Pathol. 2001;178:2802–10.

55. Hefler, LA, Reyes, CA, O'Brien, WE, and Gregg, AR. Perinatal development of endothelial nitric oxide synthase-deficient mice. Biol Reprod. 2001;64:666–73.

56. Kusinski, LC, Stanley, JL, Dilworth, MR, Hirt, CJ, Andersson, IJ, Renshall, LJ, et al. eNOS knockout mouse as a model of fetal growth restriction with an impaired uterine artery function and placental transport phenotype. Am J Physiol Integr Comp Physiol. 2012;303:R86–R93.

57. Myatt, L. Review: Reactive oxygen and nitrogen species and functional adaptation of the placenta. Placenta. 2010;31 Suppl:S66-9.

58. Oh, M-J, Lee, JK, Lee, NW, Shin, J-H, Yeo, MK, Kim, A, et al. Vascular endothelial growth factor expression is unaltered in placentae and myometrial resistance arteries from pre-eclamptic patients. Acta Obstet Gynecol Scand. 2006;85:545–50.

59. Luttun, A, Tjwa, M, and Carmeliet, P. Placental Growth Factor (PlGF) and Its Receptor Flt-1 (VEGFR-1). Ann N Y Acad Sci. 2002;979:80–93.

60. Shibuya, M. Vascular Endothelial Growth Factor (VEGF) and Its Receptor (VEGFR) Signaling in Angiogenesis: A Crucial Target for Anti- and Pro-Angiogenic Therapies. Genes Cancer. 2011;2:1097–105.

61. Zhou, CC, Ahmad, S, Mi, T, Xia, L, Abbasi, S, Hewett, PW, et al. Angiotensin II induces soluble fms-Like tyrosine kinase-1 release via calcineurin signaling pathway in pregnancy. Circ Res. 2007;100:88–95.

62. Xia, Y, Ramin, SM, and Kellems, RE. Potential roles of angiotensin receptor-activating autoantibody in the pathophysiology of preeclampsia. Hypertens. 2007;50:269–75.

63. Foidart, JM, Schaaps, JP, Chantraine, F, Munaut, C, and Lorquet, S. Dysregulation of anti-angiogenic agents (sFlt-1, PLGF, and sEndoglin) in preeclampsia--a step forward but not the definitive answer. J Reprod Immunol. 2009;82:106–11.

64. Pijnenborg, R, Vercruysse, L, and Hanssens, M. The uterine spiral arteries in human pregnancy: facts and controversies. Placenta. 2006;27:939–58.

65. Smith, SD, Dunk, CE, Aplin, JD, Harris, LK, and Jones, RL. Evidence for immune cell involvement in decidual spiral arteriole remodeling in early human pregnancy. Am J Pathol. 2009;174:1959–71.

66. Felker, AM and Croy, BA. Uterine natural killer cell partnerships in early mouse decidua basalis. J Leukoc Biol. 2016;100:645–655.

67. Felker, AM and Croy, BA. Promotion of Early Pregnancy Events in Mice and Humans by Uterine Natural Killer Cells. Neoreviews. 2016;17.

68. Rätsep, MT, Felker, AM, Kay, VR, Tolusso, L, Hofmann, AP, and Croy, BA. Uterine natural killer cells: supervisors of vasculature construction in early decidua basalis. Reproduction. 2015;149:R91-102.

69. Ricard, N and Simons, M. When It Is Better to Regress: Dynamics of Vascular Pruning. PLOS Biol. 2015;13:e1002148.

70. Trundley, A and Moffett, A. Human uterine leukocytes and pregnancy. Tissue Antigens. 2004;63:1–12.

71. Fehniger, TA, Cooper, MA, Nuovo, GJ, Cella, M, Facchetti, F, Colonna, M, et al. CD56bright natural killer cells are present in human lymph nodes and are activated by T

cell-derived IL-2: a potential new link between adaptive and innate immunity. Blood. 2003;101:3052–7.

72. Redman, CWG, Tannetta, DS, Dragovic, RA, Gardiner, C, Southcombe, JH, Collett, GP, et al. Review: Does size matter? Placental debris and the pathophysiology of pre-eclampsia. Placenta. 2012;33 Suppl:S48-54.

73. Zomer, A, Maynard, C, Verweij, FJ, Kamermans, A, Schäfer, R, Beerling, E, et al. In Vivo imaging reveals extracellular vesicle-mediated phenocopying of metastatic behavior. Cell. 2015;161:1046–57.

74. Howerton, CL and Bale, TL. Prenatal programing: At the intersection of maternal stress and immune activation. Horm Behav. 2012;62:237–242.

75. Jl, H, Jl, L, Lin, B, Zhang, J, and Foltz, G. BEX2 (brain expressed X-linked 2). Atlas Genet Cytogenet Oncol Haematol. 2012;14.

76. Tang, Y, Li, X, Wang, M, Zou, Q, Zhao, S, Sun, B, et al. Increased numbers of NK cells, NKT-like cells, and NK inhibitory receptors in peripheral blood of patients with chronic obstructive pulmonary disease. Clin Dev Immunol. 2013;2013:721782.

77. Ishikawa, H, Rattigan, Á, Fundele, R, and Burgoyne, PS. Effects of Sex Chromosome Dosage on Placental Size in Mice. Biol Reprod. 2003;69:483–488.

78. Arnold, AP. Mouse Models for Evaluating Sex Chromosome Effects that Cause Sex Differences in Non-Gonadal Tissues. J Neuroendocrino. 2009;21:377–386.

79. Kalousek, DK, Howard-Peebles, PN, Olson, SB, Barrett, IJ, Dorfmann, A, Black, SH, et al. Confirmation of CVS mosaicism in term placentae and high frequency of intrauterine growth retardation association with confined placental mosaicism. Prenat Diagn. 1991;11:743–750.

80. Yang, R, You, X, Tang, X, Gao, L, and Ni, X. Corticotropin-releasing hormone inhibits progesterone production in cultured human placental trophoblasts. J Mol Endocrinol. 2006;37:533–40.

81. Tuckey, RC. Progesterone synthesis by the human placenta. Placenta. 2005;26:273–81.

82. Hearn, JWD, Xie, W, Nakabayashi, M, Almassi, N, Reichard, CA, Pomerantz, M, et al. Association of HSD3B1 Genotype With Response to Androgen-Deprivation Therapy for Biochemical Recurrence After Radiotherapy for Localized Prostate Cancer. JAMA Oncol. 2017.

83. Zhai, P, Eurell, TE, Cooke, PS, Lubahn, DB, and Gross, DR. Myocardial ischemia-reperfusion injury in estrogen receptor-α knockout and wild-type mice. Am J Physiol Circ Physiol. 2008;278:H1640–H1647.

84. Jesmin, S, Mowa, CN, Nusrat Sultana, S, Mia, S, Islam, R, Zaedi, S, et al. Estrogen receptor alpha and beta are both involved in the cerebral VEGF/Akt/NO pathway and cerebral angiogenesis in female mice. Biomed Res. 2010;31:337–346.

85. Knabl, J, Hiden, U, Hüttenbrenner, R, Riedel, C, Hutter, S, Kirn, V, et al. GDM Alters Expression of Placental Estrogen Receptor α in a Cell Type and Gender-Specific Manner. Reprod Sci. 2015;22:1488–1495.

86. Elkin, M, Orgel, A, and Kleinman, HK. An angiogenic switch in breast cancer involves estrogen and soluble vascular endothelial growth factor receptor 1. J Natl Cancer Inst. 2004;96:875–8.

87. Albrecht, ED and Pepe, GJ. Estrogen regulation of placental angiogenesis and fetal ovarian development during primate pregnancy. Int J Dev Biol. 2010;54:397–408.

88. Losordo, DW and Isner, JM. Estrogen and Angiogenesis: A Review. Arter Thromb Vasc Biol. 2001;21:6–12.

89. Louey, S, Cock, ML, Stevenson, KM, and Harding, R. Placental Insufficiency and Fetal Growth Restriction Lead to Postnatal Hypotension and Altered Postnatal Growth in Sheep. Pediatr Res. 2000;48:808–814.

90. Gilbert, JS, Lang, AL, Grant, AR, and Nijland, MJ. Maternal nutrient restriction in sheep: hypertension and decreased nephron number in offspring at 9 months of age. J Physiol. 2005;565:137–147.

91. David, AL, Torondel, B, Zachary, I, Wigley, V, Abi-Nader, K, Nader, KA, et al. Local delivery of VEGF adenovirus to the uterine artery increases vasorelaxation and uterine blood flow in the pregnant sheep. Gene Ther. 2008;15:1344–50.

92. Liao, WX, Magness, RR, and Chen, D. Expression of Estrogen Receptors-α and -β in the Pregnant Ovine Uterine Artery Endothelial Cells In Vivo and In Vitro. Biol Reprod. 2005;72:530–537.

93. Schmidt, A, Morales-Prieto, DM, Pastuschek, J, and Fröhlich, K. Only humans have human placentas: molecular differences between mice and humans. J Reprod Immunol. 2015;108:65–71.

Chapter 4 References

1. Barker DJP, Fall CHD. Fetal and infant origins of cardiovascular disease. Arch Dis Childhood. 1993;68:797-799.

2. Barker DJP. Fetal origins of coronary heart disease. Br Heart J. 1993;69:195-196.

3. Fall CH, Osmond C, Barker DJ, et al. Fetal and infant growth and cardiovascular risk factors in women. BMJ. 1995;310:428-432.

4. Fall CH, Vijayakumar M, Barker DJ, Osmond C, Duggleby S. Weight in infancy and prevalence of coronary heart disease in adult life. BMJ. 1995;310:17-191995.

5. Mi J, Law C, Zhang KL, Osmond C, Stein C, Barker D. Effects of infant birthweight and maternal body mass index in pregnancy on components of the insulin resistance syndrome in China. Ann Intern Med. 2000;132:253-260.

6. Curhan GC, Chertow GM, Willett WC, et al. Birth weight and adult hypertension and obesity in women. Circ. 1996;94:1310-1315.

7. Curhan GC, Willett WC, Rimm EB, Spiegelman D, Ascherio AL, Stampfer MJ. Birth weight and adult hypertension, diabetes mellitus, and obesity in US men. Circ. 1996;94:3246-3250.

8. Rich-Edwards JW, Stampfer MJ, Manson JE, et al. Birth weight and risk of cardiovascular disease in a cohort of women followed up since 1976. BMJ. 1997;315:396-400.

9. Falkner B. Birth weight as a predictor of future hypertension. Am J Hypertens. 2002;15:43S-45S.

10. Eriksson J, Forsen T, Tuomilehto J, Osmond C, Barker D. Fetal and childhood growth and hypertension in adult life. Hypertension. 2000;36:790-794.

11. Woods LL, Ingelfinger JR, Nyengaard JR, Rasch R. Maternal protein restriction suppresses the newborn renin-angiotensin system and programs adult hypertension in rats. Pediatr Res. 2001;49:460-467.

12. Langley-Evans SC, Sherman RC, Welham SJ, Nwagwu MO, Gardner DS, Jackson AA. Intrauterine programming of hypertension: the role of the renin-angiotensin system. Biochem Soc Trans. 1999;27:88-93.

13. Alexander BT. Placental insuffiencey leads to development of hypertension in growth-restricted offspring. Hypertension. 2003;41:457-462.

14. Brawley L, Itoh S, Torrens C, et al. Dietary protein restriction in pregnancy induces hypertension and vascular defects in rat male offspring. Pediatr Res. 2003;54:83-90.

15. Louey S, Cock ML, Stevenson KM, Harding R. Placental insufficiency and fetal growth restriction lead to postnatal hypotension and altered postnatal growth in sheep. Pediatr Res. 2000;48:808-814.

16. Schreuder MF, Nyengaard JR, Fodor M, van Wijk JA, Delemarre-van de Waal HA. Glomerular number and function are influenced by spontaneous and induced low birth weight in rats. J Am Soc Nephrol. 2005;16:2913-2919.

17. Jeunemaitre X, Soubrier F, Kotelevtsev YV, et al. Molecular basis of human hypertension: role of angiotensinogen. Cell. 1992;71:169-180.

18. Ward K, Hata A, Jeunemaitre X, et al. A molecular variant of angiotensinogen associated with preeclampsia. Nat Genet. 1993;4:59-61.

19. Kim HS, Krege JH, Kluckman KD, et al. Genetic control of blood pressure and the angiotensinogen locus. Prod Natl Acad Sci USA. 1995;92:2735-2739.

20. Brenner BM, Chertow GM. Congenital oligonephropathy and the etiology of adult hypertension and progressive renal injury. Am J Kidney Dis. 1994;23:171-175.

21. Langley-Evans SC, Welham SJ, Jackson AA. Fetal exposure to a maternal low protein diet impairs nephrogenesis and promotes hypertension in the rat. Life Sci. 1999;64:965-974.

22. Gilbert JS, Lang AL, Grant AR, Nijland MJ. Maternal nutrient restriction in sheep: hypertension and decreased nephron number in offspring at 9 months of age. J Physiol. 2005;565:137-147.

23. Larsson L, Aperia A, Wilton P. Effect of normal development on compensatory renal growth. Kidney Int. 1980;18:29-35.

24. Thompson LP, Al-Hasan Y. Impact of oxidative stress in fetal programming. J Pregnancy. 2012;2012:582748.

25. Morgan T., Rohrwasser A., Zhao L., Hillas E., Cheng T., Ward K., J-M Lalouel. Hypervolemia of pregnancy is not maintained in mice chronically overexpressing angiotensinogen." Am J Obstet Gynecol. 2006;195(6):1700-6.

26. Houseman EA, Kile ML, Chritiani DC, Ince TA, Kelsey KT, Marsit CJ. Reference-free deconvolution of DNA methylation data and mediation by cell composition effects. BMC Bioinformatics. 2016;17:259-274.

27. Smithies, O. & Kim, H.-S. Targeted gene duplication and disruption for analyzing quantitative genetic traits in mice. Proc Natl Acad Sci USA. 1994;91:3612-3615.

28. Konecny T, Kara T, Somers VK. Obstructive sleep apnea and hypertension: an update. Hypertension. 2014;63:203-209.

29: Langley SC, Jackson AA. Increased systolic blood pressure in adult rats induced by fetal exposure to maternal low protein diets. Clin Sci. 1994;86:217-222.

30. Woods LL, Weeks DA, Rasch R. Programming of adult blood pressure by maternal protein restriction: Role of nephrogenesis. Kidney International. 2004;65:1339-48.

31. Woods LL, Ingelfinger JR, Rasch R. Modest maternal protein restriction fails to program adult hypertension in female rats. Am J Physiol Regulatory Integrative Comp Physiol. 2005;189(4):R1131-6.

32. Woods LL, Weeks DA, Rasch R: Hypertension after neonatal uninephrectomy in rats precedes glomerular damage. Hypertension. 2001;38:337-342.

33. Novick AC, Gephardt G, Guz B, et al. Long-term follow-up after partial removal of a solitary kidney, N Engl J Med. 1991;325:1058-1062.

34. Solaini G, Baracca A, Lenaz G, Sgarbi G. Hypoxia and mitochondrial oxidative metabolism. Biochim Biophys Acta Bioenergetics. 2010;1797(6-7):1171-1177.

35. Aljunaidy MM, Morton JS, Cooke C-LM, Davidge ST. Prenatal hypoxia and placental oxidative stress: linkages to developmental origins of cardiovascular disease. Am J Physiol Regul Integr Comp Physiol. 2017;313(4):R395-9.

36. Denic A, Lieske JC, Chakkera HA, Poggio ED, Alexander MP, Singh P et al. The substantial loss of nephrons in healthy human kidneys with aging. J Am Soc Nephrol. 2017;28:313-320.

37. Bagby SP, Xue H, Kupfer P, et al. Maternal protein restriction in microswine: food restriction from weaning to prevent excess intake corrects vascular dysfunction in juvenile offspring. Early Hum Dev. 2007;83(Suppl. 1), S87.

38. Anderson CM, Lopez F, Zimmer A, Benoit JN. Placental insufficiency leads to developmental hypertension and mesenteric artery dysfunction in two generations of Sprague-Dawley rat offspring. Biol Rep. 2006;74:538-544.

39. Constantine MM, Ghulmiyyah LM, Tamayo E, Hankins GDV, Saade GR, Longo M. Transgenerational effect of fetal programming on vascular phenotype and reactivity in endothelial nitric oxide synthase knockout mouse model. Am J Obstet Gynecol. 2008;199:250.e1-7.

Chapter 5 References

1. Ricard, N and Simons, M. When It Is Better to Regress: Dynamics of Vascular Pruning. PLOS Biol. 2015;13:e1002148.

2. Croy, BA, Burke, SD, Barrette, VF, Zhang, J, Hatta, K, Smith, GN, et al. Identification of the primary outcomes that result from deficient spiral arterial modification in pregnant mice. Pregnancy Hypertens. 2011;1:87–94.

3. Korn, C and Augustin, HG. Mechanisms of Vessel Pruning and Regression. Dev Cell. 2015;34:5–17.

4. Lange, C, Ehlken, C, Stahl, A, Martin, G, Hansen, L, and Agostini, HT. Kinetics of retinal vaso-obliteration and neovascularisation in the oxygen-induced retinopathy (OIR) mouse model. Graefe's Arch Clin Exp Ophthalmol. 2009;247:1205–1211.

5. Lucitti, JL, Jones, EA V, Huang, C, Chen, J, Fraser, SE, and Dickinson, ME. Vascular remodeling of the mouse yolk sac requires hemodynamic force. Development. 2007;134:3317–26.

6. Rätsep, MT, Carmeliet, P, Adams, MA, and Croy, BA. Impact of placental growth factor deficiency on early mouse implant site angiogenesis. Placenta. 2014;35:772–5.

7. Rätsep, MT, Felker, AM, Kay, VR, Tolusso, L, Hofmann, AP, and Croy, BA. Uterine natural killer cells: supervisors of vasculature construction in early decidua basalis. Reproduction. 2015;149:R91-102.

8. Yang, R, You, X, Tang, X, Gao, L, and Ni, X. Corticotropin-releasing hormone inhibits progesterone production in cultured human placental trophoblasts. J Mol Endocrinol. 2006;37:533–40.

9. Tuckey, RC. Progesterone synthesis by the human placenta. Placenta. 2005;26:273–81.

10. Hearn, JWD, Xie, W, Nakabayashi, M, Almassi, N, Reichard, CA, Pomerantz, M, et al. Association of HSD3B1 Genotype With Response to Androgen-Deprivation Therapy for Biochemical Recurrence After Radiotherapy for Localized Prostate Cancer. JAMA Oncol. 2017;1-9.

11. Elkin, M, Orgel, A, and Kleinman, HK. An angiogenic switch in breast cancer involves estrogen and soluble vascular endothelial growth factor receptor 1. J Natl Cancer Inst. 2004;96:875–8.

12. Albrecht, ED and Pepe, GJ. Estrogen regulation of placental angiogenesis and fetal ovarian development during primate pregnancy. Int J Dev Biol. 2010;54:397–408.

13. Losordo, DW and Isner, JM. Estrogen and Angiogenesis: A Review. Arter Thromb Vasc Biol. 2001;21:6–12.

14. Knabl, J, Hiden, U, Hüttenbrenner, R, Riedel, C, Hutter, S, Kirn, V, et al. GDM Alters Expression of Placental Estrogen Receptor α in a Cell Type and Gender-Specific Manner. Reprod Sci. 2015;22:1488–1495.

15. Rosmond, R, Chagnon, M, Bouchard, C, and Björntorp, P. Polymorphism in exon 4 of the human 3β-hydroxysteroid dehydrogenase type I gene (HSD3B1) and blood pressure. Biochem Biophys Res Commun. 2002;293:629–632

16. Gopalakrishnan, K, Mishra, JS, Chinnathambi, V, Vincent, KL, Patrikeev, I, Motamedi, M, et al. Elevated Testosterone Reduces Uterine Blood Flow, Spiral Artery Elongation, and Placental Oxygenation in Pregnant Rats. Hypertension. 2016;67:630–9.

17. Martins, VR, Dias, MS, and Hainaut, P. Tumor-cell-derived microvesicles as carriers of molecular information in cancer. Curr Opin Oncol. 2013;25:66–75.

18. Costa-Silva, B, Aiello, NM, Ocean, AJ, Singh, S, Zhang, H, Thakur, BK, et al. Pancreatic cancer exosomes initiate pre-metastatic niche formation in the liver. Nat Cell Biol. 2015;17:816–826.

19. Valadi, H, Ekström, K, Bossios, A, Sjöstrand, M, Lee, JJ, and Lötvall, JO. Exosome-mediated transfer of mRNAs and microRNAs is a novel mechanism of genetic exchange between cells. Nat Cell Biol. 2007;9:654–659.

20. Redman, CWG, Tannetta, DS, Dragovic, RA, Gardiner, C, Southcombe, JH, Collett, GP, et al. Review: Does size matter? Placental debris and the pathophysiology of pre-eclampsia. Placenta. 2012;33 Suppl:S48-54.

21. Rak, J and Guha, A. Extracellular vesicles - vehicles that spread cancer genes. BioEssays. 2012;34:489–497.

22. Zomer, A, Maynard, C, Verweij, FJ, Kamermans, A, Schäfer, R, Beerling, E, et al. In Vivo imaging reveals extracellular vesicle-mediated phenocopying of metastatic behavior. Cell. 2015;161:1046–57.

23. Zomer, A, Steenbeek, SC, Maynard, C, and van Rheenen, J. Studying extracellular vesicle transfer by a Cre-loxP method. Nat Protoc. 2015;11:87–101.

24. Morgan, TK, Rohrwasser, A, Zhao, L, Hillas, E, Cheng, T, Ward, KJ, et al. Hypervolemia of pregnancy is not maintained in mice chronically overexpressing angiotensinogen. Am J Obstet Gynecol. 2006;195:1700–1706.

25. Vikse, BE, Irgens, LM, Leivestad, T, Hallan, S, and Iversen, BM. Low birth weight increases risk for end-stage renal disease. J Am Soc Nephrol. 2008;19:151–7.

26. Filler, G, Ramsaroop, A, Stein, R, Grant, C, Marants, R, So, A, et al. Is Testosterone Detrimental to Renal Function? Kidney Int Reports. 2016;1:306–310.

27. Kazancioğlu, R. Risk factors for chronic kidney disease: an update. Kidney Int Suppl. 2013;3:368–371.